FINAL REPORT

" Ionospheric Refraction Corrections in the GTDS for Satellite-to-Satellite Tracking Data."

Contract # NAS 5-22423

Atlantic Science Corporation
Final Report # 76 W 117F

(NASA-CR-156834) IONOSPHERIC REFRACTION CORRECTIONS IN THE GTDS FOR SATELLITE-TO-SATELLITE TRACKING DATA Final Report (Atlantic Science Corp., Riverdale, Md.) 130 p HC A07/MF A01 N78-33654

G3/46 Unclas 35792

IONOSPHERIC REFRACTION CORRECTIONS IN THE GTDS FOR SATELLITE-TO-SATELLITE TRACKING DATA

Final Report # 76 W 117F

IONOSPHERIC REFRACTION CORRECTIONS IN THE GTDS FOR SATELLITE-to-SATELLITE TRACKING DATA

FINAL REPORT

Prepared for:

National Aeronautics and Space Administration
Goddard Space Flight Center
Greenbelt, Maryland 20771
Code 583

Contract # NAS 5-22423

Prepared by:

George Nesterczuk
Jerry K. Kozelsky

Atlantic Science Corporation
5711 Sarvis Ave., Suite 502
Riverdale, Maryland 20840

Final Report # 76 W 117 F

July 1976

TABLE OF CONTENTS

PAGE

I. INTRODUCTION 1

II. SATELLITE TO SATELLITE RAY PATH GEOMETRIES 3

A. Target Satellite Above the Ionosphere
B. Target Satellite High in the Ionosphere (above peak density)
C. Target Satellite Low in the Ionosphere (below peak density)
D. Direct Tracking of Satellite from the Ground

III. INTEGRATING TOTAL ELECTRON CONTENT ALONG SATELLITE TO SATELLITE RAY PATHS 8

A. The Gradient Function
B. The Deviation Function
C. Defining the Integration Path
D. Numerical Integration of the Total Electron Content

IV. RANGE AND RANGE RATE CORRECTIONS 18

A. Derivation of the Ionospheric Refraction Corrections to Range and Range Rate
B. Correcting the SST Data
C. Accuracy of the Corrections

V. EVALUATION OF THE SST REFRACTION CORRECTION ALGORITHM 27

A. Optimizing the Tabulation of the Deviation Function
B. Optimizing the Quadrature Integration

VI. CONCLUSIONS 33

FIGURES 35

TABLES 48

APPENDIX A. Subroutine CORSST (Flow Diagram)

APPENDIX B. Flow Diagram for Case 1

APPENDIX C. Flow Diagram for Case 2

Continued

TABLE OF CONTENTS

APPENDIX D. Flow Diagram for Case 3

APPENDIX E. Flow Diagram for Case 4

APPENDIX F. Flow Diagram for Case 5

APPENDIX G. JCL and Job Set-Up for Satellite to Satellite Ionospheric Refraction Runs

APPENDIX H. Glossary

REFERENCES.

IONOSPHERIC REFRACTION CORRECTIONS IN THE GTDS FOR SATELLITE-to-SATELLITE TRACKING DATA

I. INTRODUCTION

NASA is currently examining techniques for utilizing a Tracking Data Relay Satellite System (TDRSS) to track low orbiting satellites. Such a system, employing a relay satellite in a geostationary orbit, has the obvious advantage of being able to track satellites over a large portion of the globe with only a minimum number of ground stations. However the TDRSS concept gives rise to other difficulties not otherwise considered in the tracking of satellites from the ground. One such difficulty is in obtaining refraction corrections through large portions of the atmosphere. In the TDRSS mode the ray path between target and relay satellites frequently traverses large distances, and the inhomogeneous nature of the ionosphere becomes much more evident, presenting a far greater problem under these circumstances than in ground tracking. One must contend with geographic as well as diurnal ionospheric effects, for the line of sight between satellites can cross a day-night interface or lie within the equatorial ionosphere.

The purpose of this effort was to examine these various effects and to devise a method of computing ionospheric refraction corrections to range and range-rate measurements with sufficient accuracy to be of use in orbit determinations. The ionospheric model for satellite-to-satellite (SST) refraction corrections obviously has to be global in scope. The Bent Ionospheric Model (refs. 1a, 1b, 1c) is ideally suited for this purpose, particularly as it is already incorporated in the Goddard Trajectory Determination System (GTDS) for correcting ground

tracking data. The horizontal electron density gradients encountered along the SST ray paths can thus be generated using this model. The vertical density profiles predicted by the Bent model are of the form shown in figure (1).

Making use of the Bent Ionospheric Model a method of computing refraction corrections through lar ospheric gradients was devised and implemented into the GTDS. Herewith report on the various considerations taken in designing and implementing this SST refraction correction algorithm. The report is structured as follows. Section II is devoted to a discussion of satellite to satellite ray path geometries and of their relation to the ionospheric model. Sections III and V describe the development and eval on of the technique used to integrate the horizontal electron density grat ents encountered along a ray path through the ionosphere. Section IV describes the implementation of the technique into the GTDS, including program flow diagrams contained in Appendices B to F.

II. SATELLITE-TO-SATELLITE RAY PATH GEOMETRIES

One of the first considerations was to define all the possible ray path geometries which could be encountered in the SST mode. This was necessary to ensure that all possible ways of traversing the electron density model could be accommodated by the algorithm. Since numeric interpolation and integration schemes are employed, discontinuities of any kind have to be avoided, and particular care must be exercised whenever the ray paths cross domains where the electron density profiles take on different functional forms.

Figure 2 represents three of the general categories of orbits considered: (1) target satellite above the ionosphere, (2) target satellite high in the ionosphere (above the maximum density layer), and (3) target satellite low in the ionosphere (near or below the maximum density layer). Two additional tracking configurations are shown, ground tracking of the relay satellite and the target satellite. The ground tracking case must also be included, because the ground to relay satellite leg is an integral part of the SST tracking geometry. The important features to note about these various geometries are discussed below. In addition, five specific satellite to satellite orientations are taken up in greater detail, including program flow diagrams, in section IV and Appendices B-F. Figure 3 shows some of the parameters, to be encountered in the discussion below, which play a significant role in defining the electron density gradient function and in the integration of the densities along the ray path. Definitions of other terms and parameters used in this report can be found in the glossary (Appendix H).

A. Target Satellite Above the Ionosphere

This class of orbits gives rise to the longest transionospheric ray paths to be encountered. The geometry involved is shown in figure 2 and figure 3 . Moving from the target to the relay satellite the ionosphere is entered at point

P1 and left at point P2. Midway between P1 and P2 lies PC, the point of closest approach to the center of the earth. Tracing the target satellite in its orbit from the time it completes occultation, the following changes in the segment (P1, P2) are observed. At first, the ray path enters the ionosphere at P1, encounters a density peak at HM, exits through the bottom of the ionosphere at PB, reenters the ionosphere at a second point PB, encounters another density peak at HM and finally exits once more at P2. In effect two distinct ionospheres are encountered along the ray path. It is important that the density peaks at HM along the ray path be properly placed and the density correctly evaluated. Errors made at these locations can be significant, for the densities here are orders of magnitude larger than at the top and bottom of the ionosphere.

As the target moves on in its orbit, PC rises higher above the surface until it crosses HMYM, the bottom of the ionosphere. At this time, the segment (P1, P2) lies entirely in the ionosphere, but two density peaks are still encountered. Care must be exercised to compute these maximum densities properly in order to minimize possible errors in integrating the total electron content along the path.

Next, PC approaches the height of maximum density HM. In this case a significant portion of (P1, P2) lies within the peak density region and special attention must be paid not only to obtaining the maximum density, but also to calculating accurate density gradients.

As PC rises further, segment (P1, P2) becomes shorter, and at the same time, the electron density decreases exponentially. The net effect is a very rapid decrease in integrated electron content until the satellite to satellite ray path leaves the ionosphere entirely. It is difficult to generalize the behavior of the range and range rate corrections for satellite to satellite geometries because of the many variable ionospheric conditions that can be encountered (day to night gradients, latitudinal variations, equatorial anomaly, variable

height of maximum density, etc.). However, for those cases when the target satellite is above the ionosphere, the corrections do follow a certain pattern. As the target merges from occultation, the range correction increases from a non-zero value to a maximum, achieved when PC crosses the peak density at HM. From this maximum value, the range correction then decreases monotonically to zero. The range rate is even more difficult to generalize, for it is obtained from the time rate of change of the range correction. It attains a maximum value before PC reaches HM, a minimum value as PC rises into the exponential layers of the ionosphere, and goes to zero as PC approaches the top of the ionosphere. The sequence is repeated, (in reverse with sign changes on the range rate corrections), as the target satellite approaches occultation on the other side of its pass.

B. Target Satellite High In The Ionosphere (above peak density)

This geometry is similar to the previous case of having a satellite above the ionosphere, with the difference that the range correction never goes to zero. When the target satellite emerges from occultation,the range correction increases until PC crosses HM. The correction then declines to a minimum, which is achieved when the target passes beneath the relay satellite. As the target continues in its orbit a second range maximum is reached when PC again crosses HM. The magnitude of the peaks will depend on factors such as the height and inclination of the orbit of the target and, of course, on the ionospheric state. If the range correction peaks occur on opposite sides of a day-night interface then they could differ in magnitude by a factor of ten. Under such circumstances it is not possible to discuss the general appearance of the range rate corrections.

C. Target Satellite Low In The Ionosphere - (below peak density)

The SST configurations, in which the target is in an orbit below the peak density of the ionosphere, result in the most complex range and range rate correction signatures. The refraction correction is determined by two factors.

One factor is the geometric length of the SST ray path through the ionosphere, and the other is the ionospheric state. The geometric effect is such that maximum path lengths are achieved near occultation when the point of closest approach, PC, is still above the bottom of the ionosphere, HMYM, (fig. 3). In the presence of a homogeneous ionosphere, these positions coincide with the position of the range correction maxima. The maxima would be symmetrically situated about the midpoint of each pass of the target. The real ionosphere, however, is inhomogeneous and the large scale gradients in this complex medium will dominate the geometric effects of increased path length. Hence the presence of a day to night interface or the crossing of the equatorial ionosphere (in the course of a satellite pass), will determine the magnitude and placement of the range correction maxima (or maximum). Typical ionospheric gradients are illustrated in figures 4. For equatorial target satellite orbits, the day-night (sunrise or sunset) gradients will be of greatest significance, while for polar orbits the crossing of the equatorial ionosphere will be the dominant ionospheric effect. Orbits of intermediate inclination will be affected by a combination of both of these large gradients and the resultant range corrections will have the most complex signatures of all SST configurations. The range rate corrections are impossible to discuss in general terms for these cases.

D. Direct Tracking of Satellites From the Ground

This ray path configuration completes the satellite to satellite tracking loop by linking the relay satellite to the ground station. The SST refraction algorithm developed for the GTDS therefore has the additional capability of computing refraction corrections for direct tracking of a target satellite from the ground. When tracking the relay satellite, the ionospheric range correction to the relay will be nearly constant during the course of one pass of the target. Since the relay satellite is stationary relative to the ground station, the only variation in the range correction will be due to diurnal variations of the ionosphere.

For direct tracking of the target, the situation is quite different, for the motion of the satellite adds a significant factor to the range rate correction. Combining geometric and ionospheric effects one can obtain a variation in the range correction of a factor of 30 just in the visible sky over one tracking station (ref. 6). The variation in range correction will depend on the orbit of the target as well as on the ionospheric state, just as it does for SST configurations. The dominant factor in the range rate correction under these conditions is the velocity of the target relative to the ground station. In general the rate correction should achieve a positive maximum as the satellite rises in the sky over the station, and a negative maximum as the satellite sets over the station. The relative magnitude and placement of these maxima depends on the ionospheric state.

III. INTEGRATING TOTAL ELECTRON CONTENT ALONG SATELLITE TO SATELLITE RAY PATHS

The major problem in computing range and range rate corrections lies in accurately defining the horizontal electron density gradients which are encountered along the large distances characteristic of satellite to satellite (SST) geometries. A satellite at 1000 km can achieve SST ray path which will subtend earth central angles of 80° to 90° totally immersed in the ionosphere. Figure 4a gives some idea of the magnitude of the gradients. It is a world map of the ionospheric critical frequency f0F2 projected onto a shpere at height 300 km above the surface of the earth. f0F2 is related to the maximum electron density by the equation

$$N_m = 1.24 \times 10^{10} \times (f0F2)^2 \quad el/m^3 \qquad (1)$$

where f0F2 is in MHz. Figure 4b is a world map of the height of the maximum electron density HM. It too shows a highly complicated structure. Both of these parameters play a critical role in predicting the vertical density profile using the Bent model. In addition to providing N_m, f0F2 is also one of the key parameters used to compute the thickness of the parabolic regions of the profile, and the decay constants in the exponential layers (figure 1).

Integrating the profile vertically gives the vertical electron content

$$N_v = \int_{h_m - y_m}^{h_{top}} N(h)\, dh \qquad (2)$$

Figure 4c shows how this quantity varies globally on a typical day. The extent to which the ionosphere is inhomogeneous becomes strikingly obvious in this figure.

A. The Gradient Function

The total electron content between any two points, P1 and P2, in the ionosphere is obtained by integrating

$$N_T = \int_{P1}^{P2} N(s)\, ds \qquad (3)$$

where N(s) is the electron density function, giving the electron density at position $s = s(x, y, z)$ or $s(\lambda, \theta, h)$ along the path, and λ, θ, h are the longitude, latitude, and height above the surface, respectively. Since N(s) does not have a simple analytic representation some new means had to be devised to perform the integration in eq. 3. Accordingly we chose a quadrature integration technique. Using quadrature integration it is not necessary to know the exact functional form of the integrand. It suffices to have values of the integrand at specific "quadrature" points.

The problem of dealing with a complicated function like N(s) was then reduced to computing N(s) at some specific points along the path. To simplify these computations N(s) was separated into 2 parts. The approach was to consider the ionosphere as a three dimensional medium having a vertical electron density distribution given by the profile in figure 1. If the ionosphere were homogeneous then one such vertical density profile would suffice to define the ionosphere any place on the globe. However, the ionosphere is not homogeneous, therefore, each location on the globe has its own profile. But, since the profiles all have the same basic shape it is possible to separate this basic height dependence from the positional variations. The basic height dependence is represented by a reference profile $N_{ref}(\lambda_{ref}, \theta_{ref}, h)$. The positional dependence is then reduced to perturbations or deviations from the reference profile which are represented mathematically by a function G(s), called the gradient function. Along any ray path the line of sight electron density distribution N(s) is then given by <u>one</u> reference profile modified by a gradient function, as in eq. 4.

$$N(s) = N_{ref}(\lambda_{ref}, \theta_{ref}, h) * G(s) \qquad (4)$$

Figure 5 may be helpful in illustrating the relationship between the functions N, N_{ref} and G. It now remains to evaluate the gradient function G which, b equation 4, is

$$G(s) = \frac{N(s)}{N_{ref}(\lambda_{ref}, \theta_{ref}, h)} \quad . \qquad (5)$$

B. The Deviation Function

During the course of numerical evaluations of the function G it became expedient to represent the gradient function as

$$G(s) = 1 + \delta(s) \qquad (6)$$

In this form $\delta(s)$ isolates the deviation of the density at s from the reference profile density. For this reason $\delta(s)$ is called the deviation function. Now, by equations 5 and 6

$$\delta(s) = \frac{N(s)}{N_{ref}(\lambda_{ref}, \theta_{ref}, h)} - 1 \qquad (7a)$$

Equation 7a is the defining equation of the deviation function.

If the variable s is replaced by spherical positional parameters λ, θ, and h, it may become clearer how δ is evaluated in a practical application.

$$\delta(s) = \frac{N(\lambda, \theta, h)}{N_{ref}(\lambda_{ref}, \theta_{ref}, h} - 1 \qquad (7b)$$

$\delta(s)$ is defined at several discrete points (up to 22 points in the SST formulation) between the ends of the ray path, thereby producing a table of values, $\delta_i(s_i)$, where

$$\delta_i(s_i) = \frac{N_i(\lambda_i, \theta_i, h_i)}{N_{ref,i}(\lambda_{ref}, \theta_{ref}, h_i)} - 1 \qquad (7c)$$

Theoretically any reference profile could be used to evaluate the δ_i in eq. 7c. However, when defining $\delta(s)$ using only a few discrete points, it was found necessary (in order to maximize numerical accuracy) to choose the reference profile at the point $(\lambda_{ref}, \theta_{ref}, HM)$ along the ray path where the maximum electron density is encountered. All the profile parameters are generated at the location $(\lambda_{ref}, \theta_{ref})$ using the Bent Ionospheric Model. They are later used, as needed, to compute the densities $N_{ref,i}$ at the heights h_i. Once the reference profile has been chosen, the densities N_i are computed. To do this a complete ionospheric profile, i.e. a complete set of profile parameters, is predicted by the Bent Model, at each location (λ_i, θ_i) in turn. Using the profile parameters, the density N_i at each point $(\lambda_i, \theta_i, h_i)$ is obtained by substituting the height h_i into the equations defining the profile. The profile equations are listed on figure 1.

To obtain values of δ at intermediate points of the $\delta_i(s_i)$ table, several numerical techniques were investigated. The first approach was to represent δ by a simple polynomial. Based on examinations of world maps of f0F2 and N_v (figures 4a and 4c) it appeared that a polynomial of 1st or 2nd order would suit the mid and high latitude regions of the ionosphere while a 3rd or 4th order polynomial would fit the equatorial regions. Accordingly, δ was computed at numerous points along various ray paths and polynomials were fitted to these data in a least squares sense. It was necessary to go to sixth order fits before numerical results became stable enough to perform range differencing. Fits of this order would require too many data points, hence, the polynomial representation of δ was

abandonned, and instead, numerical interpolation schemes were investigated. Interpolation using a cubic spline technique (ref. 3) was finally chosen as the most satisfactory means of defining δ at intermediate points in the δ_i (s_i) table. Details concerning the number of points needed to accurately define δ, as well as the placement of those points, are discussed in section V below.

As previously mentioned, the reference profile is always chosen at the point of highest density along a ray path. For direct tracking of satellites from the ground, this point occurs when the ray path crosses HM. In the SST mode it is possible for the ray path to cross HM twice. In such cases, the ray path is divided into two legs, the division being made at the point of closest approach, PC . A separate reference profile and deviation function are then obtained for each leg. For the cases when PC is above HM, the reference profile is chosen at PC, for, being the lowest point in the ionosphere, PC becomes the highest density point on the ray path. For those geometries where the target satellite itself is the lowest point in the ionosphere, the reference profile is chosen at the target satellite.

This concludes the description of how the electron density is computed, at any point along an integration path through the ionosphere, as the product of a reference profile and a gradient function. Both the reference profile and the gradient function have been defined and discussed. Let us now turn to the problem of actually integrating the electron density N(s) from point P1 to point P2, as required by equation 3.

C. Defining The Integration Path

The integration of the total electron content now proceeds according to equation 8, obtained by substituting eqs. 6 and 4 into eq. 3.

$$N_T = \int_{P1}^{P2} (N_{ref} * (1+\delta)) \, ds \qquad (8)$$

The integration in eq. 8 is executed assuming the path (P1, P2) is a straight line (refer to figure 3 for definition of points). To assume straight line radio propagation means that effects of refractive bending are being neglected. This assumption is valid for satellite to satellite tracking, since at S-band frequencies refractive bending is negligible.

The integration interval (P1, P2) is not always treated as a single interval. The interval is sometimes split into two intervals (PC, P1) and (PC, P2) and the integrations then summed. The distinction between these two modes of integration is made on the basis of the position of the point of closest approach, PC, relative to the height of maximum density HM. If PC is above HM, then only one deviation function is defined for the entire path (with reference profile at PC) and the interval (P1, P2) is not split at PC. If PC falls below HM, and PC lies between P1 and P2, the path is divided at PC into the two intervals (PC, P1) and (PC, P2). Each of these two intervals has its own deviation function, defined with respect to a reference profile computed at the intersection of the ray path with HM. In the event that PC falls below the ionosphere, the intervals become (PB, P1) and (PB, P2).

For those SST configurations in which the target satellite lies on the near side of the earth, as seen from the relay satellite, i.e. PC lies outside the interval (P1, P2) (see figure 3), then the interval (P1, P2) is not divided. A single deviation function is computed in these cases, relative to a reference profile chosen either at HM, or at the target, if the target is above HM.

The purpose in distinguishing between these various ray path configurations, is to ensure an accurate definition of the density gradients along the path (P1, P2), particularly when the path traverses the region around the peak electron density at HM.

In performing an actual integration, the interval (P1, P2) is further subdivided into segments, so chosen as to reflect the boundaries of the seven layers of the

reference profile (fig. 1). The end points of these segments correspond to the layer heights HMYM (bottom of the ionosphere), HM, H0, H1, H2, 1000 km, 2000 km, and 3500 km. This segmentation of the integration interval is necessitated by the requirement of quadrature integration that the function to be integrated and its derivatives be continuous over the integration interval. To meet these requirements, the integration of equation 8 by quadrature must therefore proceed in steps through the layers over which the reference profile does not change analytical form.

D. Numerical Integration of the Total Electron Content

The Gaussian quadrature method (ref. 4) was selected to evaluate the total electron content according to equation 8. Gaussian integration is performed as follows:

$$\int_a^b f(y)\,dy = \frac{b-a}{2} \sum_{i=1}^{n} w_i\, f(y_i) + R_n \qquad (9)$$

$$y_i = \left(\frac{b-a}{2}\right) x_i + \left(\frac{b+a}{2}\right) \qquad (10)$$

x_i = Zeros of the Legendre Polynomials $P_n(x)$

$$\text{weights } w_i = \frac{2}{(1-x_i)^2} \left[P_n'(x)\right]^2$$

$$\text{remainder } R_n = \frac{(b-a)^{2n+1}\,(n!)^4}{(2n+1)\,[(2n)!]^3}\; 2^{2n+1}\; f^{(2n)}(\xi)$$

Tables of the values of x_i and w_i can be found in many standard texts on numerical techniques, including ref. 4.

Equation 8 can now be rewritten according to equation 9 to produce the form which is implemented in the GTDS for SST refraction correction calculations.

$$\int_{Pa}^{Pb} N_{ref}\,(1+\delta)\,ds = \sum_{j=\ell}^{m} \left(\int_{S_j}^{S_{j+1}} N_{ref}\,(s)\;(1+\delta\;(s))\;ds \right)$$

$$= \sum_{j=\ell}^{m} \left(\frac{S_{j+1} - S_j}{2} \sum_{i=1}^{n_j} w_i \;\; N_{ref}\,(s_i)\,(\,1+\delta(s_i)\;) \right) \qquad (11)$$

$$\text{where} \quad s_i = \left(\frac{S_{j+1} - S_j}{2} \right) x_i + \frac{S_{j+1} + S_j}{2} \qquad (12)$$

and S_j = position along the ray path (Pa, Pb) which intersects the height of the bottom of the jth layer of the reference profile

ℓ = index of the lowest profile layer encountered along the interval (Pa, Pb)

m = index of the highest profile layer encountered along the interval (Pa, Pb)

S_ℓ = position corresponding to lowest height attained by path (Pa, Pb) in traversing the ionosphere

S_m = position corresponding to highest height attained by path (Pa, Pb) in traversing the ionosphere

Pa, Pb = limits of integration corresponding to integration intervals (P1, P2), (PC, P2), (PC, P1), (PB, P1), (PB, P2), as appropriate for each SST ray path

N_{ref} = reference profile

δ = deviation function defining density gradients between points Pa and Pb in the ionosphere

n_j = number of quadrature points used to integrate electron density in j^{th} layer; $n_j = 4$ for $j=1$ and $n_j=3$ for $j=2,3,\ldots 7$

Equation 11 is the form in which integrations are carried out for SST configurations. The first step in evaluating equation 11 is to determine the limits of the j - sum, i.e. the summation over layers, as set by the configuration geometry. This procedure was described in section III C, above. Integration then proceeds from layer 1 to layer m.

The quadrature weights and points, w_i and x_i, appropriate for each layer are obtained from tables. The minimum number of points, n_j, required to accurately integrate N_{ref} $(1+\delta)$ through each layer, was determined in a series of evaluation runs in which quadrature integrations were compared with ray tracing calculations. In the course of these evaluations it was found that at least 4 quadrature points were needed to integrate through the first (bi-parabolic) layer of the ionosphere, and at least 3 quadrature points were needed for each of the six topside layers (one parabolic and five exponential layers).

Using the appropriate quadrature points for the layer lying between points S_j and S_{j+1} along the ray path, equation 12 provides the positions s_i at which the deviation function δ and the reference electron density N_{ref} are to be evaluated. The reference density is obtained by substituting the height h_i corresponding to the point s_i (i.e. $s_i = s(\lambda_i, \theta_i, h_i)$) into the ionospheric profile equations (fig. 1) containing the reference profile parameters. The deviation function is interpolated at s_i using a cubic spline interpolation as described in section III-B, above. The products $w_i * N_{ref}(s_i) * (1+\delta(s_i))$ are then formed and summed, and the totals for each layer added according to equation 11 .

If the integration interval (P1, P2) (see figure 2) has been split into two intervals, as described in section III-C, then this summation procedure is repeated seperately for each interval and the results are then added to produce

a total electron content, N_T , between points P1 and P2. This is the basic quantity which is used to compute the ionospheric refraction correction to range measurements. As described in section IV, a simple scaling of N_T by the tracking frequency produces the range correction.

Details of some of the evaluations undertaken during the development of this refraction correction technique are discussed in section V below. These include studies of the definition of the deviation function, the selection of the integration paths, and the definition of the minimum number of points required to perform accurate quadrature integration of equation 8.

IV. RANGE AND RANGE RATE CORRECTIONS

A. Derivation of the Ionospheric Refraction Corrections to Range and Range Rate

The refraction corrections to range and range rate are obtained according to the following equations.

Range: $$\Delta R = \frac{40.3}{f^2} N_T \tag{13}$$

Range-rate: $$\Delta \dot{R} = \frac{\Delta R\,(t+\Delta t) - \Delta R\,(t)}{\Delta t} \tag{14}$$

where the total content N_T is defined in equation (3) and evaluated according to equation 8, f is the tracking frequency in Hz, Δt is in seconds and ΔR and $\Delta \dot{R}$ are in meters and meters/sec., respectively. The range and the range rate corrections so defined have opposite effects on their respective observable quantities because of the different manner of propagation of the signals from which the ranges and rates are extracted.

Ranges are obtained from the modulation of the carrier wave of the tracking signal, whereas range rates are deduced from doppler counts (phase measurements). The modulated carrier propagates as a wave group through the ionosphere and its behavior is characterized by the group index of refraction n_g. Since the ionosphere is a dispersive medium the group and phase (n_p) indices of refraction are not equal. Hence, phase propagation must be characterized by the phase index of refraction. Fortunately, at S-band frequencies n_g and n_p are simply related (ref. 2) by

$$n_g \simeq \frac{1}{n_p} \tag{15}$$

For satellite tracking frequencies, the Appleton- Hartree equation (ref. 2) simplifies to

$$n_p^2 = 1 - k\frac{N}{f^2} \tag{16a}$$

where $k = (e^2/4\pi^2 \epsilon_0 m) = 80.5$ and f is in Hz. By using the binomial expansion and equation (15), we get

$$n_g^2 = 1 + k\frac{N}{f^2} \tag{16b}$$

Using the binomial expansion again and substituting for k, eqs. (16) reduce to the more familiar

$$n_p = 1 - \frac{40.3\,N}{f^2} \tag{17a}$$

$$n_g = 1 + \frac{40.3\,N}{f^2} \tag{17b}$$

One can now define the radio path R of a signal propagating through the ionosphere (figure 6)

$$R = \int_{P_1}^{P_2} n \; ds \; . \tag{18}$$

Substituting eqs. (17)

$$R = \int_{P_1}^{P_2} \left(1 \mp \frac{40.3\,N}{f^2}\right) ds$$

$$= R_0 \mp \frac{40.3}{f^2} \int_{P_1}^{P_2} N \, ds \tag{19}$$

where R_o is the straight line range in the absence of any ionosphere. Equation (19) defines the range correction ΔR (equation 13), such that

$$R = R_o \mp \Delta R$$

Hence for phase and group measurements the radio paths are

$$R_{phase} = R_o - \Delta R \tag{20a}$$

$$R_{group} = R_o + \Delta R \tag{20b}$$

Range measurements are then corrected according to

$$\text{Range}_{measured} = \text{Range}_{vacuum} + \Delta R \tag{21b}$$

while range - rates (phase measurements) according to the time derivative of eq. (20a)

$$\text{Range-rate}_{measured} = \text{Range-rate}_{vacuum} - \Delta \dot{R} \tag{21a}$$

In applying corrections to observations in the GTDS, the convention is such that the corrections are always subtracted from the observations, therefore

$$\text{Range-rate}_{measured,\,corrected} = \text{Range-rate}_{measured} - (-\Delta \dot{R}) = \text{Range-rate}_{vacuum} \tag{22a}$$

$$\text{Range}_{measured,\,corrected} = \text{Range}_{measured} - \Delta R = \text{Range}_{vacuum} \tag{22b}$$

Equation (22a) shows why the sign on the range rate correction is always changed before it is applied to the tracking observation.

An excellent discussion of this phenomenon from an electrical engineering standpoint can be found in ref. 1c.

B. Correcting the SST Data

Integration of the total electron content encountered along SST ray paths through the ionosphere is controlled in the GTDS by subroutine IONSST. The selection of integration paths and the definitions of gradient functions is all performed in this subroutine. Program flow diagrams of IONSST can be found in Appendix B.

For illustration purposes, five test cases have been traced through the flow diagrams of IONSST for various SST geometries. The flow of the logic for each case is traced by a heavy line in Appendices B through F. Included are three cases involving a single integration path but with differently defined reference profiles, one case involving two integration paths requiring two separate reference profiles, and one case depicting direct tracking from the ground. The geometries are illustrated in figures 7 through 11, and the significant points to note for each case are summarized below.

Case 1 (figure 7) - The target satellite is in the topside ionosphere above HM, and is located between PC and P2. The deviation function is defined relative to a reference profile at P1, and from 2 to 9 points are used to define the function over the interval (P1, P2). The exact number of points depends on the height of the point of closest approach, PC, and on the length of the path (P1, P2). The closer PC approaches HM, the larger the number of points used to specify the deviation function. The integration interval (P1, P2) is divided into segments corresponding to the topside layers of the reference profile, and three-point Gaussian quadrature is used to integrate the electron content through each of these segments. The flow diagram for case 1 is in Appendix B.

Case 2 (figure 8) - The target satellite is above the ionosphere. PC lies above HM so only one reference profile (at PC) is used to define the deviation function between P1 and P2. Again, depending on the height of PC and the length of the path (P1, P2), anywhere from 3 to 17 points, spaced at intervals of equal earth central angle, are used to specify the deviation function over the interval (P1, P2). Integration then proceeds in layer segment from P1 to P2 using this deviation function and the reference profile. The integration through each segment is executed by a 3-point Gaussian quadrature. The flow diagram for case 2 is in Appendix C.

Case 3 (figure 9) - The target satellite is in the bottomside ionosphere below the maximum density layer HM. The position of HM along the path (P1, P2) is obtained by an iterative process. This being the maximum density encountered along the path, the reference profile is computed at this location. Next, a profile is computed at P1 in order to define the deviation function at this point. A comparison is made between the bottomside ionospheres at P1 and at the reference profile. If it is found that the ionosphere at P1 extends to a lower height than at the reference point HM, then the bottomside of the reference profile is modified to reflect this difference. This is achieved by setting the reference profile parameter YM (ref) to the value of YM at P1. This precaution is taken to avoid divisions by zero when defining the bottom of the ionosphere. The deviation function definition is then completed using up to 9 points spaced at equal earth central angles along (P1, P2). An additional point is placed halfway between P1 and HM to improve numerical accuracy. In the event that the earth central angle subtended by (P1, P2) is less than three degrees, gradients are neglected and the deviation function is set to zero. Integration proceeds from P1 to P2 in layer segments. The first segment from P1 to HM is integrated using 4 quadrature points, while the six topside segments are integrated with 3 quadrature points. The flow diagram for case 3 is in Appendix D.

Case 4 (figure 10) - The target satellite is within the ionosphere in a position near occultation. PC falls below the bottom of the ionosphere, HMYM, so that the ray path exits and reenters the ionosphere at the points PB. These points

must be solved for iteratively. The path (P1, P2) is now subdivided into 2 intervals, (PB, P1) and (PB, P2). Reference profiles for each of these intervals are computed at the points HM, which must also be found by iteration. Tests are made to determine if the bottomside reference profiles need to be extended relative to the bottomside at the points PB. This is to ensure properly defined deviation functions in the bottomside ionosphere, as discussed in the example of case 3. A separate deviation function is defined for each interval using up to 9 points, spaced at equal earth central angles. An additional point is placed midway between PB and HM. Two integrations are then performed, layer by layer, from PB to P1, and from PB to P2. The results of the separate integrations are added to produce a net total electron content for the path (P1, P2). The flow diagram for case 4 is in Appendix E.

Case 5 (figure 11) - Direct tracking of a satellite from the ground. The integration interval is (PB, P2). If the satellite is above the ionosphere, P2 corresponds to the top of the ionosphere at 3500 km. If the satellite is within the ionosphere, P2 coincides with the satellite position. The intersections at PB and at HM are found iteratively. The reference profile is computed at HM along the interval (PB, P2), and from 2 to 7 points are used to define the deviation function over this interval. For high elevation angles when the earth central angle subtended by (PB, P2) is less than 3°, gradients are neglected and the deviation function is set to zero. Integration now proceeds by quadrature from the first layer up to a maximum of seven layers. The flow diagram for case 5 is in Appendix F.

Once the integration has been completed a return is made to subroutine CORSST. It is here that the one-way range and range rate corrections are computed and applied to the observations, as specified by equations 23, 24 and 25.

$$DMR = \frac{40.3\, N_T\,(\text{relay})}{2} \left(\frac{1}{f^2_{up}} + \frac{1}{f^2_{dwn}} \right) + \frac{40.3\, N_T\,(SST)}{f^2_{SST}} \qquad (23)$$

$$DRATE = -\frac{DMR\ (T+DELT) - DMR(T)}{DELT} \tag{24}$$

$$OM2 = OM2 - DMR/1000 \text{ (Range Observations)} \tag{25a}$$

$$OM2 = OM2 - DRATE/1000 \text{ (Range rate Observations)} \tag{25b}$$

where N_T (relay) = total electron content for the ground to relay satellite link

N_T (SST) = Total electron content for the relay to target satellite link

f_{up}, f_{dwn}, f_{SST} = uplink, downlink, and satellite to satellite tracking frequencies.

DMR =range correction in meters

DRATE = range rate correction in meters/sec

OM2 = tracking data observation (GTDS notation) in km of range or km/sec of range rate.

The program flow diagram for subroutine CORSST is found in Appendix A.

Since it takes two successive range observations to compute a range difference, the range rate correction is set to zero if the first observation in any pass is a range rate. Furthermore, if the time interval, DELT, between successive range rate observations is too large ($>$ 10 minutes), DRATE is again set to zero and the range differencing is reinitialized, as for the beginning of a new pass. For those cases when the time interval is too small ($<$ 1 second), DRATE is not evaluated, and instead, the last computed value of DRATE is used.

C. Accuracy of the Corrections

The ionospheric refraction correction algorithm for satellite to satellite tracking data described in this report has not yet been evaluated. Test runs using tracking data from the ATS-6 to GEOS-3 SST configuration indicate that the algorithm has been successfully integrated into the GTDS. The refraction corrections computed by the algorithm, for this configuration, range from 0.5 to 10 meters for range measurements and from 0.1 to 1.0 cm/sec for range rates, at frequencies near 2 GHz. Although they are of the right order of magnitude, the corrections appear to be lower than expected by perhaps a factor of 2 or 3 in the range correction. Some numeric inconsistencies have also been noted, between the integrations in the ground to relay link and the relay to target link. Hence, definitive conclusions regarding the accuracy of the SST refraction correction algorithm must be put off pending further testing and evaluations.

Some comments can, however, be made regarding the expected accuracy of the refraction corrections. The approach of using a reference profile, in conjunction with a gradient function, to represent electron density variations between two points in the ionosphere, was thoroughly tested in a ground tracking configuration for a satellite above the ionosphere. Though this did not provide a complete test of the technique, the ground tracking mode did allow an in-depth evaluation of all the requisite numerical techniques including quadrature integration through the ionospheric profile, definition of the deviation function and spline interpolation of the deviation function. Furthermore, some similarities do exist between the two modes. For example, the longest path through the ionosphere for ground tracking occurs at 0° elevation when the path subtends an earth central angle of about 40°. The longest path in the SST mode is about 50°, as measured from the point of closest approach to the top of the ionosphere. Although the total path in the SST case is 100°, for integration purpose it would be treated as two 50° intervals. Hence, the low elevation angle lines of sight in the ground tracking mode can provide a

fair approximation of SST geometries.

Range corrections in the ground tracking tests were found to agree with ray trace results to within 1% (though with some exceptions) when the deviation function was defined by as few as 7 points. The limiting accuracy in computing the corrections was entirely dependent on the definition of the deviation function, and not on the quadrature integration or spline interpolation. Hence, with deviation functions defined by using a few more points (up to 9 or 10), it should be possible to achieve the same 1% accuracy in range correction for any SST configuration.

The accuracy of the range rate corrections will vary with the accuracy of the range corrections. Experience with ground tracking geometries indicates that for accuracies of 1% in the range corrections the range rates should be good to within 2% to 4%. Confirmation of this estimate will have to await further testing.

A more detailed discussion of the ground based evaluation runs can be found in section V of this report.

V. EVALUATION OF THE SST REFRACTION CORRECTION ALGORITHM

To date, the refraction correction algorithm as it is implemented in the GTDS, has not been evaluated. However, the numerical techniques employed in the algorithm were thoroughly tested in the course of program development. The tests were made using a configuration in which a ground station tracks a satellite in orbit above the ionosphere (ref. 7). At low elevation angles, ground to satellite ray paths in the ionosphere can be as large as 40° of earth central angle. Though this is not as long as some of the SST ray paths, these low elevation cases traverse enough ionosphere to encounter substantial density gradients. As a result it was possible to confirm the validity of representing the variations in electron density in the ionosphere as the product of a reference profile and a gradient function.

The ground station at which the evaluation tests were made, was located at Kashima, Japan (lat = 35.°95, long = 140.°7) and the evaluations were run for 12h U.T. on 15 January 1969. The date was chosen to coincide with solar maximum, and the location was selected because of its proximity to the geomagnetic equator where electron density gradients are high. The ionospheric state for this date and time is illustrated in the world maps of figures 4. Integrations of total electron content were carried out by ray tracing along lines of sight selected at 30° intervals in azimuth and for 19 elevations. From 0° to 10° the elevations were incremented in steps of 1°, from 10° to 30° the elevations were incremented in steps of 5°, and from 30° to 90° in steps of 15°.

At low elevations, up to 150 density points were computed to define the electron density variations along each line of sight. The points were generated at intervals of 20 km along the path, from the bottom of the ionosphere to a height of 1000 km, then at 200 km intervals from 1000 km to 3500 km. At this height the ionosphere was cut off. As the line of sight approached vertical incidence, the total number of generated points decreased to approximately 60.

The ray tracing program (ref. 5) is a double precision arithmetic application of Snell's Law in spherical form. Numerical integration of the equations, relating ray bending and electron content to changing local elevation angle and refractivity, was performed layer by layer through the ionosphere to provide the total electron content. The integration steps were 1 km in height below 1000 km and 5 km for heights above 1000 km. Integration of the density through each step was carried out using a 3-point Simpson's rule. Electron densities at positions in between the 60 to 150 precomputed density points were provided to the ray trace program by interpolation. Below the maximum density the interpolation was of fourth order. Above maximum density the interpolation was quadratic in the parabolic layer and logarithmic in the exponential layers. Comparisons with analytic integration at vertical incidence indicated the ray trace total electron content was accurate to 1 part in 10^8.

The ray trace results served as benchmarks for evaluating the gradient function technique. The main items of interest were to determine the minimum number of points needed for accurate Gaussian integration through the gradients and to optimize the calculation of the deviation function.

A. Optimizing the Tabulation of the Deviation Function

The deviation function δ defining the electron density gradients between two points P1 and P2 in the ionosphere is computed at equally spaced intervals of earth central angle between the two points. The number of intervals to be used is obtained using the empirically determined function, NOPF.

$$\mathrm{NOPF} = \frac{48\mathrm{x}10^5}{\mathrm{H}+18\mathrm{x}10^5} + \frac{\mathrm{ECA}}{7.5}$$

where ECA is the earth central angle (in degrees) subtended by the interval (P1, P2), and H (in meters) is the height of closest approach to the surface of the earth of the line segment (P1, P2). The function is integerized in the

computer so that it returns a fractionless integer. The definition of NOPF is such that more weight is placed on the lower regions of the ionosphere, where the gradients are expected to be the most significant. Hence, for ray paths crossing through or near the peak density, NOPF returns its maximum value of 8 intervals. For the cases when the point of closest approach, PC, lies between P1 and P2 (see figure 3), the ECA is measured from PC, and NOPF is then separately determined for (PC, P1) and (PC, P2). This means that as many as 16 intervals may be used in defining δ along some of the longer transionospheric ray paths. Up to two more points may be added to these, as follows: (1) the point HM, if it lies on the ray path, and (2) a point halfway between HM and the lowest point encountered along the path. It is therefore possible to have a δ defined by as many as 22 points (counting end points).

The function NOPF was determined on the basis of comparisons with the ground based ray tracing calculations. For each line of sight in the benchmark cases described above, the deviation function was computed at fifteen heights. In each case, the reference profile was at the peak electron density. Different combinations of the heights, varying from as few as 6 to all 15 points, were then used to define the deviations along the lines of sight. Quadrature integration produced a set of range corrections which could be compared to the exact ray trace calculations along each ray path. Some of the results of these comparisons are presented in Tables 1, 2, and 3. The labels in the tables mean the following:

analytical - analytic integration thru the ionosphere assuming a homogeneous profile at HM

numerical - Gaussian quadrature integration through the ionosphere assuming a homogeneous profile at HM

numerical - (least squares) - quadrature integration with gradients given by 6th order polynomial fitted by least squares

numerical - (spline) - quadrature integration with gradients given by cubic spline interpolation through different sets of points

The range and range difference corrections are in meters. Angle corrections are in mrad. The percentage difference for each entry is taken relative to the ray trace result and is given by

$$\% \text{ diff} = \frac{\text{computed value - ray trace}}{\text{ray trace}} .$$

The range differences were obtained by differencing the printed value of the range correction with the value at the previous elevation angle. Below 10° elevation this meant differencing range corrections over a 1° angle interval. From 15° to 30° the differencing was over 5° angle interval, and from 45° to 90° the interval was 15°. This exercise was not meant to simulate range rate corrections but rather to check for numerical stability in successive calculations of the range corrections.

The heights at which δ was computed were HM-0.75YM, HM-0.58YM, HM-0.5YM, HM -0.33YM, HM, HM+150 km, $\frac{H0+H1}{2}$, H1, $\frac{H1+H2}{2}$, H2, 650 km, 850 km, 1500 km, and 3000 km. The quantities YM, H0, H1, and H2 are profile parameters as defined in figure 1. In early tests, only one point was used below HM and the highest point taken was at 1500 km. This proved to be inadequate to properly define the slopes of δ at the end points, and since the spline interpolation exhibited a marked dependence on the slopes of δ at these points, additional heights had to be included. Therefore the points at HM - 0.75YM and at 3000 km were added into the calculation of δ, for the sole purpose of allowing more accurate calculations of the first and second derivatives at HM-0.58YM and at 1500 km.

The combination of points marked 1, 2, 13, 9 and 10 in Tables 1, 2 and 3, was the smallest number of points which still provided a consistently accurate set of range and range difference corrections at all elevations and all azimuths. The apparently large relative errors in the range differences seen in Tables 1b, 1c, and 1d can be ascribed to the small absolute value of these quantities,

in that particular azimuthal direction. In other words, percentage errors can sometimes be deceiving.

The combination 1, 2, 13, 9, 10 corresponded to the seven heights HM-0.75YM, HM-0.58YM, HM, HM+150, 850, 1500, and 3000. It should be noted that this deviation function, derived at a combination of heights which are not tied to the reference profile parameters, proved to be numerically more stable than the deviation functions whose defining heights were dependent on the reference profile. Furthermore it became evident in the course of this study that the points which most affected the accuracy of δ were the three points HM-.58YM, HM, and HM+150. This indicates that great care must be taken to properly define the gradients along that portion of ray path which traverses the ionosphere within $\pm$ 150 km of the peak density.

The optimum number of points needed for ground tracking at low elevation angles is seven. Since SST ray paths may be as much as 20% longer than such low angle cases, the optimum number of points for the longest SST ray paths was therefore set to nine. This seems a reasonable first guess at the optimum number of points to use in defining deviation functions in SST geometries. Further work must be done in this area to properly define the point function NOPF.

B. Optimizing the Quadrature Integration

The initial evaluations of Gaussian quadrature integration of the Bent ionospheric profile (fig. 1) were performed assuming a homogeneous ionosphere with no gradients (ref. 8). Under these assumptions, integration errors of less than 0.01% at all elevations were achieved using 3-point Gaussian quadrature in the bottomside bi-parabolic layer and 2 quadrature points in each of the six topside layers (a total of 15 points). Increasing the number of quadrature points to 4 and 3, respectively, was sufficient to cut the errors to less than 0.00001%.

In an attempt to reduce the total number of quadrature points, the integration limits were modified by merging several layers. Thus, instead of integrating through 7 distinct profile layers, the number of integration layers was reduced to 3. The integration tests were again repeated using 4 and 5 layers. The fewer the number of layers, the more quadrature points were required to obtain accurate integrations. In fact, it took from 25 to 30 quadrature points in these tests to achieve the 0.01% accuracies obtained when integrating thru the seven analytic layers of the profile. Hence, it was resolved that all quadrature integration of the Bent ionospheric profile would be carried out between the limits of the ionospheric layers. As expected, in the presence of gradients, more quadrature points are required to maintain integration accuracy. The results of the numerical integrations listed in Tables 1,2, and 3 were all obtained using 4 quadrature points in the bottomside and 3 points in each of the topside layers. The range corrections are found to agree with ray trace results to within 1% relative accuracy. Increasing the number of quadrature points to 6 and 5, respectively, had little or no effect on the range corrections. The changes that were noted were in no case larger than 0.05% in the range and they provided no net improvement to the corrections. However, the increased number of points did add some numerical stability to the calculations, for the range difference error were reduced by as much as a factor of 2 ! The number of quadrature points used in the GTDS formulation of the SST refraction correction algorithm has been left at 4 and 3 pending evaluations using real range rate data, at which time these numbers may be increased as necessary.

One can conclude from these comparisons that in the present formulation, it is the spline function and not the quadrature integration which sets the limit on the accuracy of the refraction corrections.

VI. CONCLUSIONS

Comparison of the refraction correction algorithm against ray trace calculations confirms the hypothesis that electron density variations in the ionosphere can be represented as the product of a reference profile and a gradient function. The reference profile represents the basic vertical distribution of electrons while the gradient function modifies the vertical distribution to fit the actual density along a particular line of sight. The gradient function is computed, in tabular form at specified points, as the deviation of the electron density from the reference profile density. Up to twenty two such points may be used to specify the deviations. Values of the deviations at points between table entries are obtained by interpolation using a cubic spline. The reference profile for any integration path is defined at the point at which maximum electron density is encountered.

Integration of the reference profile and deviation function proceeds in layers corresponding to the layers over which the reference profile maintains its analytical form. The integration is performed by Gaussian quadrature using 4 quadrature points in the bottomside layer of the ionosphere and 3 quadrature points in each of the topside layers.

The refraction correction algorithm has been successfully implemented into the GTDS, and it was used to correct SST range and range rate observations of the GEOS-3 satellite as relayed from ATS-6. At S-band, computed corrections for this orbit varied from 0.5 to 10 meter for range measurements and 0.1 to 1 cm/sec for range rates. The accuracy of these values is not known at present, and in light of certain inconsistencies which have been noted in some range correction calculations, not much more can be said about the GEOS refraction corrections at this time.

Ground tracking of a satellite, at low elevation angles and through regions of large electron density gradients was used to simulate SST geometries.

Comparison of algorithm calculations with ray trace results at these low elevations indicates that errors of less than 1% can be achieved for range corrections and error levels of 2% to 4% can be achieved for range differences. The limiting factor in achieving or improving these error levels is the deviation function. From ground based results it is expected that 22 points, properly distributed, should suffice to attain these accuracies for the worst case SST configurations. Confirmation of this will have to await further evalution studies.

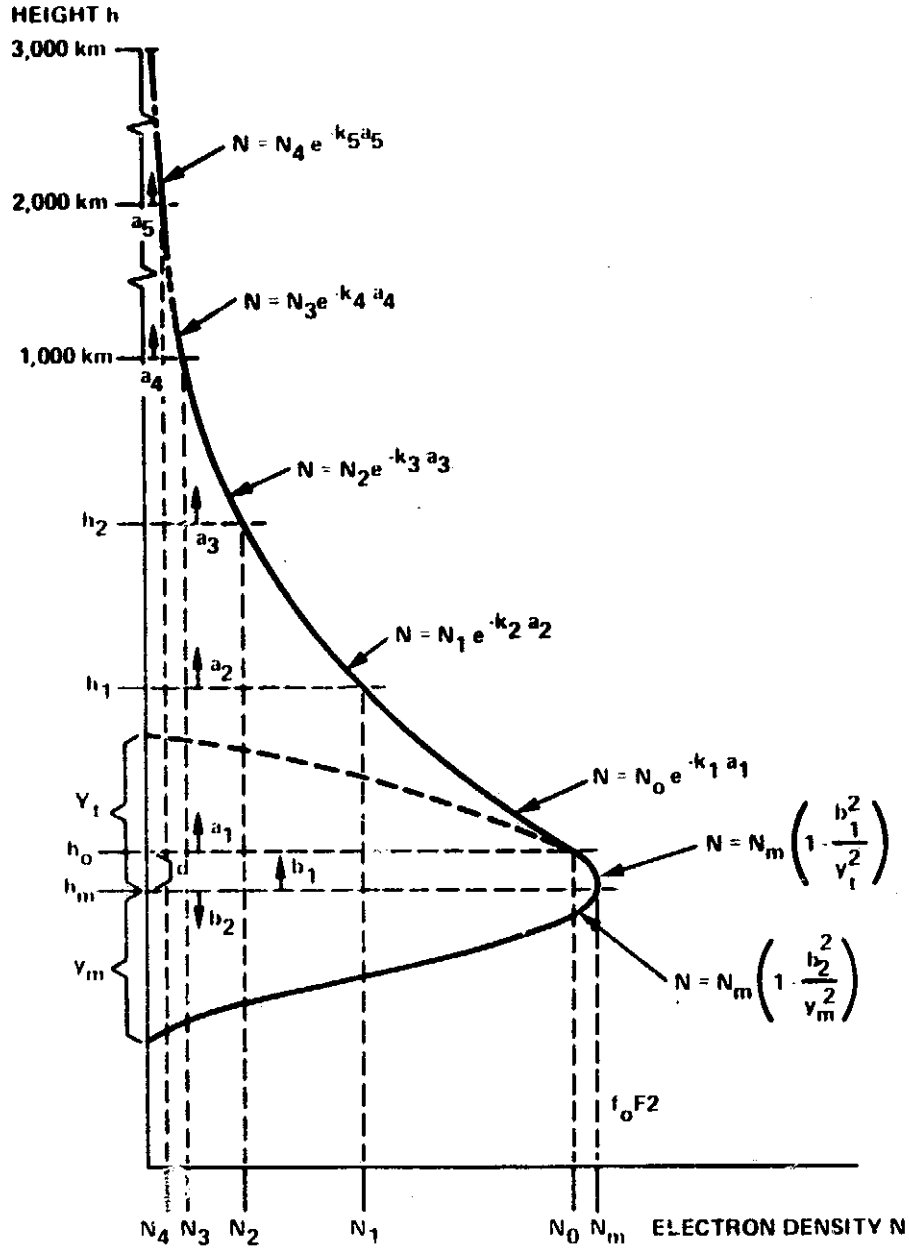

Figure 1. The electron density profile of the Bent Ionospheric Model.

ORIGINAL PAGE IS
OF POOR QUALITY

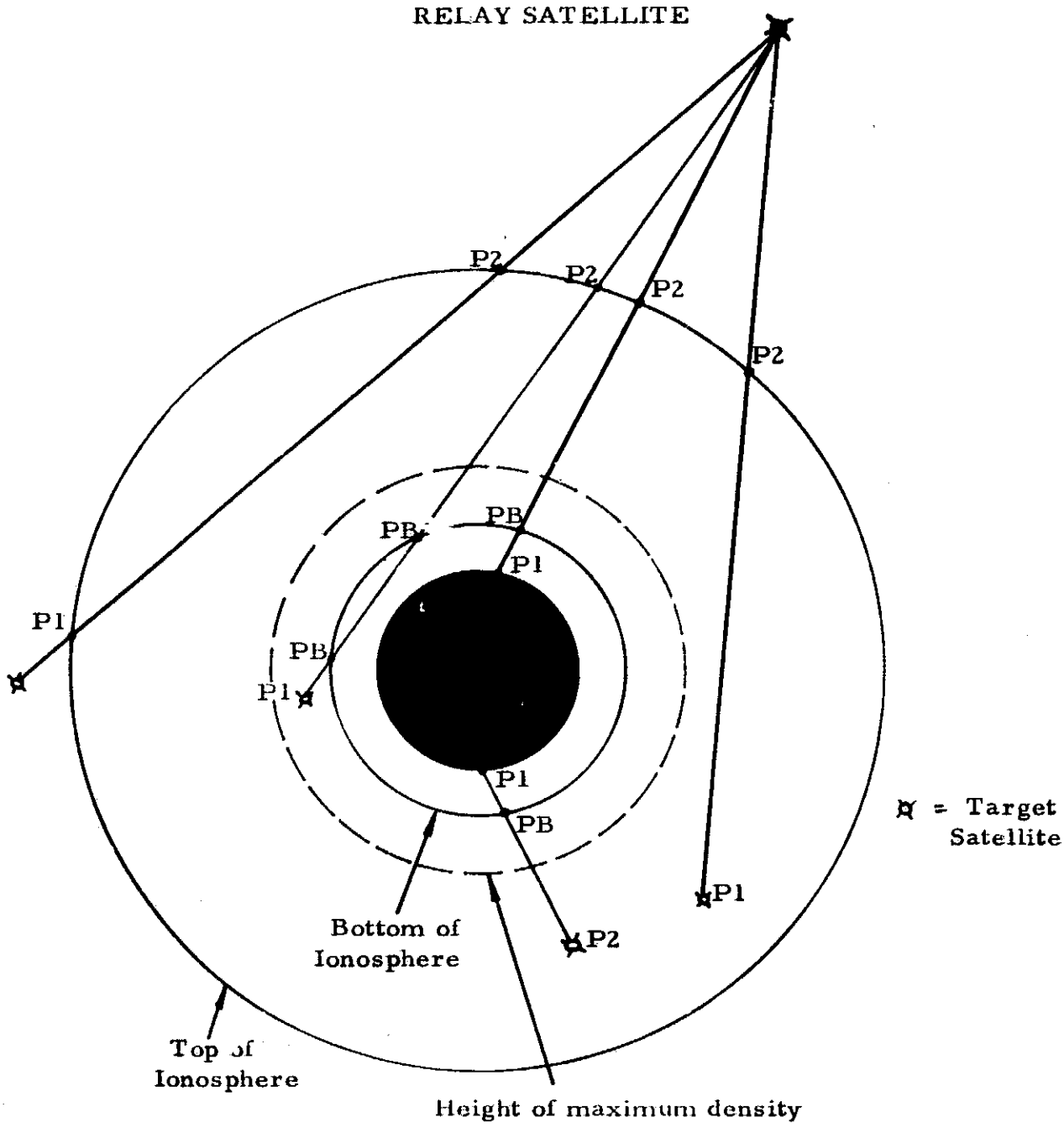

Figure 2. Example of 3 types of SST configurations and 2 types of ground track configurations. (P1, P2), (P1, PB), and (PB, P2) are those segments of the ray paths for which ionospheric refraction needs to be computed.

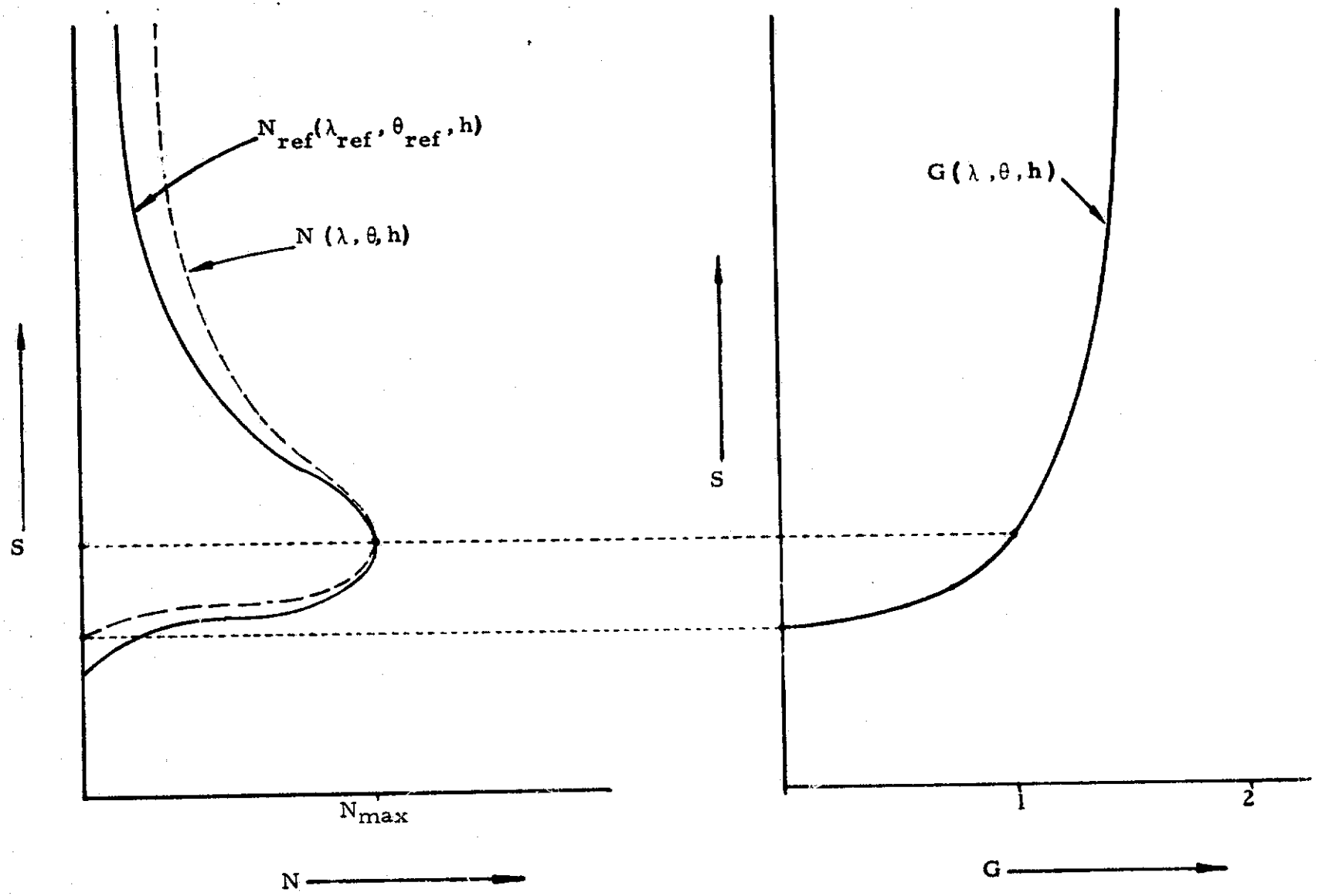

Figure 5. A hypothetical situation showing the relationship between the profiles N and N_{ref}, and the corresponding gradient function $G = N / N_{ref}$.

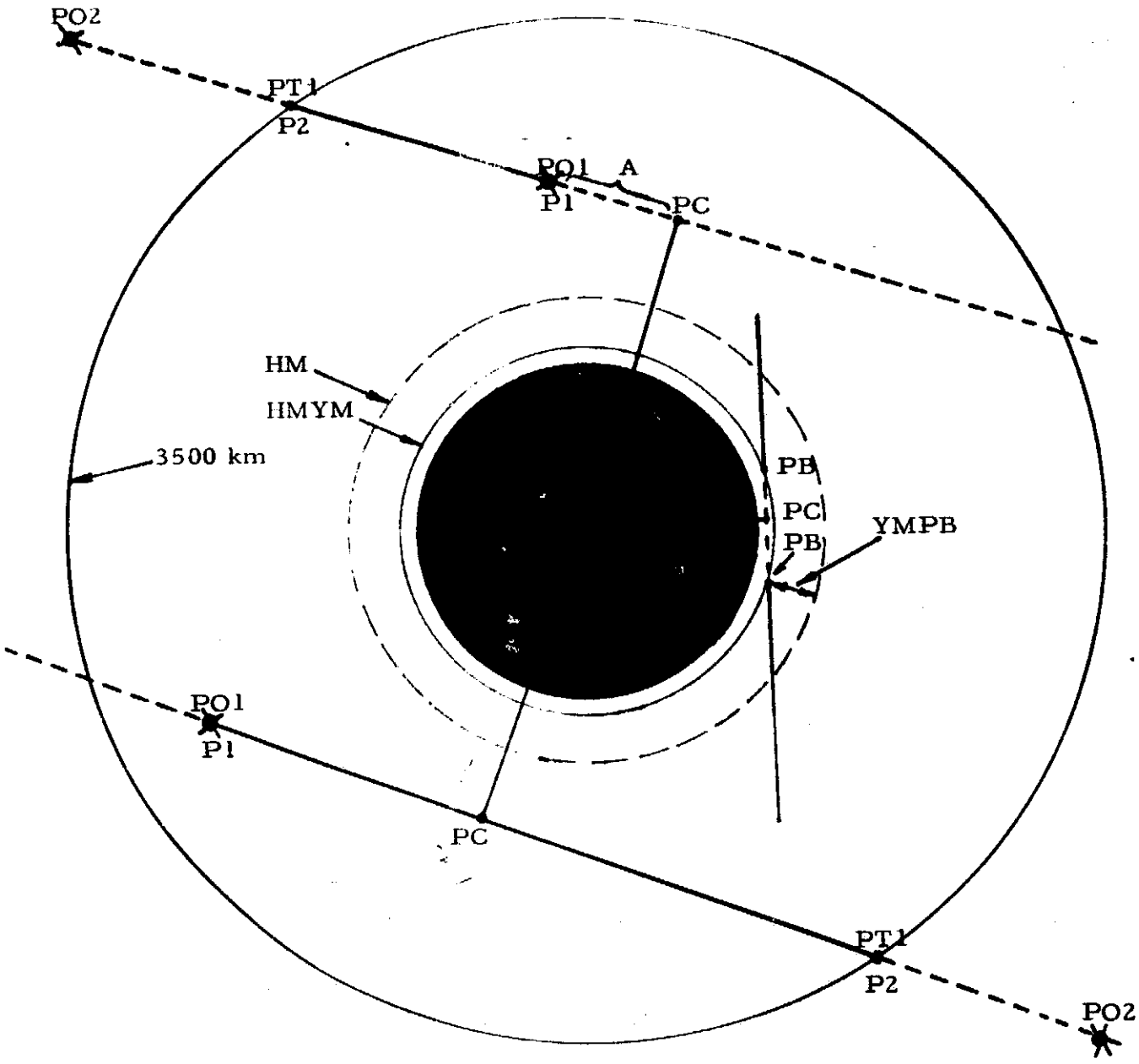

Figure 3. Definitions of some of the important points and parameters used in obtaining satellite-to-satellite ionospheric refraction corrections. Further explanations and definitions can be found in the glossary (Appendix H).

Fig. 4.a. World Map of Ionospheric Critical Frequency fOF2 in MHz at 12 h U.T. on 15 January 1969. Contours are Plotted Every 1.0 MHz.

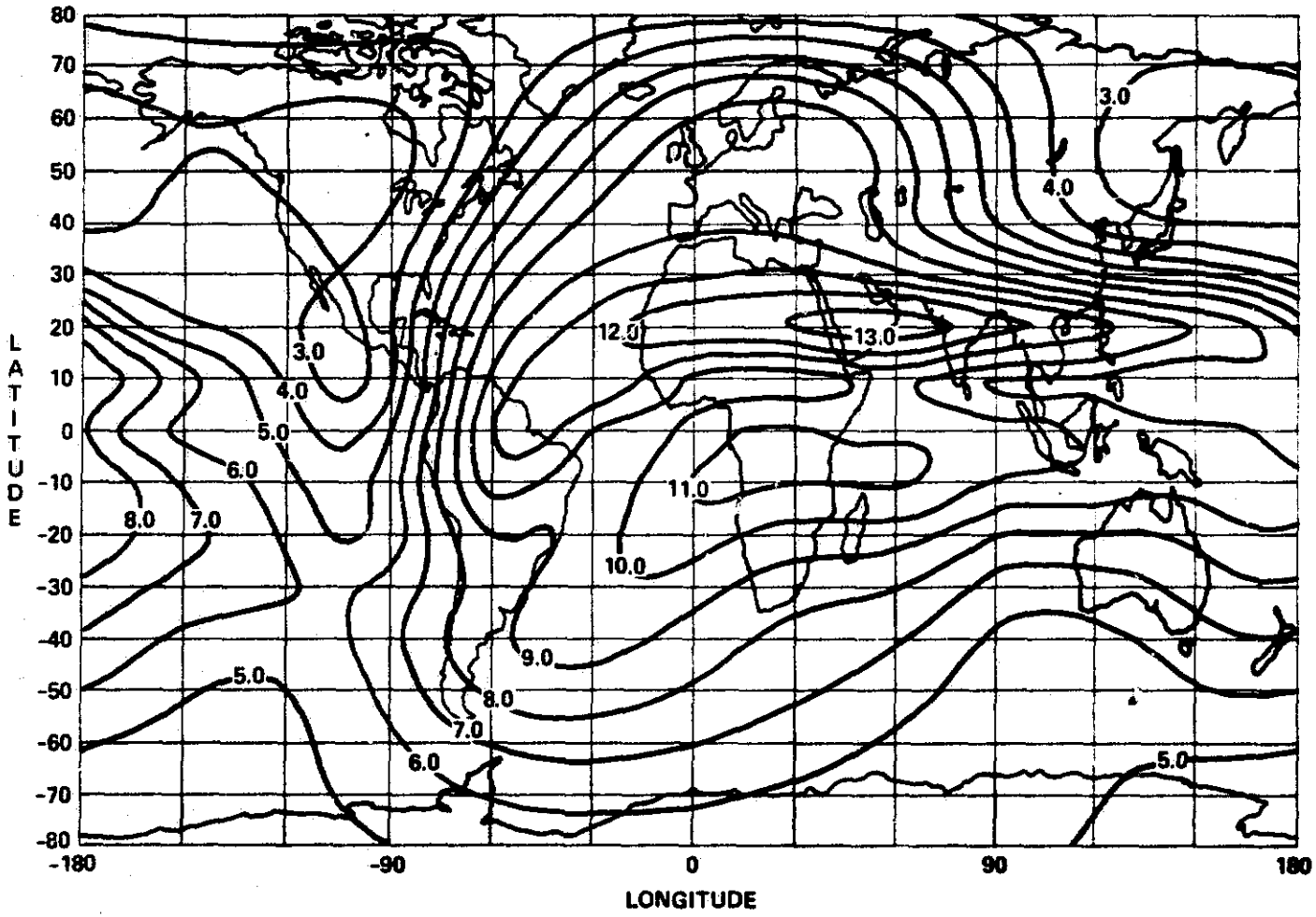

ORIGINAL PAGE IS
OF POOR QUALITY

Fig. 4.b. World Map of Height of Maximum Ionospheric Electron Density Hmax at 12 h U.T. on 15 January 1969. Contours Every 20 km.

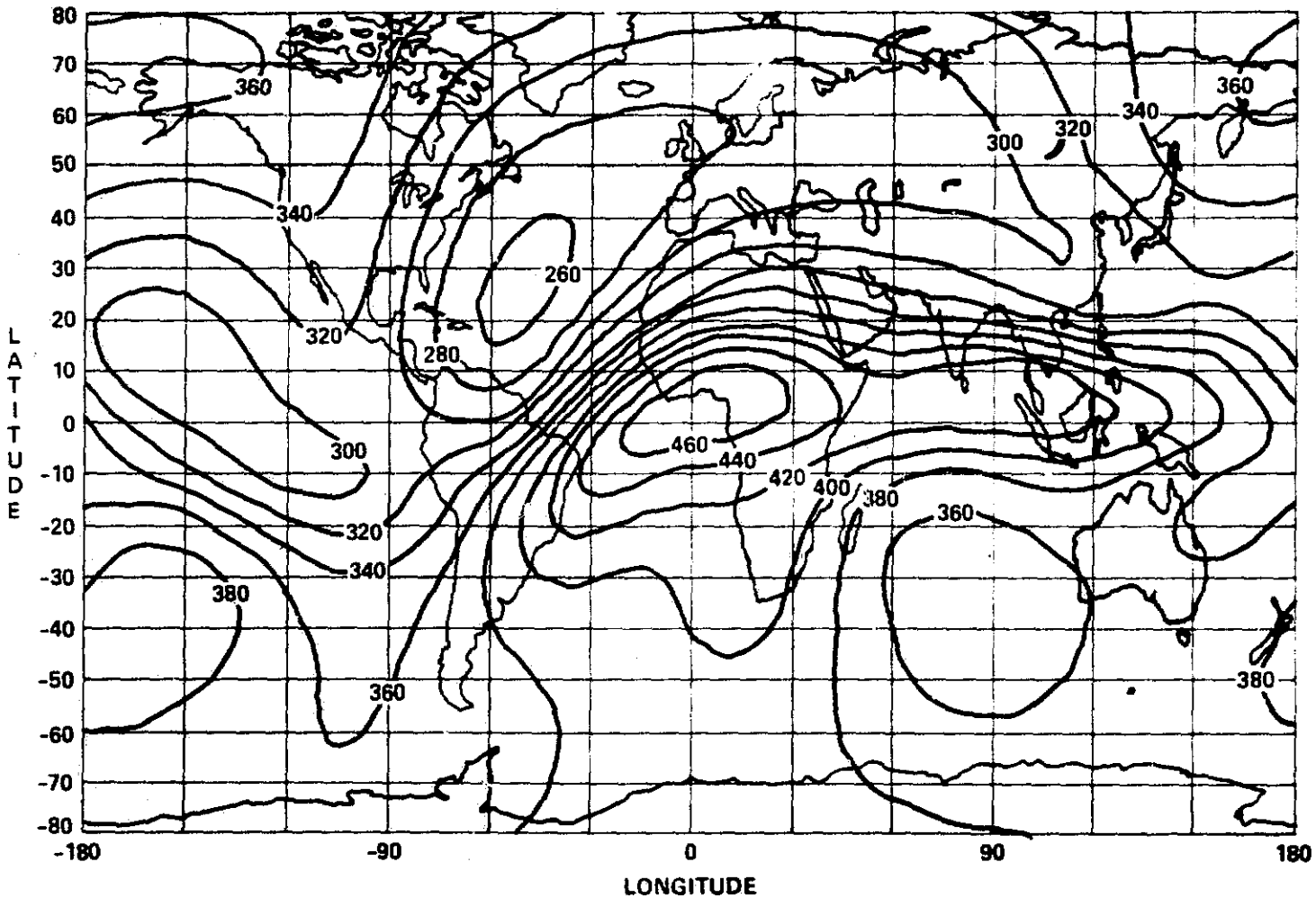

ORIGINAL PAGE IS
OF POOR QUALITY

Fig. 4.c. World Map of Integrated Vertical Electron Content N_T as Predicted by Bent Ionospheric Model in Units of 10^{17} el/sq. meter at 12 h U.T. on 15 January 1969. Contours Every 5 x 10^{16} el/sq.m.

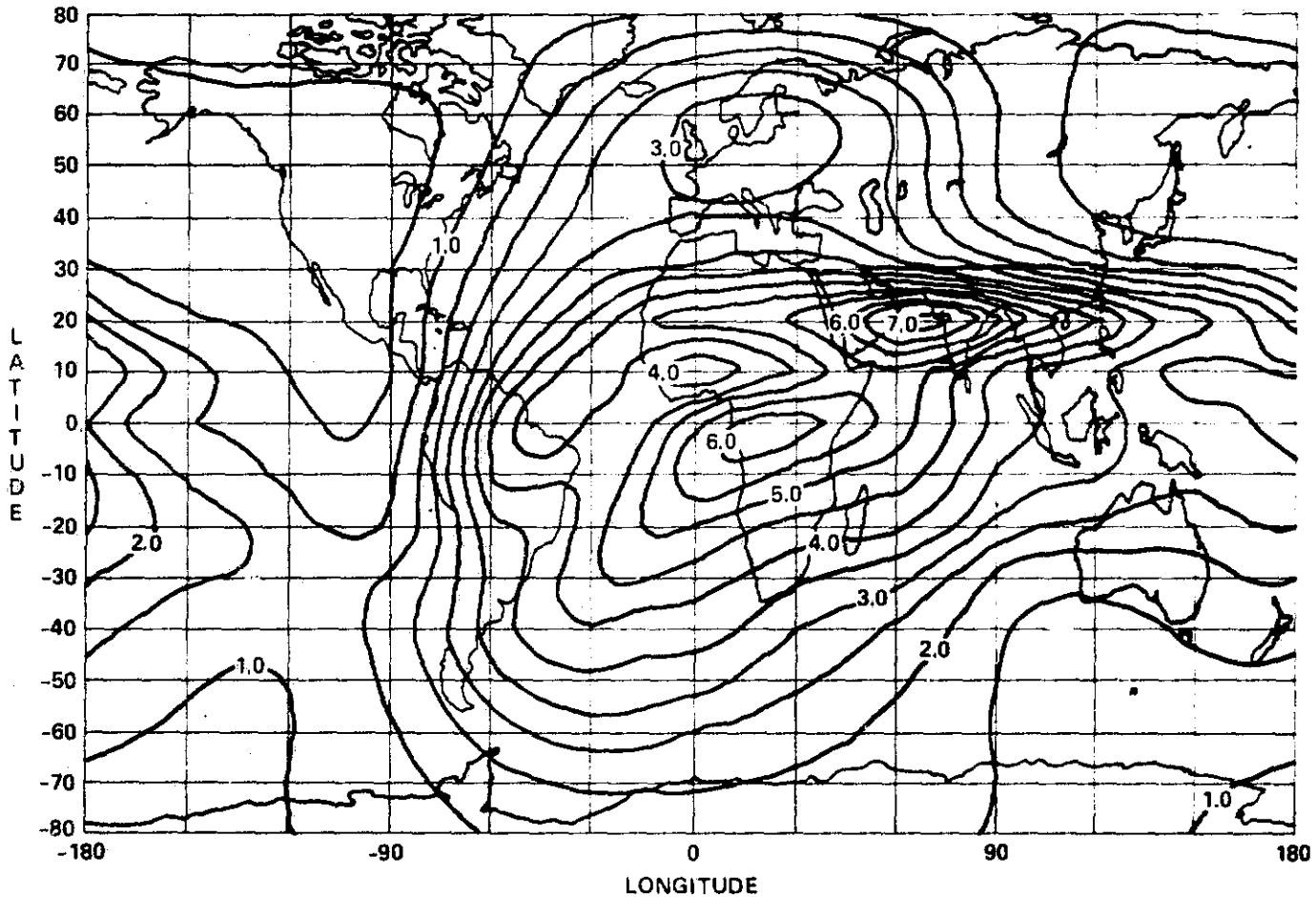

ORIGINAL PAGE IS OF POOR QUALITY

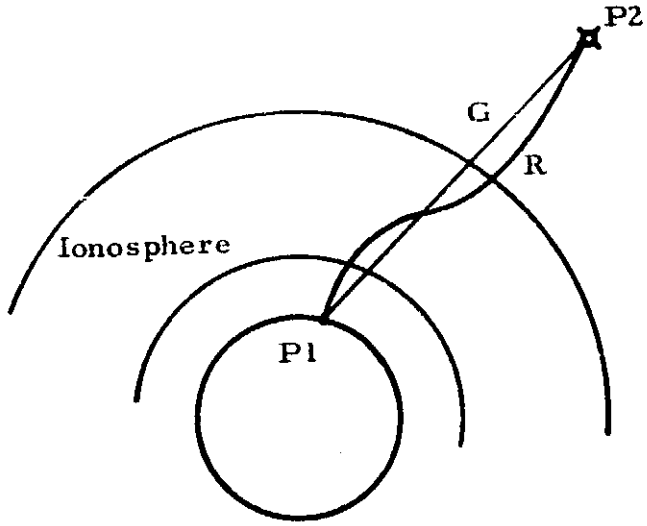

Figure 6. Radio propagation through the ionosphere. R is the radio path, G is the straight line or in vacuo path

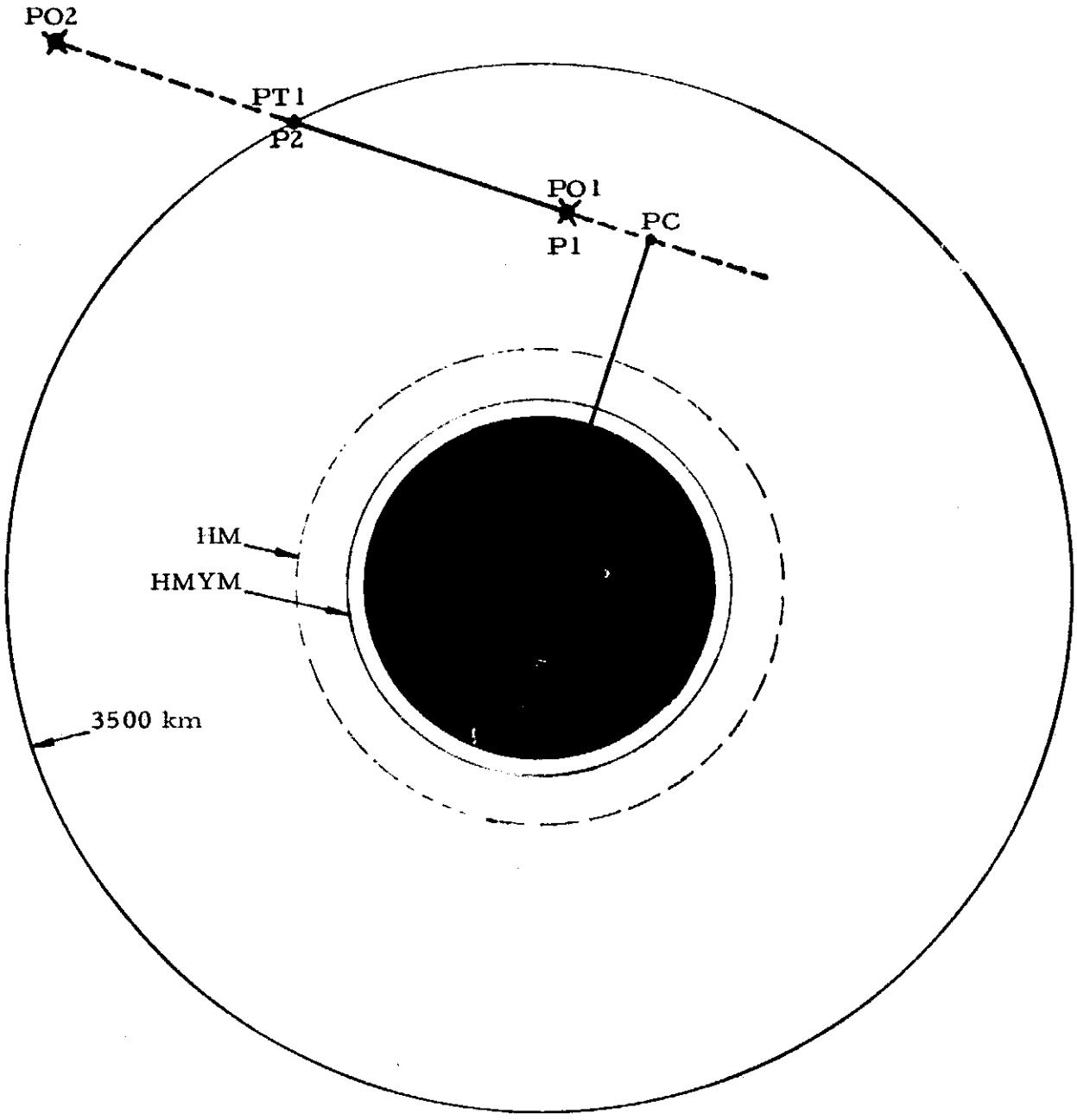

CASE 1

Figure 7. Target satellite in the ionosphere above maximum density layer HM; single integration path from P1 to P2; reference profile at P1.

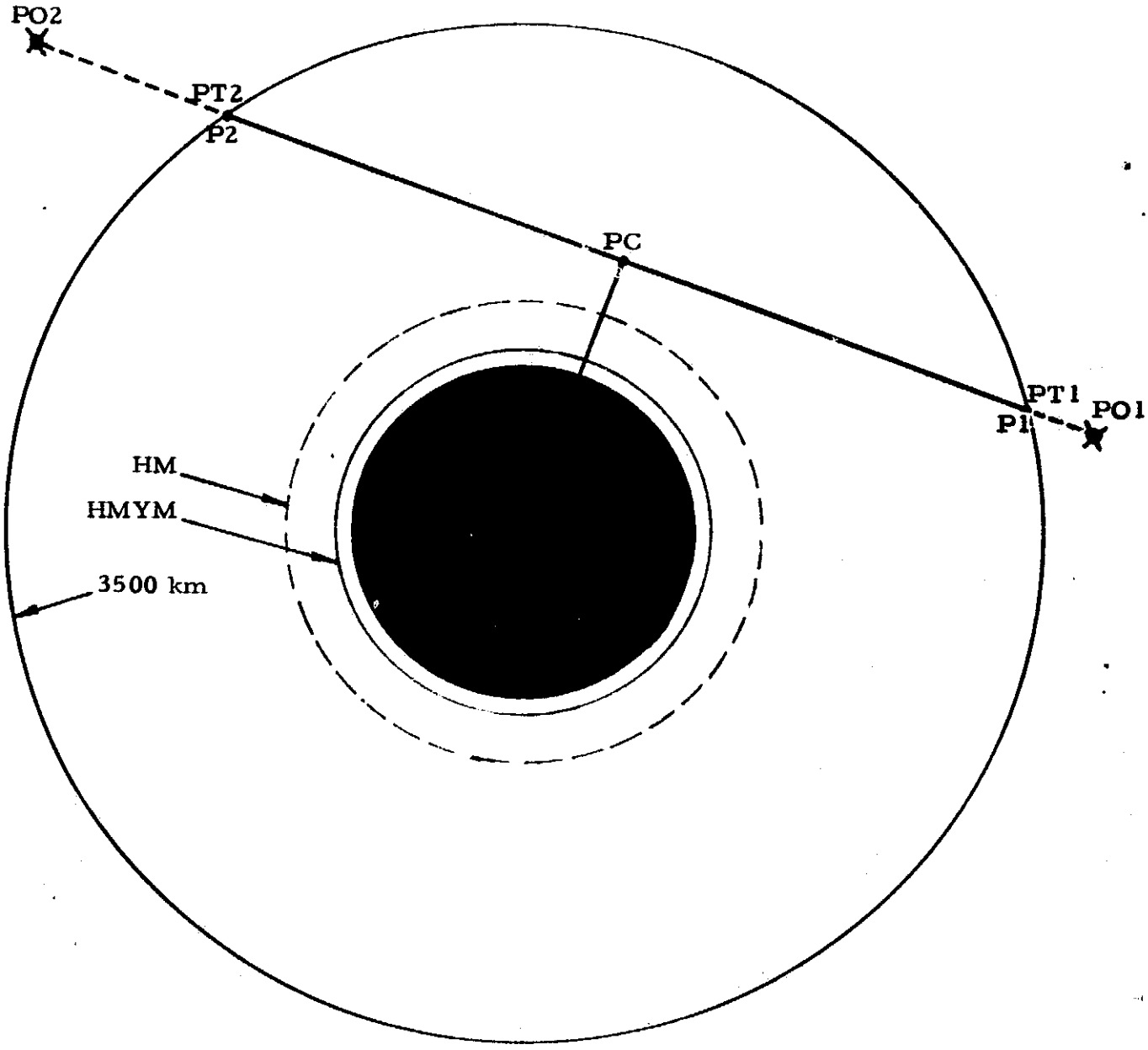

CASE 2

Figure 8. Target satellite above the ionosphere; single integration path from P1 to P2; reference profile at PC.

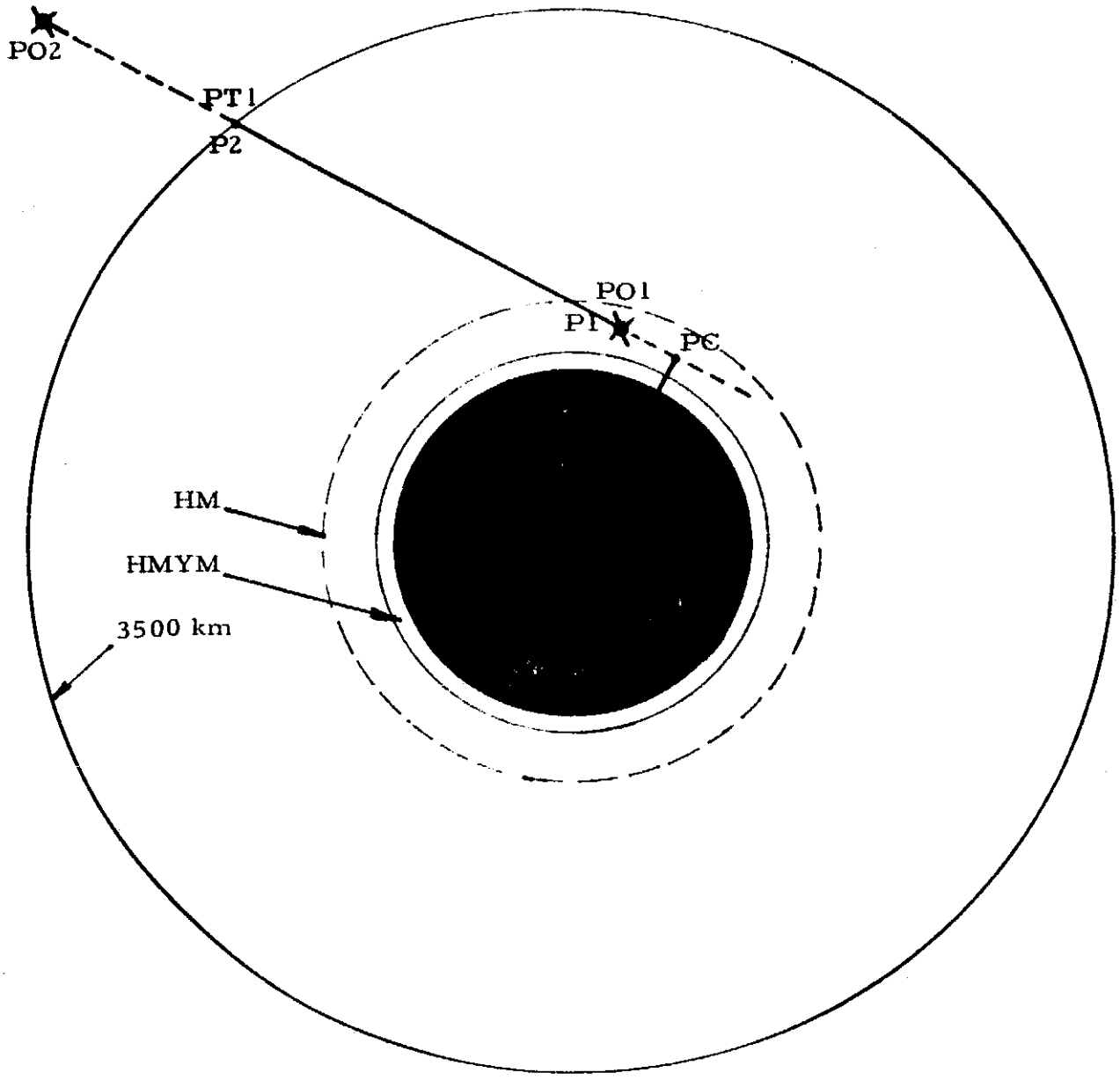

CASE 3

Figure 9. Target satellite in the lowest layer of the ionosphere (below height of maximum density HM); single integration path from P1 to P2; reference profile at HM.

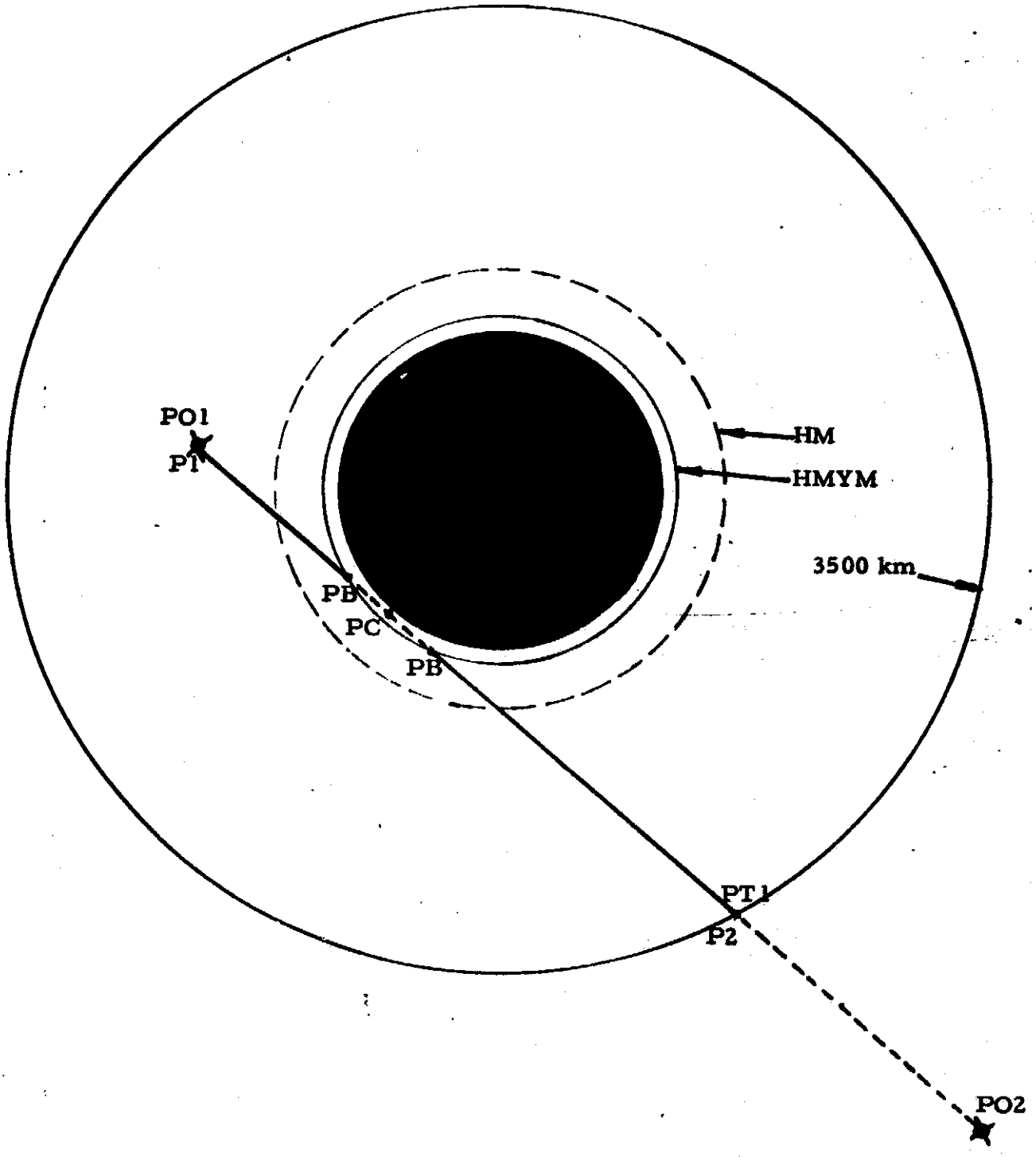

CASE 4

Figure 10. Target satellite near occultation so that ray path exits and reenters the ionosphere through the bottom (HMYM); two integration paths (PB, P1) and (PB, P2); two reference profiles at HM along each path.

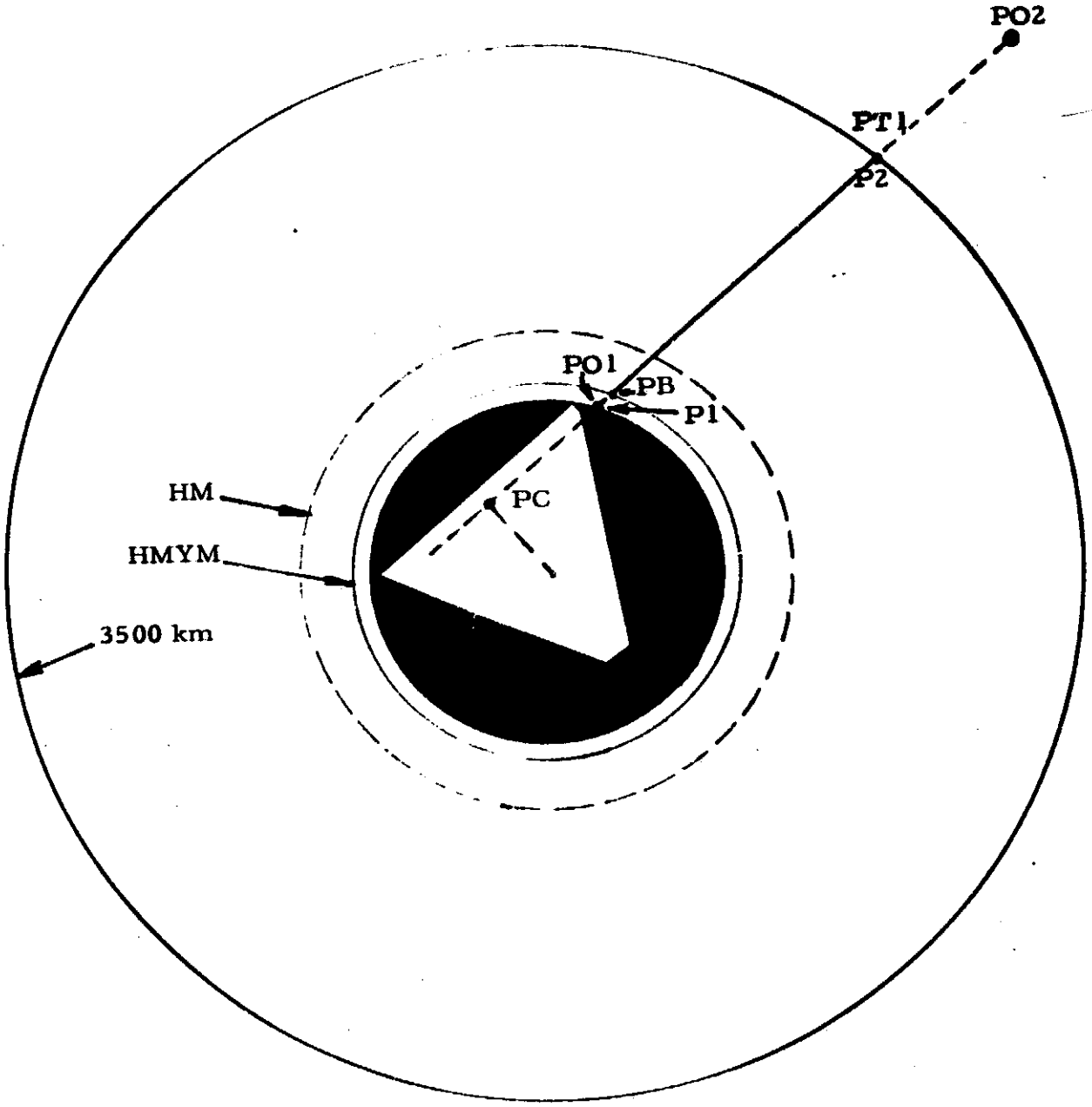

CASE 5

Figure 11. Ground tracking configuration; single integration path PB to P2; reference profile at HM.

AZIMUTH = 0 ELEVATION = 0

FREQUENCY = 2000.0 MHZ SATELLITE RANGE = 5000000. METERS

NORMAL PROFILE PARAMETERS ARE

FOF2 = 2.32 MHZ RHM = 0.346013C3D 06 YM = 81129. METERS YT = 81129. METERS D = 17452. METERS

DECAY CONSTANTS 0.55605255880-C5 0.5221329591D-C5 0.2425628.51D-05 0.14388754430-05 0.86463051010-06

HEIGHTS 0.36346547520-06 0.57964365280-06 0.79582182640-06 0.10000000000-07 0.20000000000-07 0.39000000000-07

	RANGE DIFFERENCE	PERC.DIFF.	RANGE CORRECTION	PERC.DIFF.	ANGLE CORRECTION	PERC.DIFF.
RAY-TRACE	0.59858698700 00		0.59858698700 00		0.57350572430-C3	
ANALYTIC	0.51909656920 00	-13.280	0.51909656920 00	-13.280	0.57C9785761D-C3	-0.441
NUMERICAL(QUADRATURE)	0.48326461410 00	-19.266	0.48326461410 00	-19.266	0.51055564570-C3	-10.969
NUMERICAL(LEAST SQUARE)	0.55668700150 00	-0.317	0.59668709150 00	-0.317	0.56859200240-C3	-0.857
NUMERICAL(SPLINE)						
1 2 11 6	0.59917329540 00	0.098	0.59917329540 00	0.098	0.57277414C90-C3	-0.127
1 7 2 13 9 10	0.55839973C60 00	-0.031	0.59839973060 00	-0.031	0.57267781650-C3	-0.144
1 2 13 8 9 10	0.59936293220 00	0.133	0.59936293220 00	0.133	0.57405744420-C3	0.096
1 2 13 9 10	0.59943369200 00	0.141	0.59943369200 00	0.141	0.57410579200-C3	0.105
1 7 2 13 8 9 10	0.59770579680 00	-0.147	0.59770579680 00	-0.147	0.57207166650-C3	-0.250
1 2 3 12 10	0.59541213320 00	-0.530	0.59541213320 00	-0.530	0.57129485700-C3	-0.386
ALL POINTS 15	0.59922056150 00	0.106	0.59922056150 00	0.106	0.57371885560-C3	0.037

Table 1a. Azimuth = 0°, Elevation = 0°

Comparison of ray trace refraction corrections vs. homogeneous ionosphere modified by a density gradient function. Test case at Kashima, Japan. 12^h U.T. on 15 January 1969.

ORIGINAL PAGE IS OF POOR QUALITY

AZIMUTH = 0 ELEVATION = 10

FREQUENCY = 2000.0 MHZ SATELLITE RANGE = 5000000. METERS

NORMAL PROFILE PARAMETERS ARE

FOF2 = 2.44 MHZ RHM = 0.33556236D 06 YM = 8217C. METERS YT = 82170. METERS D = 20493. METERS

DECAY CONSTANTS 0.64729929560-05 0.49907585550-05 0.22883053940-05 0.12415978390-05 0.75770158490-06

HEIGHTS 0.36005540970-06 0.57337027310-06 0.79468513660-06 0.10000000000-07 0.20000000000-07 0.25000000000-07

	RANGE DIFFERENCE	PERC.DIFF.	RANGE CORRECTION	PERC.DIFF.	ANGLE CORRECTION	PERC.DIFF.
RAY-TRACE	-0.53006687670-02		0.48757762420 00		0.46453667390-03	
ANALYTIC	0.13570741830-02	-125.602	0.50221233090 00	3.002	0.52467113410-03	12.945
NUMERICAL(QUADRATURE)	0.16627424270-02	-131.369	0.46725613310 00	-4.166	0.45591821040-03	-1.856
NUMERICAL(LEAST SQUARE)	-0.81459083810-02	53.677	0.49339715710 00	1.194	0.46870607100-03	0.897
NUMERICAL(SPLINE)						
1 2 11 6	-0.57652487990-02	9.142	0.48357783630 00	-0.820	0.46103383610-03	-0.754
1 7 2 13 9 10	-0.67277456250-02	26.923	0.48292817150 00	-0.954	0.45952625880-03	-1.079
1 2 13 8 9 10	-0.54109333000-02	5.853	0.49054158670 00	0.660	0.46745053720-03	0.635
1 2 13 9 10	-0.56225872430-02	6.073	0.48795295430 00	0.077	0.46570558860-03	0.251
1 7 2 13 8 9 10	-0.67714031080-02	27.746	0.48323144500 00	-0.891	0.45970746430-03	-1.040
1 2 3 12 10	-0.60144905150-02	13.467	0.48080163250 00	-1.390	0.45631384840-03	-1.771
ALL POINTS 15	-0.60531816270-02	14.197	0.48732475520 00	-0.052	0.46391440070-03	-0.121

Table 1b. Azimuth = 0°, Elevation = 10°

Comparison of ray trace refraction corrections vs. homogeneous ionosphere modified by a density gradient function. Test case at Kashima, Japan. 12^h U.T. on 15 January 1969.

ORIGINAL PAGE IS OF POOR QUALITY

AZIMUTH = 0 ELEVATION = 30

FREQUENCY = 2000.0 MHZ SATELLITE RANGE = 5000000. METERS

NORMAL PROFILE PARAMETERS ARE

FOF2 = 3.03 MHZ RHM = 0.33132280D 06 YM = 87178. METERS YT = 87178. METERS D = 25156. METERS

DECAY CONSTANTS 0.72212222220-05 0.48656455590-05 0.23628855660-05 0.10792725270-05 0.66971759270-06

HEIGHTS 0.35647840210-06 0.57495560140-06 0.79349280070-06 0.10000000000-07 0.20000000000-07 0.30000000000-07

	RANGE DIFFERENCE	PERC.DIFF.	RANGE CORRECTION	PERC.DIFF.	ANGLE CORRECTION	PERC.DIFF.
RAY-TRACE	-0.11106000860-01		0.42443562460 00		0.21047644510-03	
ANALYTIC	-0.65584454750-02	-40.947	0.49903949260 00	17.577	0.26135500800-03	24.173
NUMERICAL(QUADRATURE)	-0.15173709330-02	-82.195	0.48036866230 00	13.178	0.23096755850-03	9.736
NUMERICAL(LEAST SQUARE)	-0.15755243160-02	-85.814	0.44220859730 00	4.187	0.21687467540-03	3.990
NUMERICAL(SPLINE)						
1 2 11 6	-0.87993115340-02	-20.770	0.42627157950 00	0.433	0.21033874470-03	-0.065
1 7 2 13 9 10	-0.95665457200-02	-13.862	0.42170439040 00	-0.643	0.20901503900-03	-0.694
1 2 13 8 9 10	-0.71318247360-02	-35.784	0.42767056840 00	0.762	0.21198176440-03	0.715
1 2 13 9 10	-0.81410941350-02	-26.696	0.42556507460 00	0.266	0.21152301500-03	0.497
1 7 2 13 8 9 10	-0.96086422030-02	-13.482	0.42147473630 00	-0.698	0.20921410740-03	-0.600
1 2 3 12 10	-0.15340652220-01	38.130	0.41632194290 00	-1.912	0.20587034580-03	-2.188
ALL POINTS 15	-0.10183591280-01	-8.306	0.42447611370 00	0.010	0.21033874470-03	-0.065

Table 1c. Azimuth = 0° , Elevation = 30°

Comparison of ray trace refraction corrections vs. homogeneous ionosphere modified by a density gradient function. Test case at Kashima, Japan. 12^h U.T. on 15 January 1969.

ORIGINAL PAGE IS OF POOR QUALITY

AZIMUTH = 0 ELEVATION = 60

FREQUENCY = 2060.0 MHZ SATELLITE RANGE = 5000000. METERS

NORMAL PROFILE PARAMETERS ARE

FOF2 = 3.57 MHZ RHM = 0.326742E5D 06 YM = 55544. METERS YT = 95544. METERS D = 30800. METERS

DECAY CONSTANTS 0.75305870310-05 0.48735103490-05 0.25374332990-05 0.10233727080-05 0.63108269620-06

HEIGHTS 0.35754 3450 06 0.57565516390 06 0.79384758190 06 0.10000000000 07 0.20000000000 07 0.30000000000 07

	RANGE DIFFERENCE	PERC.DIFF.	RANGE CORRECTION	PERC.DIFF.	ANGLE CORRECTION	PERC.DIFF.
RAY-TRACE	-0.91938059360-02		0.39845633830 00		0.68882704650-04	
ANALYTIC	-0.17075683820-01	85.730	0.45022919230 00	12.993	0.80934021560-04	17.495
NUMERICAL(QUADRATURE)	-0.11819780850-01	28.562	0.44711422590 00	12.212	0.74677408300-04	8.703
NUMERICAL(LEAST SQUARE)	-0.43261518370-02	-52.945	0.41450397570 00	4.027	0.72619276830-04	5.425
NUMERICAL(SPLINE)						
1 2 11 6	-0.43637611620-03	-95.254	0.40561731920 00	1.797	0.70878481830-04	2.897
1 7 2 13 9 10	0.95401782830-03	-110.377	0.40335120480 00	1.228	0.68892655040-04	0.015
1 2 13 8 9 10	-0.13579746790-02	-85.029	0.40404940760 00	1.404	0.70090918700-04	1.754
1 2 13 9 10	-0.65151235990-03	-92.914	0.40383241290 00	1.349	0.70090918700-04	1.754
1 7 2 13 8 9 10	0.11254033870-02	-112.241	0.40322906250 00	1.198	0.69454386390-04	0.888
1 2 3 12 10	0.19187632220-02	-120.870	0.40354546350 00	1.277	0.68892655040-04	0.015
ALL POINTS 14	0.29774113950-04	-100.324	0.40438824160 00	1.489	0.70878481830-04	2.897

Table 1d. Azimuth = 0°, Elevation = 60°

Comparison of ray trace refraction corrections vs. homogeneous ionosphere modified by a density gradient function. Test case at Kashima, Japan. 12^h U.T. on 15 January 1969.

ORIGINAL PAGE IS OF POOR QUALITY

AZIMUTH = 90 ELEVATION = 0

FREQUENCY = 2000.0 MHZ SATELLITE RANGE = 5000000. METERS

NORMAL PROFILE PARAMETERS ARE

FOF2 = 4.11 MHZ RHM = 0.32833592D 06 YM = 102988. METERS YT = 102988. METERS D = 35586. METERS

DECAY CONSTANTS 0.7619932385D-05 0.4854001913D-05 0.2692371742D-05 0.1040412221D-05 0.6221613534D-06

HEIGHTS 0.3639217360D 06 0.5799470265D 06 0.7959739103D 06 0.1000000000D 07 0.2000000000D 07 0.3000000000D 07

	RANGE DIFFERENCE	PERC.DIFF.	RANGE CORRECTION	PERC.DIFF.	ANGLE CORRECTION	PERC.DIFF.
RAY-TRACE	0.1464782655D 01		0.1464782655D 01		0.1736720138D-02	
ANALYTIC	0.1542558739D 01	5.310	0.1542558739D 01	5.310	0.1881769470D-02	8.352
NUMERICAL(QUADRATURE)	0.1443498537D 01	-1.453	0.1443498537D 01	-1.453	0.1725571661D-02	-0.619
NUMERICAL(LEAST SQUARE)	0.1458982899D 01	-0.396	0.1458982899D 01	-0.396	0.1729457746D-02	-0.418
NUMERICAL(SPLINE)						
1 2 11 6	0.1466913661D 01	0.145	0.1466913661D 01	0.145	0.1740673488D-02	0.193
1 7 2 13 9 10	0.1468858123D 01	0.278	0.1468858123D 01	0.278	0.1741532375D-02	0.277
1 2 13 8 9 10	0.1467631288D 01	0.194	0.1467631288D 01	0.194	0.1740225140D-02	0.202
1 2 13 9 10	0.1467946445D 01	0.216	0.1467946445D 01	0.216	0.1740424370D-02	0.213
1 7 2 13 8 9 10	0.1468968558D 01	0.286	0.1468968558D 01	0.286	0.1741622029D-02	0.282
1 2 3 12 10	0.1466370267D 01	0.108	0.1466370267D 01	0.108	0.1738516670D-02	0.126
ALL POINTS 15	0.1465678841D 01	0.061	0.1465678841D 01	0.061	0.1737950136D-02	0.071

Table 2a. Azimuth = 90°, Elevation = 0°

Comparison of ray trace refraction corrections vs. homogeneous ionosphere modified by a density gradient function. Test case at Kashima, Japan. 12^h U.T. on 15 January 1969.

ORIGINAL PAGE IS OF POOR QUALITY

AZIMUTH = 90 ELEVATION = 10

FREQUENCY = 2000.0 MHZ SATELLITE RANGE = 5000000. METERS

NORMAL PROFILE PARAMETERS ARE

FOF2 = 3.95 MHZ RHM = 0.32586648D 06 YM = 102896. METERS YT = 102896. METERS D = 35512. METERS

DECAY CONSTANTS 0.76153627210-05 0.48320645840-05 0.26305290110-05 0.10297808900-05 0.62182458360-06

HEIGHTS 0.36537881580-06 0.58091921320-06 0.75645960660-06 0.10000000000-07 0.20000000000-07 0.35000000000-07

	RANGE DIFFERENCE	PERC.DIFF.	RANGE CORRECTION	PERC.DIFF.	ANGLE CORRECTION	PERC.DIFF.
RAY-TRACE	-0.27112455580-01		0.12414575390 01		0.12038551340-02	
ANALYTIC	-0.32068932120-01	18.358	0.12877236800 01	3.727	0.14127935370-02	10.043
NUMERICAL(QUADRATURE)	-0.29435474520-01	8.568	0.12077013550 01	-2.719	0.12613355060-02	-1.754
NUMERICAL(LEAST SQUARE)	-0.29942066760-01	10.436	0.12356[illegible]5169D 01	-0.471	0.12756017550-02	-0.628
NUMERICAL(SPLINE)						
1 2 11 6	-0.26662303000-01	-1.660	0.12439191920 01	0.198	0.12047553570-02	0.070
1 7 2 13 9 10	-0.25167728140-01	7.580	0.12401556540 01	-0.057	0.12034801000-02	-0.030
1 2 13 8 9 10	-0.28354271170-01	4.580	0.12405629640 01	-0.072	0.12032205710-02	-0.050
1 2 13 9 10	-0.29096523830-01	7.318	0.12405462760 01	-0.073	0.12031985410-02	-0.051
1 7 2 13 8 9 10	-0.28428145300-01	4.853	0.12409411160 01	-0.042	0.12035882220-02	-0.021
1 2 3 12 10	-0.26901524750-01	-0.778	0.12419746280 01	0.042	0.12046473330-02	0.061
ALL POINTS 15	-0.27508120060-01	1.459	0.12414543160 01	-0.000	0.12039995020-02	0.011

Table 2b. Azimuth = 90°, Elevation = 10°

Comparison of ray trace refraction corrections vs. homogeneous ionosphere modified by a density gradient function. Test case at Kashima, Japan. 12^h U.T. on 15 January 1969.

ORIGINAL PAGE IS OF POOR QUALITY

AZIMUTH = 90 ELEVATION = 20

FREQUENCY = 2000.0 MHZ SATELLITE RANGE = 5000000. METERS

NORMAL PROFILE PARAMETERS ARE

FOF2 = 3.91 MHZ RHM = 0.328801870 06 YM = 100472. METERS YT = 100472. METERS D = 34064. METERS

DECAY CONSTANTS 0.762535531OD-05 0.490387776OD-05 0.266923513OD-05 0.102277947OD-05 0.619224704OD-06

HEIGHTS 0.362865405OD 06 0.579243603OD 06 0.795621801OD 06 0.100000000OD 07 0.200000000OD 07 0.300000000OD 07

	RANGE DIFFERENCE	PERC.DIFF.	RANGE CORRECTION	PERC.DIFF.	ANGLE CORRECTION	PERC.DIFF.
RAY-TRACE	-0.120914530OD 00		0.982861467OD 00		0.700256019D-03	
ANALYTIC	-0.139395338OD 00	15.284	0.100368633OD 01	2.119	0.777613382D-03	11.047
NUMERICAL(QUADRATURE)	-0.123754801OD 00	2.349	0.954224720OD 00	-2.914	0.686202113D-03	-2.007
NUMERICAL(LEAST SQUARE)	-0.119601565OD 00	-1.081	0.982832903OD 00	-0.003	0.695382548D-03	-0.125
NUMERICAL(SPLINE)						
1 2 11 6	-0.120230213OD 00	-0.566	0.982401929OD 00	-0.047	0.655856674D-03	-0.051
1 7 2 13 9 10	-0.121333261OD 00	0.346	0.982925723OD 00	0.007	0.699720156D-03	-0.077
1 2 13 8 9 10	-0.120712588OD 00	-0.167	0.983613263OD 00	0.071	0.700354297D-03	0.020
1 2 13 9 10	-0.120933765OD 00	0.016	0.983567076OD 00	0.072	0.700354576D-03	0.014
1 7 2 13 8 9 10	-0.121263103OD 00	0.288	0.982595510OD 00	-0.027	0.695640659OD-03	-0.088
1 2 3 12 10	-0.123296579OD 00	1.970	0.982211018OD 00	-0.066	0.695244034D-03	-0.145
ALL POINTS 15	-0.122326055OD 00	1.167	0.983206742OD 00	0.035	0.700176215D-03	-0.012

Table 2c. Azimuth = 90°, Elevation = 20°

Comparison of ray trace refraction corrections vs. homogeneous ionosphere modified by a density gradient function. Test case at Kashima, Japan. 12^h U.T. on 15 January 1969.

AZIMUTH = 90 ELEVATION = 45

FREQUENCY = 2000.0 MHZ SATELLITE RANGE = 5000000. METERS

NORMAL PROFILE PARAMETERS ARE

FOF2 = 3.92 MHZ RHM = 0.32652907D 06 YM = 100612. METERS YT = 100612. METERS D = 34234. METERS

DECAY CONSTANTS 0.76495388C4D-C5 0.49011234140-C5 0.26739496770-05 0.10169016050-05 0.6153648384D-C6

HEIGHTS 0.36076346290-C6 0.57784230860 C6 0.79492115430 06 0.10000000000-07 0.20000000000 C7 0.30000000000 07

	RANGE DIFFERENCE	PERC.DIFF.	RANGE CORRECTION	PERC.DIFF.	ANGLE CORRECTION	PERC.DIFF.
RAY-TRACE	-0.17C95953020 00		0.62581325670 00		0.18132667570-C3	
ANALYTIC	-0.17712463840 00	3.606	0.63006084400 00	0.679	0.19585250560-C3	8.010
NUMERICAL(QUADRATURE)	-0.16016765540 00	-6.312	0.61952735990 00	-1.004	0.18005141580-C3	-0.705
NUMERICAL(LEAST SQUARE)	-0.17125359240 00	0.172	0.62634631600 00	0.085	0.18150956740-C3	0.100
NUMERICAL(SPLINE)						
1 2 11 6	-0.17263760940 00	0.982	0.62449998330 00	-0.210	0.18112727670-C3	-0.111
1 7 2 13 9 10	-0.17027652910 00	-0.400	0.62530466930 00	-0.081	0.18150956740-C3	0.100
1 2 13 8 9 10	-0.17033027260 00	-0.368	0.62611399430 00	0.048	0.18173915500-C3	0.226
1 2 13 9 10	-0.17039821080 00	-0.328	0.62588788820 00	0.012	0.18173915500-C3	0.226
1 7 2 13 8 9 10	-0.17018206580 00	-0.455	0.62520028380 00	-0.098	0.18135658800-C3	0.016
1 2 3 12 10	-0.17006989010 00	-0.520	0.62492631960 00	-0.142	0.18135658800-C3	0.016
ALL POINTS 15	-0.17042162580 00	-0.315	0.62580060530 00	-0.002	0.18135658800-C3	0.016

Table 2d. Azimuth = 90°, Elevation = 45°

Comparison of ray trace refraction corrections vs. homogeneous ionosphere modified by a density gradient function. Test case at Kashima, Japan. 12^h U.T. on 15 January 1969.

ORIGINAL PAGE IS OF POOR QUALITY

AZIMUTH = 90 ELEVATION = 60

FREQUENCY = 2000.0 MHZ SATELLITE RANGE = 5000000. METERS

NORMAL PROFILE PARAMETERS ARE

FOF2 = 3.93 MHZ RHM = 0.32561972D 06 YM = 100838. METERS YT = 100838. METERS D = 34405. METERS

DECAY CONSTANTS 0.7658608324D-05 0.4901865315D-05 0.2680558592D-05 0.1015559779D-05 0.6139712817D-06

HEIGHTS 0.3002458010D 06 0.5773457200D 06 0.7946748600D 06 0.1000000000D 07 0.2000000000D 07 0.3000000000D 07

	RANGE DIFFERENCE	PERC.DIFF.	RANGE CORRECTION	PERC.DIFF.	ANGLE CORRECTION	PERC.DIFF.
RAY-TRACE	-0.9072771296D-01		0.5350855438D 00		0.9119181207D-04	
ANALYTIC	-0.9331436007D-01	2.851	0.5367464839D 00	0.310	0.9700072234D-04	6.370
NUMERICAL(QUADRATURE)	-0.8633624912D-01	-4.840	0.5331911108D 00	-0.354	0.9002570788D-04	-1.279
NUMERICAL(LEAST SQUARE)	-0.9096013552D-01	0.256	0.5353861805D 00	0.056	0.9155426716D-04	0.397
NUMERICAL(SPLINE)						
1 2 11 6	-0.8596321950D-01	-0.843	0.5345367638D 00	-0.103	0.9155426716D-04	0.397
1 7 2 13 9 10	-0.9142557494D-01	0.774	0.5338750944D 00	-0.226	0.9048658655D-04	-0.773
1 2 13 8 9 10	-0.9178513143D-01	1.165	0.5343288629D 00	-0.141	0.9155426716D-04	0.397
1 2 13 9 10	-0.9172556326D-01	1.100	0.5341623249D 00	-0.173	0.9155426716D-04	0.397
1 7 2 13 8 9 10	-0.9142945491D-01	0.773	0.5337708289D 00	-0.246	0.8956205309D-04	-1.787
1 2 3 12 10	-0.9154934617D-01	0.906	0.5333769734D 00	-0.319	0.9048658655D-04	-0.773
ALL POINTS 14	-0.9163135920D-01	0.996	0.5341692461D 00	-0.171	0.9109835246D-04	-0.102

Table 2e. Azimuth = 90°, Elevation = 60°

Comparison of ray trace refraction corrections vs. homogeneous ionosphere modified by a density gradient function. Test case at Kashima, Japan. 12^h U.T. on 15 January 1969.

ORIGINAL PAGE IS OF POOR QUALITY

AZIMUTH = 180 ELEVATION = 0

FREQUENCY = 2000.0 MHZ SATELLITE RANGE = 5000000. METERS

NORMAL PROFILE PARAMETERS ARE

FOF2 = 10.45 MHZ RHM = 0.33081878D 06 YM = 168534. METERS YT = 168534. METERS D = 92645. METERS

DECAY CONSTANTS 0.9348368401D-05 0.6849161858D-05 0.3228796597D-05 0.1337545455D-05 0.4512727273D-06

HEIGHTS 0.4234642127D 06 0.6196428085D 06 0.8158214042D 06 0.1000000000D 07 0.2000000000D 07 0.3000000000D 07

	RANGE DIFFERENCE	PERC.DIFF.	RANGE CORRECTION	PERC.DIFF.	ANGLE CORRECTION	PERC.DIFF.
RAY-TRACE	0.1124995592D 02		0.1124995592D 02		0.1509225659D-01	
ANALYTIC	0.1097850506D 02	-2.413	0.1097850506D 02	-2.413	0.1433461752D-01	-5.020
NUMERICAL(QUADRATURE)	0.1082624113D 02	-3.766	0.1082624113D 02	-3.766	0.1499146613D-01	-0.668
NUMERICAL(LEAST SQUARE)	0.1124277700D 02	-0.064	0.1124277700D 02	-0.064	0.1522801565D-01	0.899
NUMERICAL(SPLINE)						
1 2 11 6	0.1109687000D 02	-1.361	0.1109687000D 02	-1.361	0.1507603229D-01	-0.095
1 7 2 13 9 10	0.1124806615D 02	-0.017	0.1124806619D 02	-0.017	0.1514545440D-01	0.352
1 2 13 8 9 10	0.1124846657D 02	-0.013	0.1124846657D 02	-0.013	0.152[illegible]291D-01	0.921
1 2 13 9 10	0.1125679913D 02	0.061	0.1125679913D 02	0.061	0.1523270246D-01	0.930
1 7 2 13 8 9 10	0.1124670205D 02	-0.029	0.1124670205D 02	-0.029	0.1514530562D-01	0.351
1 2 3 12 10	0.1152597225D 02	2.453	0.1152597225D 02	2.453	0.1552755159D-01	2.884
ALL POINTS 15	0.1139575714D 02	1.296	0.1139575714D 02	1.296	0.1532017200D-01	1.510

Table 3a. Azimuth = 180°, Elevation = 0°

Comparison of ray trace refraction corrections vs. homogeneous ionosphere modified by a density gradient function. Test case at Kashima, Japan. 12^h U.T. on 15 January 1969.

ORIGINAL PAGE IS OF POOR QUALITY

AZIMUTH = 180 ELEVATION = 10

FREQUENCY = 2000.0 MHZ SATELLITE RANGE = 5000000. METERS

NORMAL PROFILE PARAMETERS ARE

FOF2 = 8.08 MHZ RHM = 0.31368803D 06 YM = 109786. METERS YT = 109786. METERS D = 42129. METERS

DECAY CONSTANTS 0.61978516C7D-C5 0.62083485380-C5 C.31487341610-05 0.12334067530-C5 0.4625778255C-C6

HEIGHTS 0.35581696640 06 0.57454460420 06 0.79327230210 06 0.10000000000 07 0.20000000000 07 0.35000000000 07

	RANGE DIFFERENCE	PERC.DIFF.	RANGE CORRECTION	PERC.DIFF.	ANGLE CORRECTION	PERC.DIFF.
RAY-TRACE	-0.48954356C7D 00		0.57364265350 01		0.61717364540-C2	
ANALYTIC	-0.34240317320 00	-30.057	0.49247973070 01	-14.149	0.57877537260-C2	-6.222
NUMERICAL(QUADRATURE)	-0.33C05835C30 00	-32.578	0.47230398400 01	-17.666	C.5416CC5841D-C2	-12.265
NUMERICAL(LEAST SQUARE)	-0.337C4528330 00	-31.151	0.54199976920 01	-5.516	0.58686453410-C2	-4.9C8
NUMERICAL(SPLINE)						
1 2 11 6	-0.47802846830 00	-2.352	0.57348038200 01	-0.028	0.61780814520-C2	0.103
1 7 2 13 9 10	-0.45552336980 00	1.222	0.57378387830 01	0.025	C.61647672580-C2	0.211
1 2 13 8 9 10	-0.48936542200 00	-0.036	0.57039340120 01	-0.566	C.61574439740-C2	-0.232
1 2 13 9 10	-0.500177746CD 00	2.172	0.57254728800 01	-0.191	0.61707C4711C-C2	-0.017
1 7 2 13 8 9 10	-0.48454CE270D 00	-1.022	0.57206984250 01	-0.274	C.61141222130-C2	0.039
1 2 3 12 10	-0.51687513130 00	5.583	0.56893252270 01	-0.821	C.61415457660-C2	-C.489
ALL POINTS 15	-0.49537139C7D 00	1.190	0.57156558280 01	-0.362	0.61652365200-C2	-0.105

Table 3b. Azimuth = 180°, Elevation = 10°

Comparison of ray trace refraction corrections vs. homogeneous ionosphere modified by a density gradient function. Test case at Kashima, Japan. 12^h U.T. on 15 January 1969.

AZIMUTH = 180 ELEVATION = 20

FREQUENCY = 2000.0 MHZ SATELLITE RANGE = 5000000. METERS

NORMAL PROFILE PARAMETERS ARE

FOF2 = 6.29 MHZ RHM = 0.31543705D 06 YM = 102811. METERS YT = 102811. METERS D = 37212. METERS

DECAY CONSTANTS 0.81024386 51D-05 0.54565552040D-05 0.33302442250D-05 0.11155984700D-05 0.52801587360D-06

HEIGHTS 0.35264672660D 06 0.57243248440D 06 0.79221624220D 06 0.10000000000D 07 0.20000000000D 07 0.30000000000D 07

	RANGE DIFFERENCE	PERC.DIFF.	RANGE CORRECTION	PERC.DIFF.	ANGLE CORRECTION	PERC.DIFF.
RAY-TRACE	-0.10759815420 01		0.28846601570 01		0.20479412220-02	
ANALYTIC	-0.96405643170 00	-10.402	0.23245518070 01	-19.417	0.18602743560-02	-9.184
NUMERICAL(QUADRATURE)	-0.51793260190 00	-14.689	0.22337326780 01	-22.565	0.16866614680-02	-17.631
NUMERICAL(LEAST SQUARE)	-0.10105048500 01	-6.085	0.27185042120 01	-5.760	0.19283654550-02	-5.839
NUMERICAL(SPLINE)						
1 2 11 6	-0.10827031670 01	0.625	0.28813568840 01	-0.115	0.20461646570-02	-0.087
1 7 2 13 9 10	-0.10728930670 01	-0.287	0.28703668280 01	-0.455	0.20395003270-02	-0.412
1 2 13 8 9 10	-0.10564614550 01	-1.814	0.28859551900 01	0.045	0.20470326130-02	-0.044
1 2 13 9 10	-0.10712029030 01	-0.444	0.28675069040 01	-0.595	0.20365538530-02	-0.537
1 7 2 13 8 9 10	-0.10595116770 01	-1.531	0.28912700790 01	0.229	0.20509338680-02	0.146
1 2 3 12 10	-0.10415133840 01	-3.203	0.28826529600 01	-0.070	0.20417105530-02	-0.304
ALL POINTS 14	-0.10609557270 01	-1.396	0.28917010330 01	0.244	0.20498712410-02	0.094

Table 3c. Azimuth = 180°, Elevation = 20°

Comparison of ray trace refraction corrections vs. homogeneous ionosphere modified by a density gradient function. Test case at Kashima, Japan. 12^h U.T. on 15 January 1969.

AZIMUTH = 180 ELEVATION = 45

FREQUENCY = 2000.0 MHZ SATELLITE RANGE = 5000000. METERS

NORMAL PROFILE PARAMETERS ARE

FOF2 = 4.78 MHZ RHM = 0.320127030 06 YM = 101954. METERS YT = 101954. METERS D = 35753. METERS

DECAY CONSTANTS 0.784302857 4D-05 0.501208730 2D-05 0.306920461 1D-05 0.102467529 0D-05 0.579364451 1D-06

HEIGHTS 0.355080244 6D 06 0.574586826 7D 06 0.793293414 9D 06 0.100000000 0D 07 0.200000000 0D 07 0.350000000 0D 07

	RANGE DIFFERENCE	PERC.DIFF.	RANGE CORRECTION	PERC.DIFF.	ANGLE CORRECTION	PERC.DIFF.
RAY-TRACE	-0.706641670 8D 00		0.103965023 7D 01		0.295545324 1D-03	
ANALYTIC	-0.539703753 5D 00	-23.624	0.893139988 6D 00	-14.092	0.279421006 5D-03	-5.456
NUMERICAL(QUADRATURE)	-0.511697335 8D 00	-27.587	0.879524388 3D 00	-15.402	0.256686415 9D-03	-12.471
NUMERICAL(LEAST SQUARE)	-0.649069152 7D 00	-8.147	0.100841643 5D 01	-3.004	0.286047962 6D-03	-3.214
NUMERICAL(SPLINE)						
1 2 11 6	-0.737357938 7D 00	4.347	0.103903901 1D 01	-0.059	0.295357028 3D-03	-0.064
1 7 2 13 9 10	-0.700986612 4D 00	-0.800	0.104335913 2D 01	0.357	0.295920328 9D-03	0.127
1 2 13 8 9 10	-0.700531077 0D 00	-0.865	0.104416655 7D 01	0.434	0.296295267 7D-03	0.254
1 2 13 9 10	-0.699655359 0D 00	-0.989	0.104298505 0D 01	0.321	0.295779604 3D-03	0.079
1 7 2 13 8 9 10	-0.702310539 9D 00	-0.613	0.104457029 2D 01	0.512	0.296435747 5D-03	0.301
1 2 3 12 10	-0.652734236 7D 00	-1.968	0.104734410 9D 01	0.760	0.297090441 5D-03	0.523
ALL POINTS 14	-0.703756616 2D 00	-0.408	0.104479355 9D 01	0.455	0.296295267 7D-03	0.294

Table 3d. Azimuth = 180°, Elevation = 45°

Comparison of ray trace refraction corrections vs. homogeneous ionosphere modified by a density gradient function. Test case at Kashima, Japan. 12^h U.T. on 15 January 1969.

AZIMUTH = 180 ELEVATION = 60

FREQUENCY = 2000.0 MHZ SATELLITE RANGE = 5000000. METERS

NORMAL PROFILE PARAMETERS ARE

FOF2 = 4.41 MHZ RHM = 0.32179735D 06 YM = 101887. METERS YT = 101887. METERS D = 35493. METERS

DECAY CONSTANTS 0.77824370470-C5 0.49571713450-C5 0.28920313050-05 0.10157900400-05 0.59325876500-C6

HEIGHTS 0.35729020450-C6 0.57552680300-06 0.79376340150-06 0.10000000000-07 0.20000000000-C7 0.30000000000-C7

	RANGE DIFFERENCE	PERC.DIFF.	RANGE CORRECTION	PERC.DIFF.	ANGLE CORRECTION	PERC.DIFF.
RAY-TRACE	-0.30856111250 00		0.73108912470 00		0.12265552370-C3	
ANALYTIC	-0.23809320580 00	-22.838	0.65504678280 00	-10.401	0.11897623110-C3	-3.000
NUMERICAL(QUADRATURE)	-0.22860107010 00	-25.914	0.65092331830 00	-10.965	0.11113605290-C3	-9.392
NUMERICAL(LEAST SQUARE)	-0.29120203310 00	-5.626	0.71721440160 00	-1.858	0.12036781330-C3	-1.865
NUMERICAL(SPLINE)						
1 2 11 6	-0.30999528590 00	0.465	0.72904372500 00	-0.280	0.12253883630-C3	-0.095
1 7 2 13 9 10	-0.31105819840 00	0.809	0.73230093360 00	0.166	0.12215860750-C3	-0.373
1 2 13 8 9 10	-0.31204157270 00	1.130	0.73211898410 00	0.141	0.12287812310-C3	0.181
1 2 13 9 10	-0.31082562220 00	0.734	0.73215942800 00	0.146	0.12215660750-C3	-0.373
1 7 2 13 8 9 10	-0.31262453060 00	1.317	0.73234576120 00	0.172	0.12253883630-C3	-0.095
1 2 3 12 10	-0.31067399030 00	0.685	0.73667011830 00	0.763	0.12433766770-C3	1.371
ALL POINTS 14	-0.31160975500 00	0.988	0.73318376380 00	0.287	0.12287812310-C3	0.181

Table 3e. Azimuth = 180°, Elevation = 60°

Comparison of ray trace refraction corrections vs. homogeneous ionosphere modified by a density gradient function. Test case at Kashima, Japan. 12^h U.T. on 15 January 1969.

ORIGINAL PAGE IS OF POOR QUALITY

APPENDIX A

SUBROUTINE CORSST

(Flow diagram)

SUBROUTINE CORSST

INTERFACE BETWEEN GTDS SST ROUTINES AND IONOSPHERIC SST ROUTINES

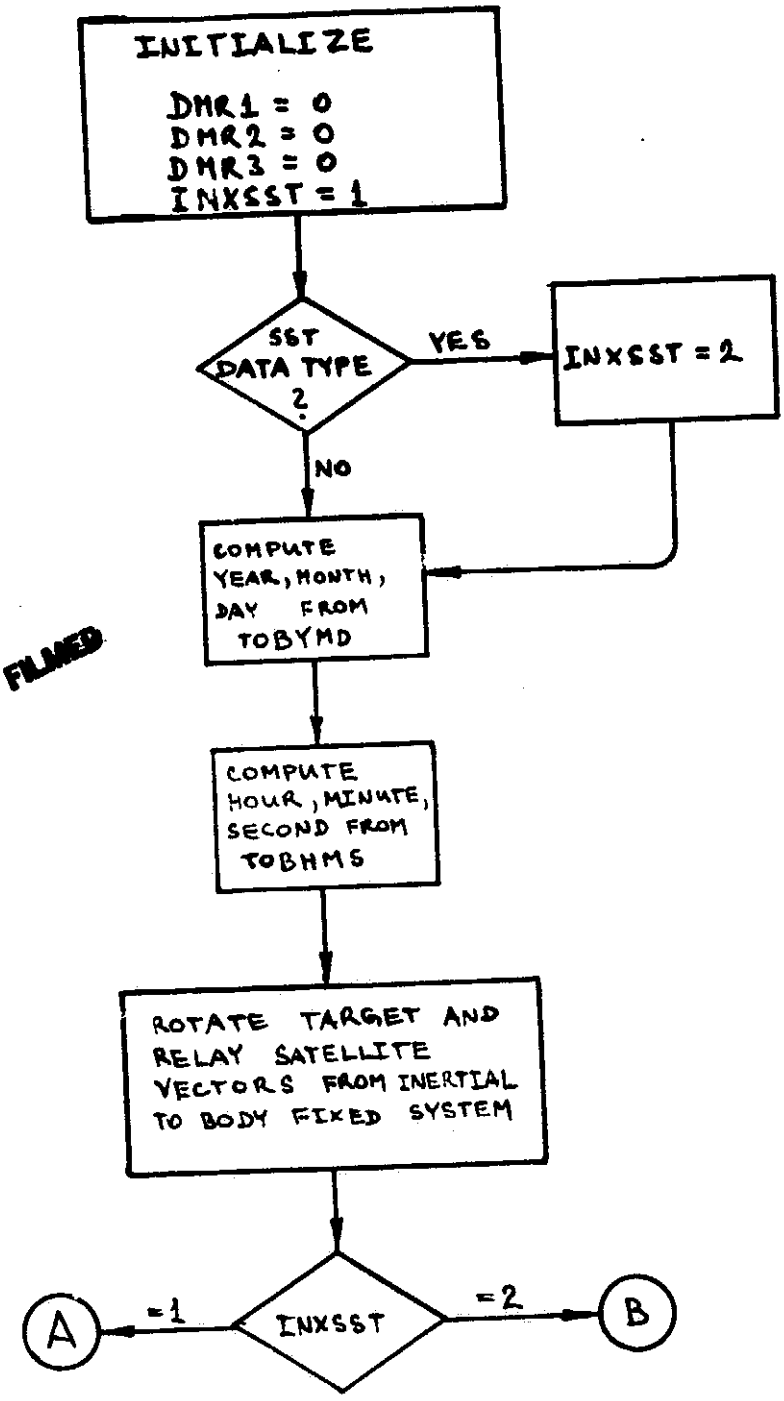

PRECEDING PAGE BLANK NOT FILMED

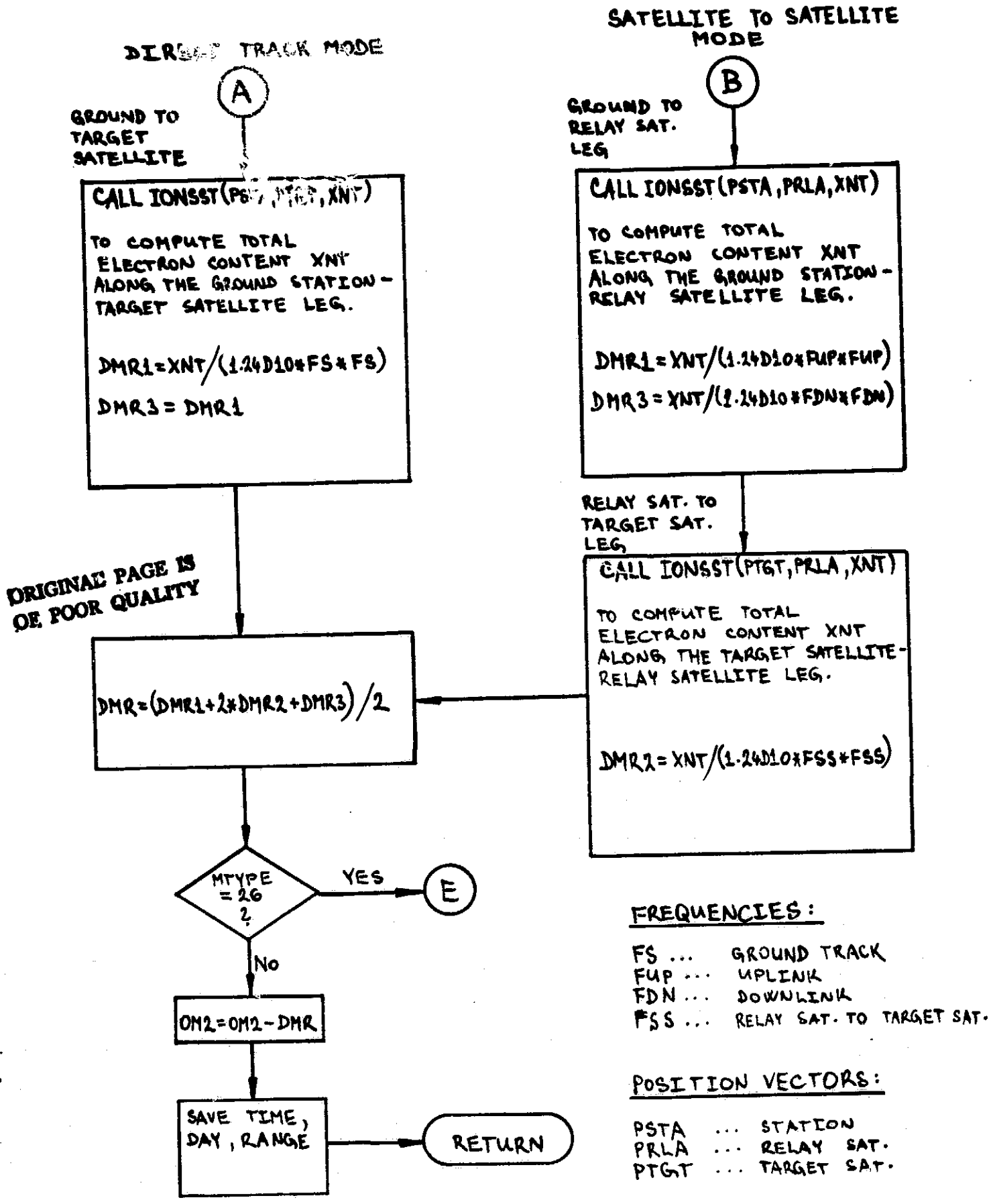

ORIGINAL PAGE IS OF POOR QUALITY

RANGE RATE COMPUTATION

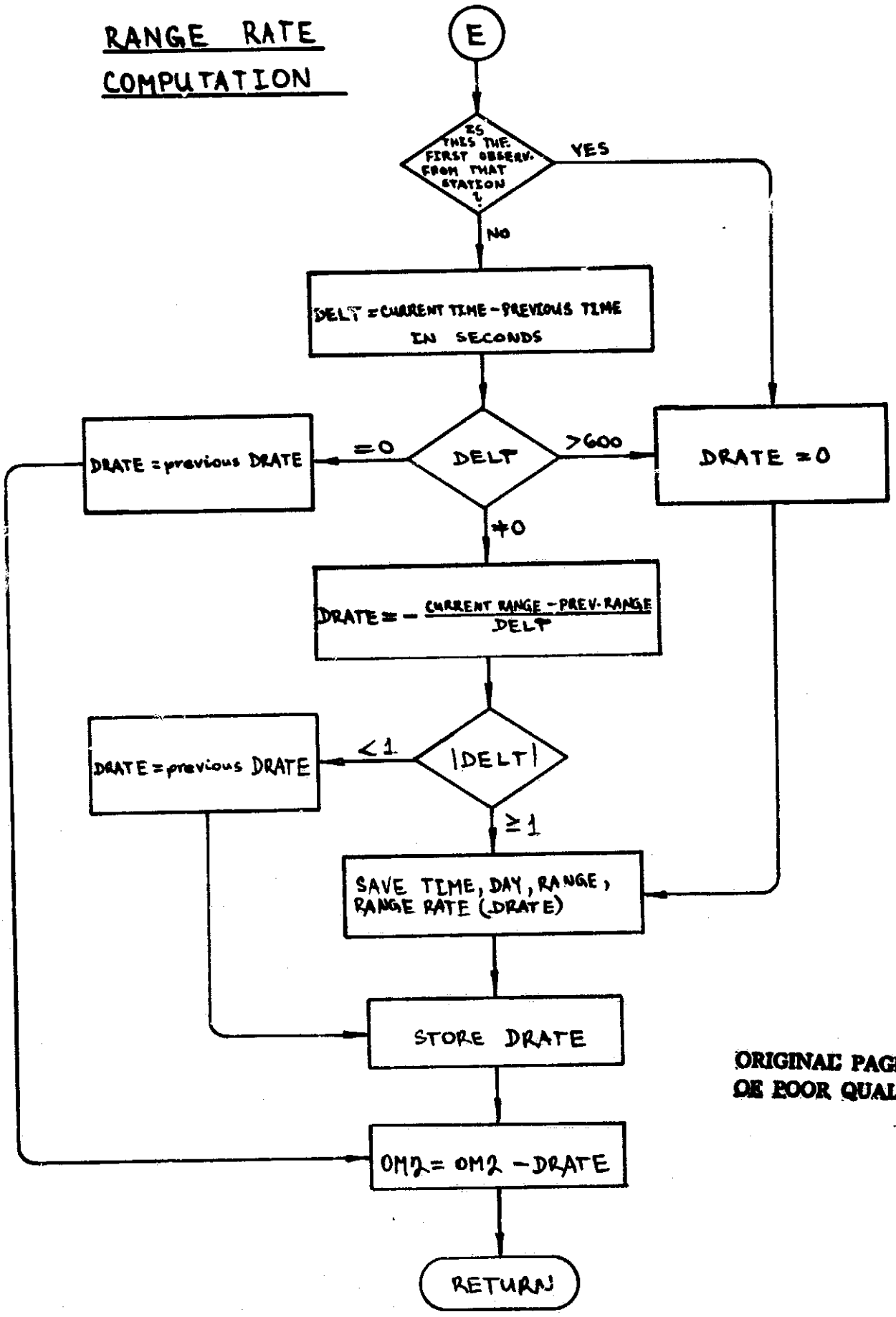

ORIGINAL PAGE IS OF POOR QUALITY

APPENDIX B

SUBROUTINE IONSST

Flow diagram for Case 1 (Figure 6)

PRECEDING PAGE BLANK NOT FILMED

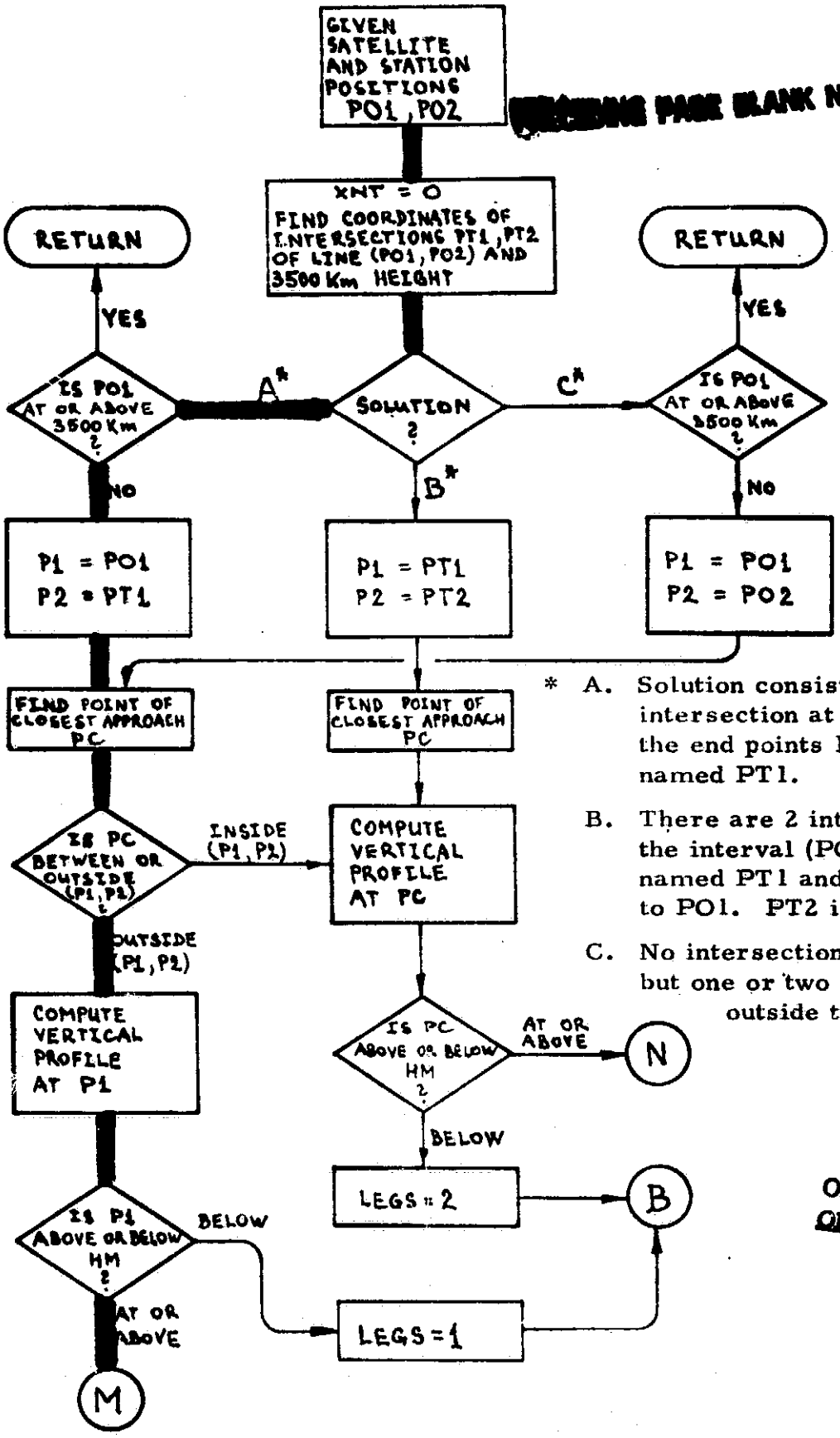

* A. Solution consists of one point of intersection at height 3500 km between the end points PO1 and PO2. It is named PT1.

B. There are 2 intersection points inside the interval (PO1, PO2). They are named PT1 and PT2. PT1 is closer to PO1. PT2 is closer to PO2.

C. No intersections between PO1 and PO2, but one or two intersections may exist outside the interval.

ORIGINAL PAGE IS OF POOR QUALITY

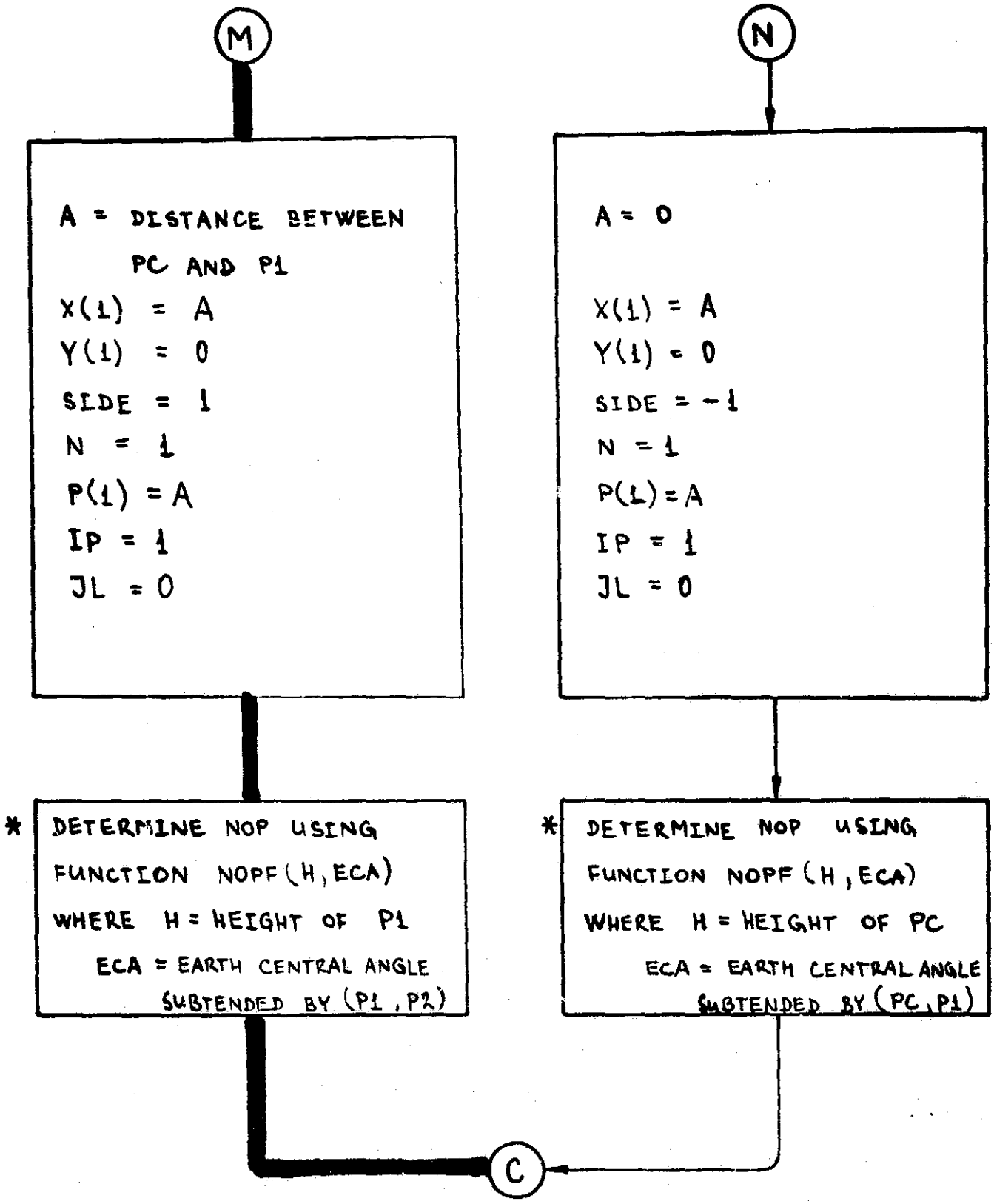

* NOP IS USUALLY ONE LESS THAN THE NUMBER OF POINTS NEEDED TO PROPERLY EVALUATE THE ELECTRON DENSITY DEVIATION FUNCTION BETWEEN TWO POINTS IN THE IONOSPHERE.

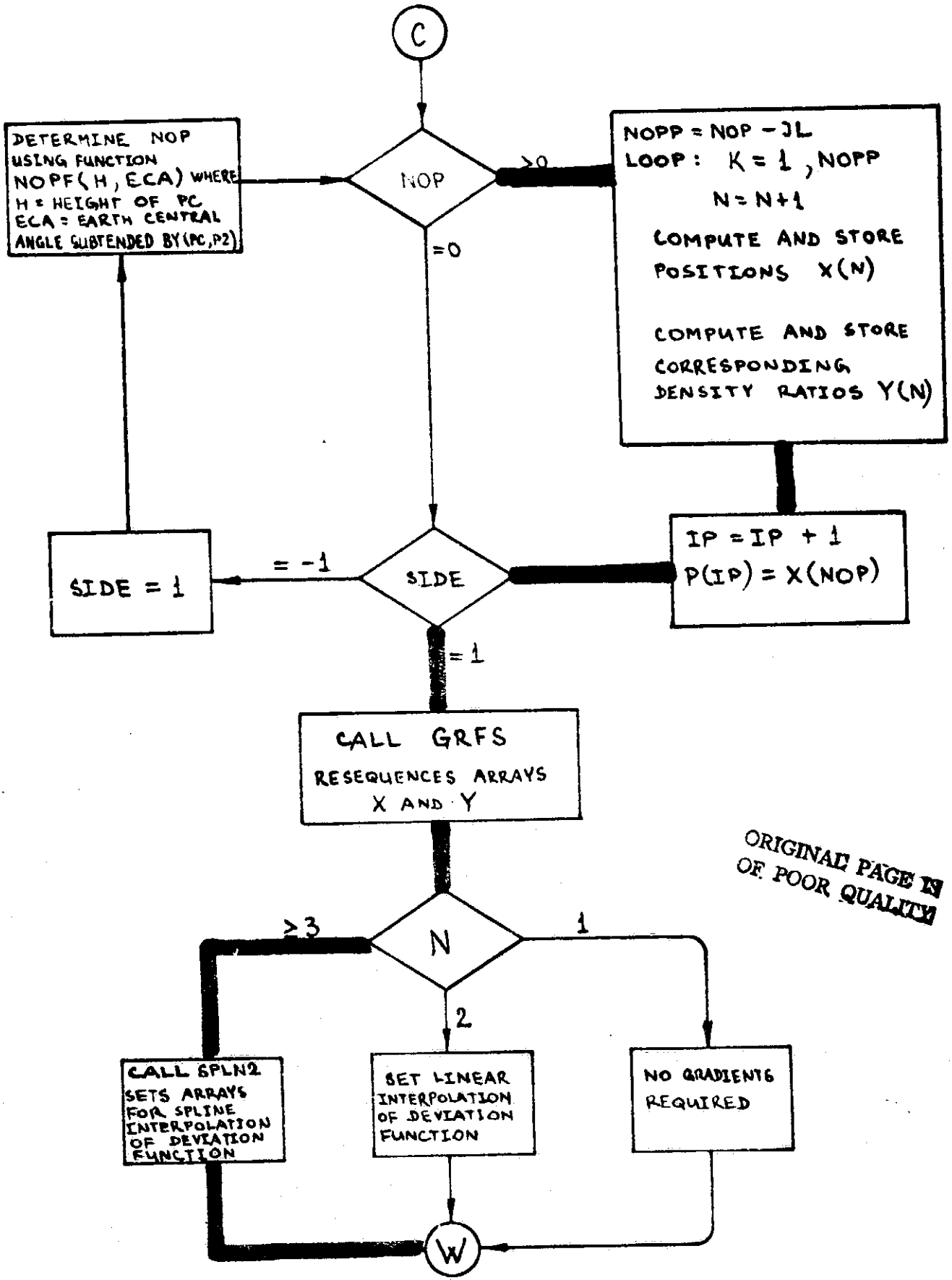

ORIGINAL PAGE IS OF POOR QUALITY

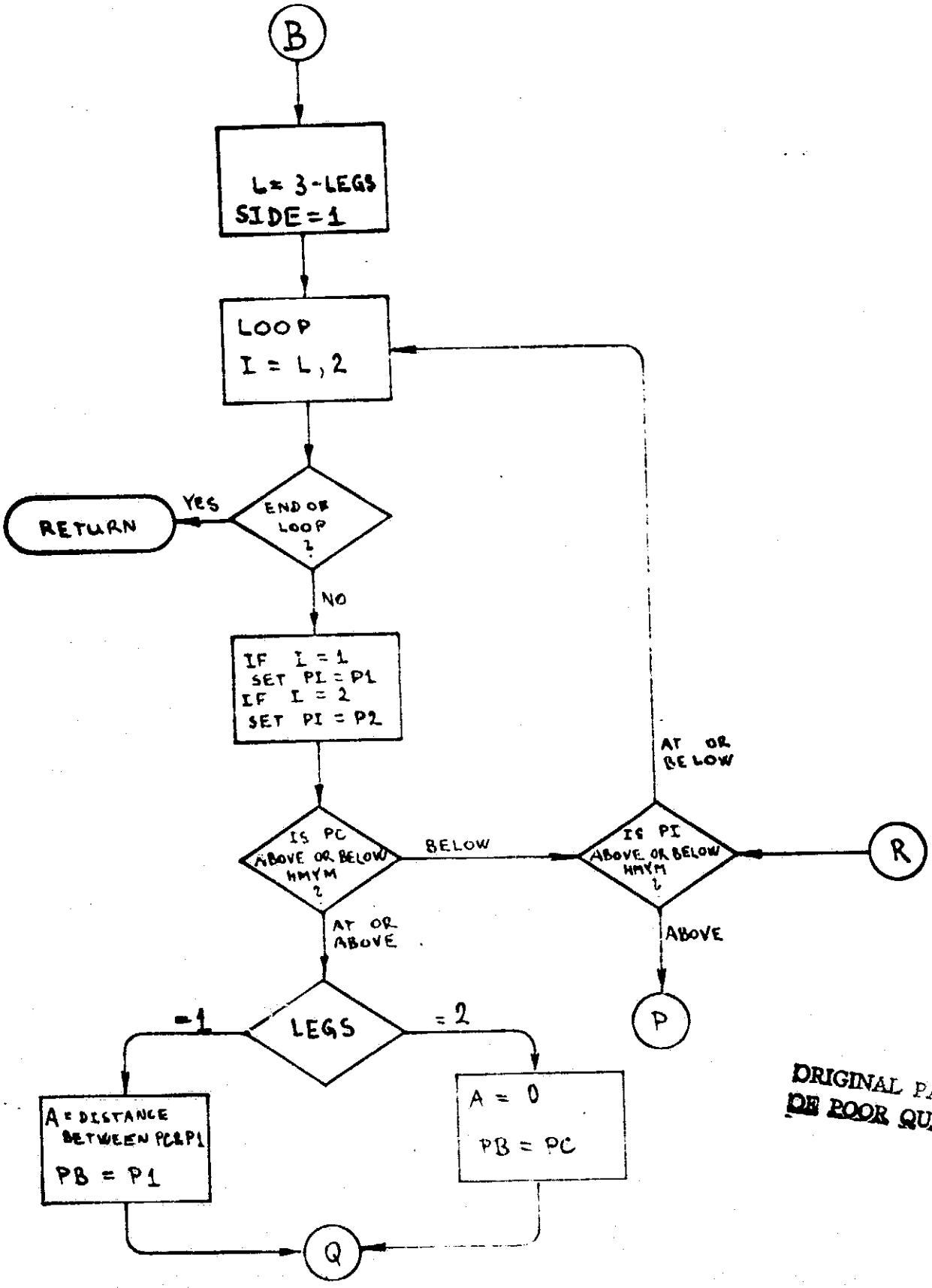

ORIGINAL PAGE IS
OF POOR QUALITY

CONVERGE TO BOTTOM OF IONOSPHERE HMYM

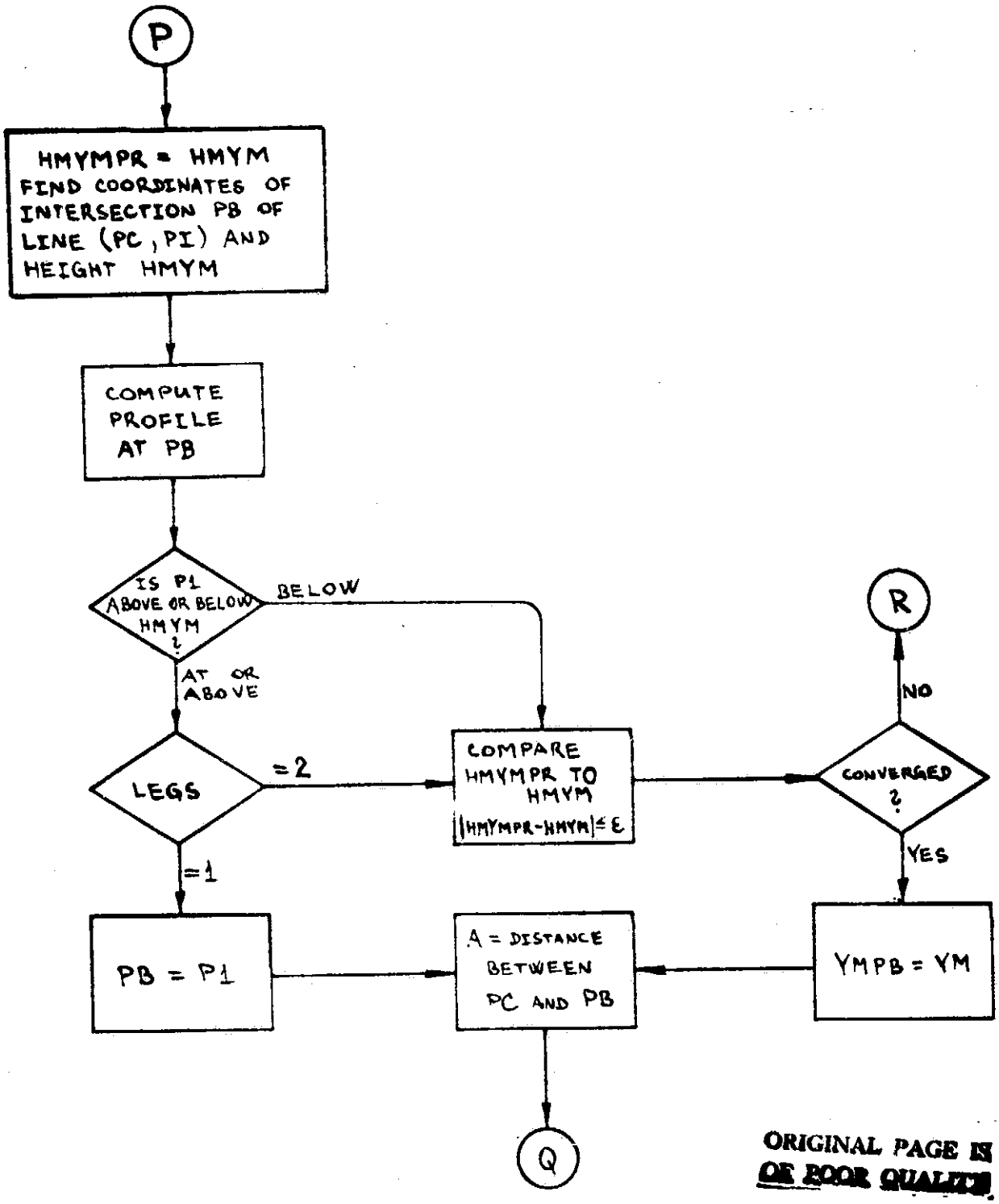

ORIGINAL PAGE IS OF POOR QUALITY

CONVERGE TO HEIGHT OF MAXIMUM ELECTRON DENSITY HM

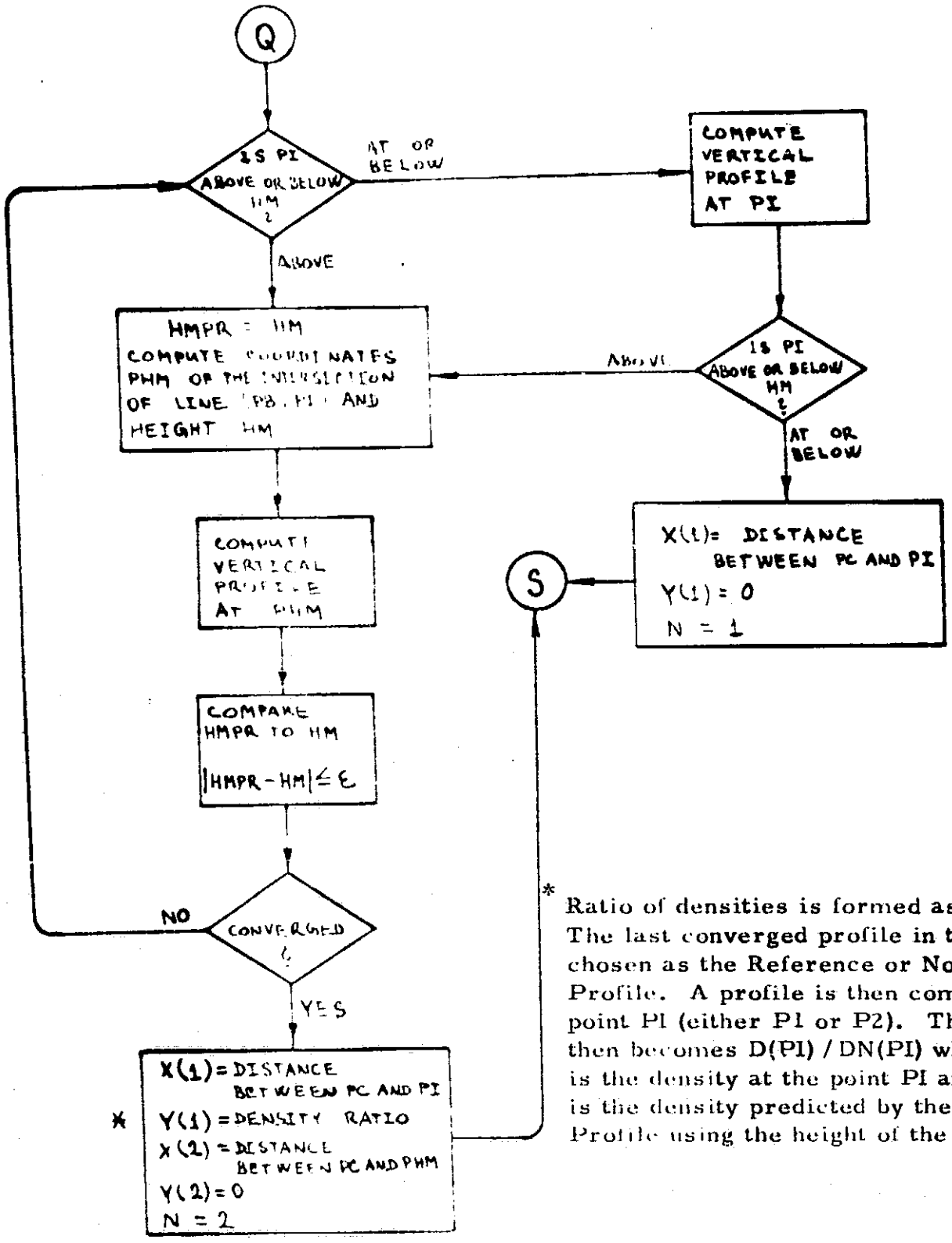

* Ratio of densities is formed as follows: The last converged profile in the loop is chosen as the Reference or Normalized Profile. A profile is then computed at the point PI (either P1 or P2). The ratio Y(1) then becomes D(PI) / DN(PI) where D(PI) is the density at the point PI and DN(PI) is the density predicted by the Reference Profile using the height of the point PI.

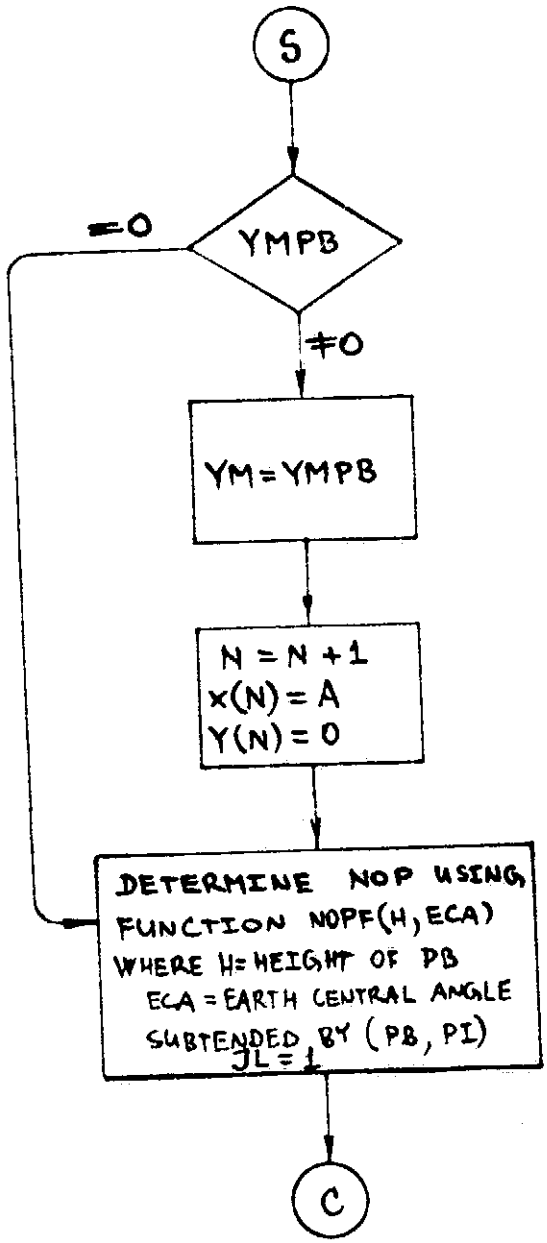

ORIGINAL PAGE IS
OF POOR QUALITY

INTEGRATOR 1

DETERMINE LIMITS OF INTEGRATION

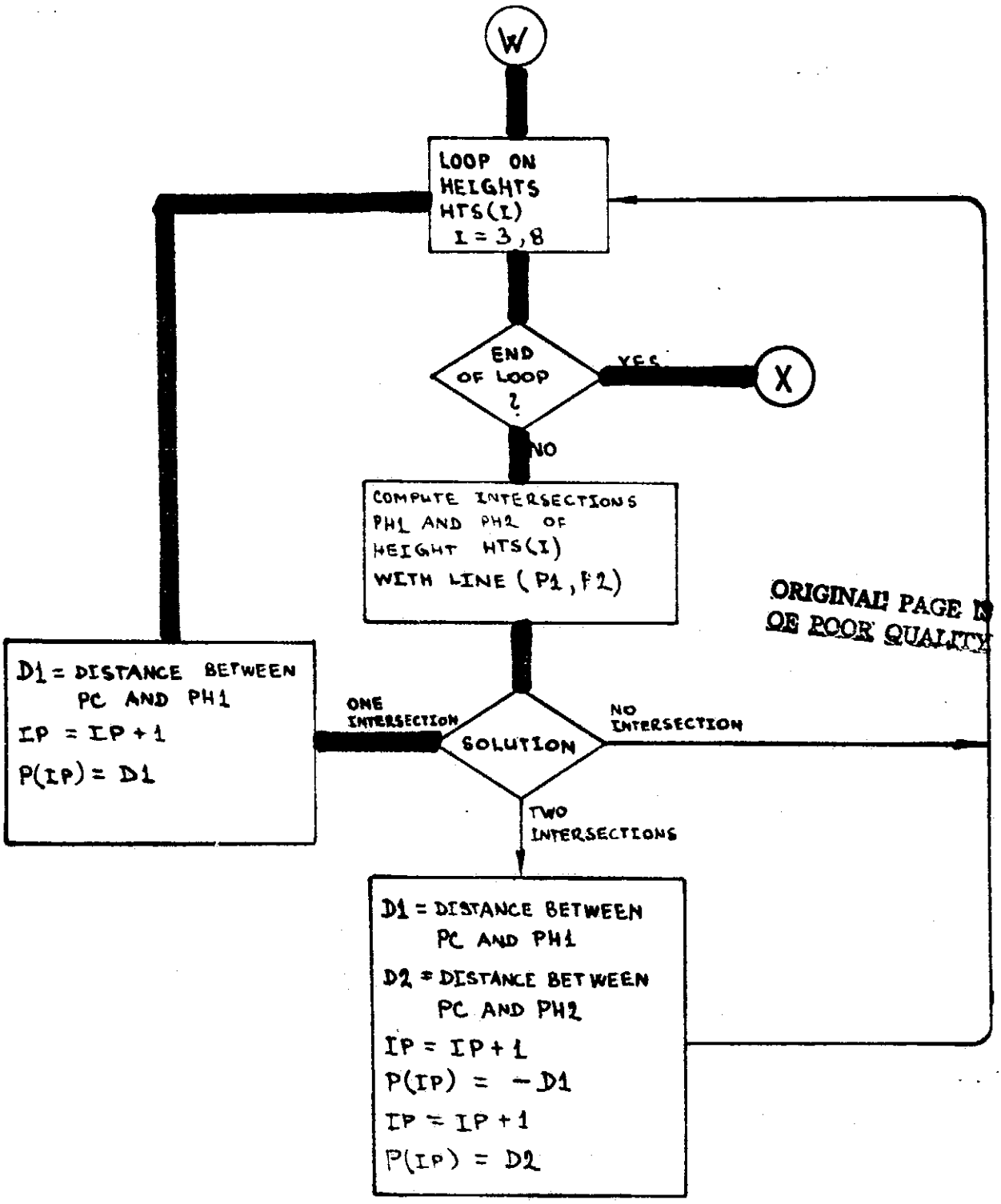

ORIGINAL PAGE IS OF POOR QUALITY

INTEGRATOR 2

PERFORM NUMERICAL INTEGRATION OF TOTAL ELECTRON CONTENT

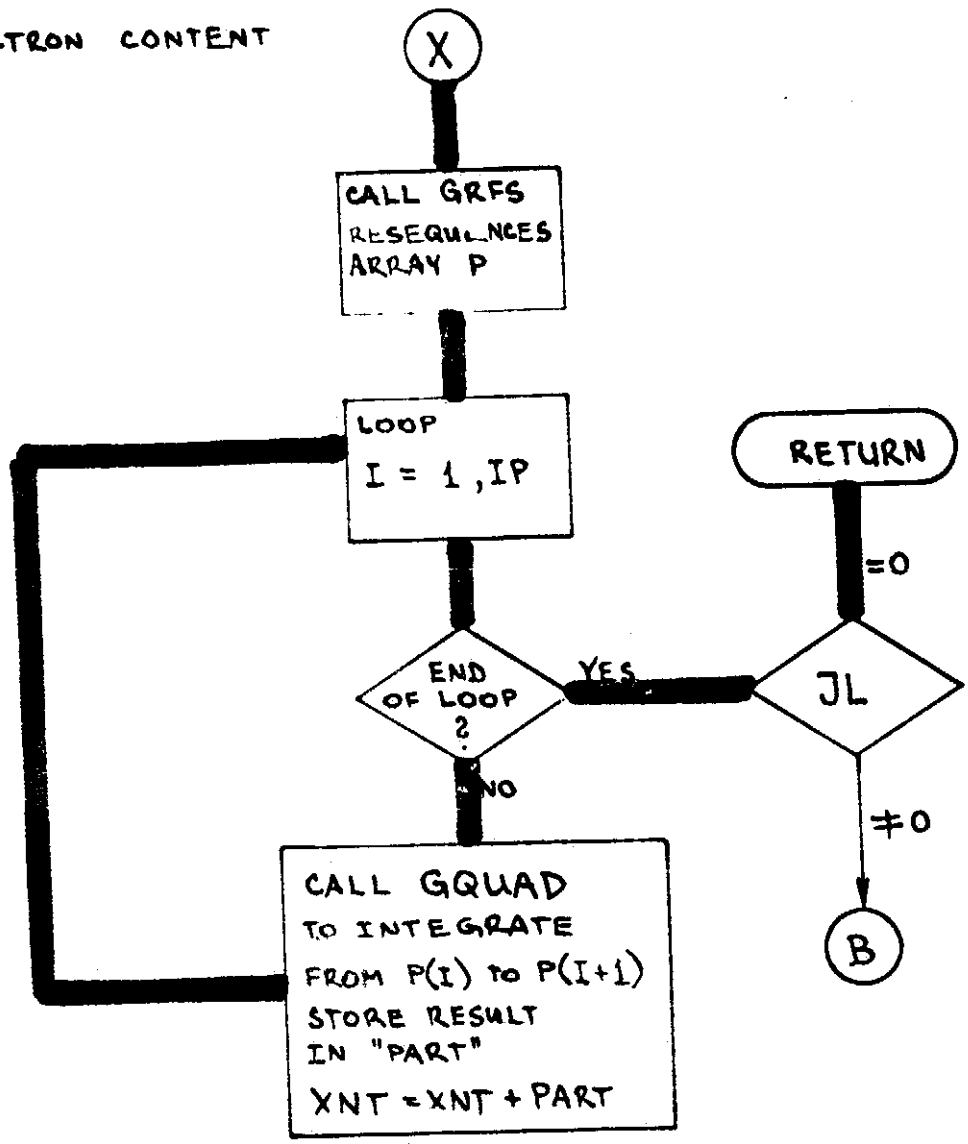

ORIGINAL PAGE IS
OF POOR QUALITY

APPENDIX C

SUBROUTINE IONSST

Flow diagram for Case 2 (Figure 7)

PRECEDING PAGE BLANK NOT FILMED

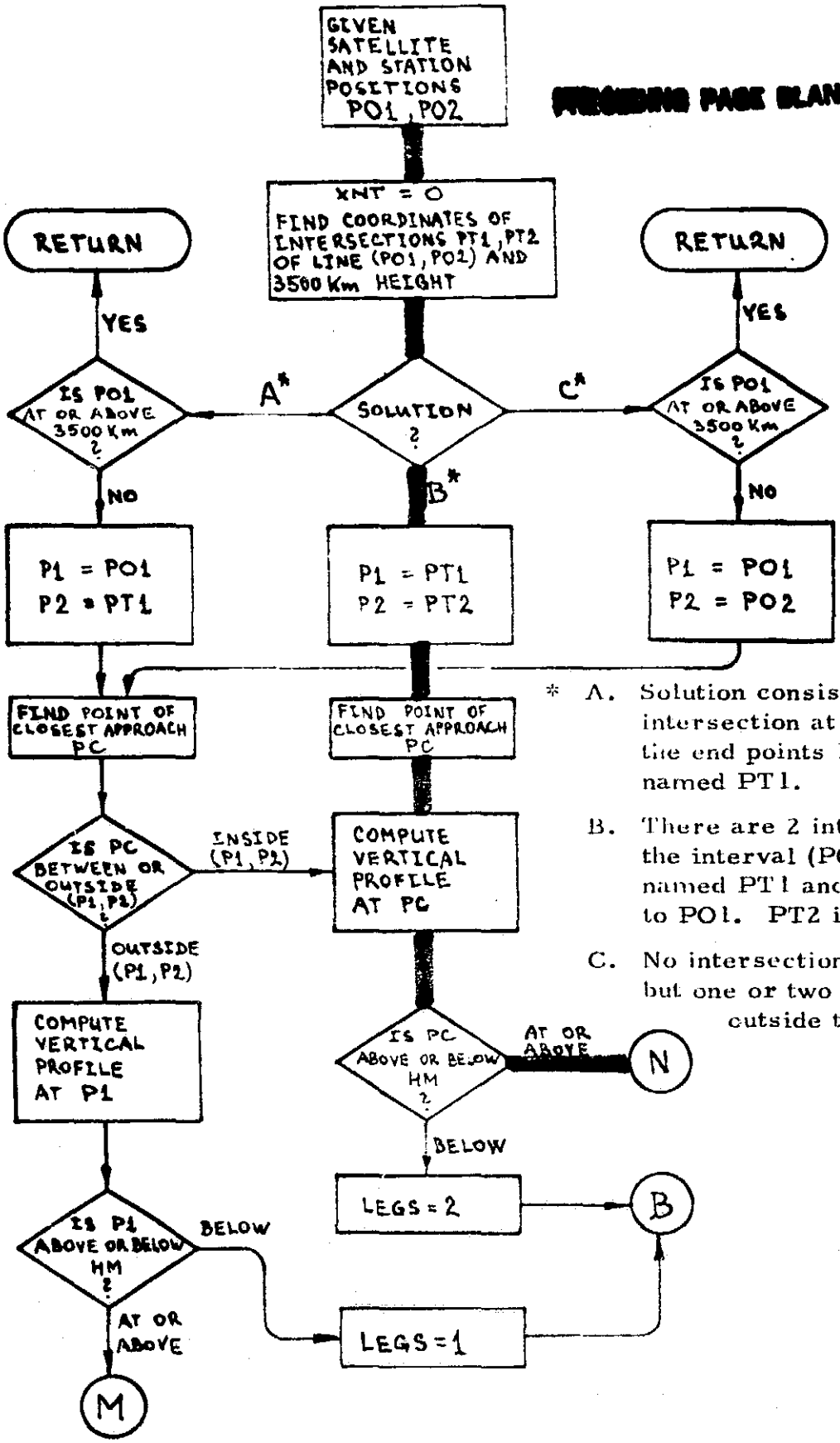

* A. Solution consists of one point of intersection at height 3500 km between the end points PO1 and PO2. It is named PT1.

B. There are 2 intersection points inside the interval (PO1, PO2). They are named PT1 and PT2. PT1 is closer to PO1. PT2 is closer to PO2.

C. No intersections between PO1 and PO2, but one or two intersections may exist outside the interval.

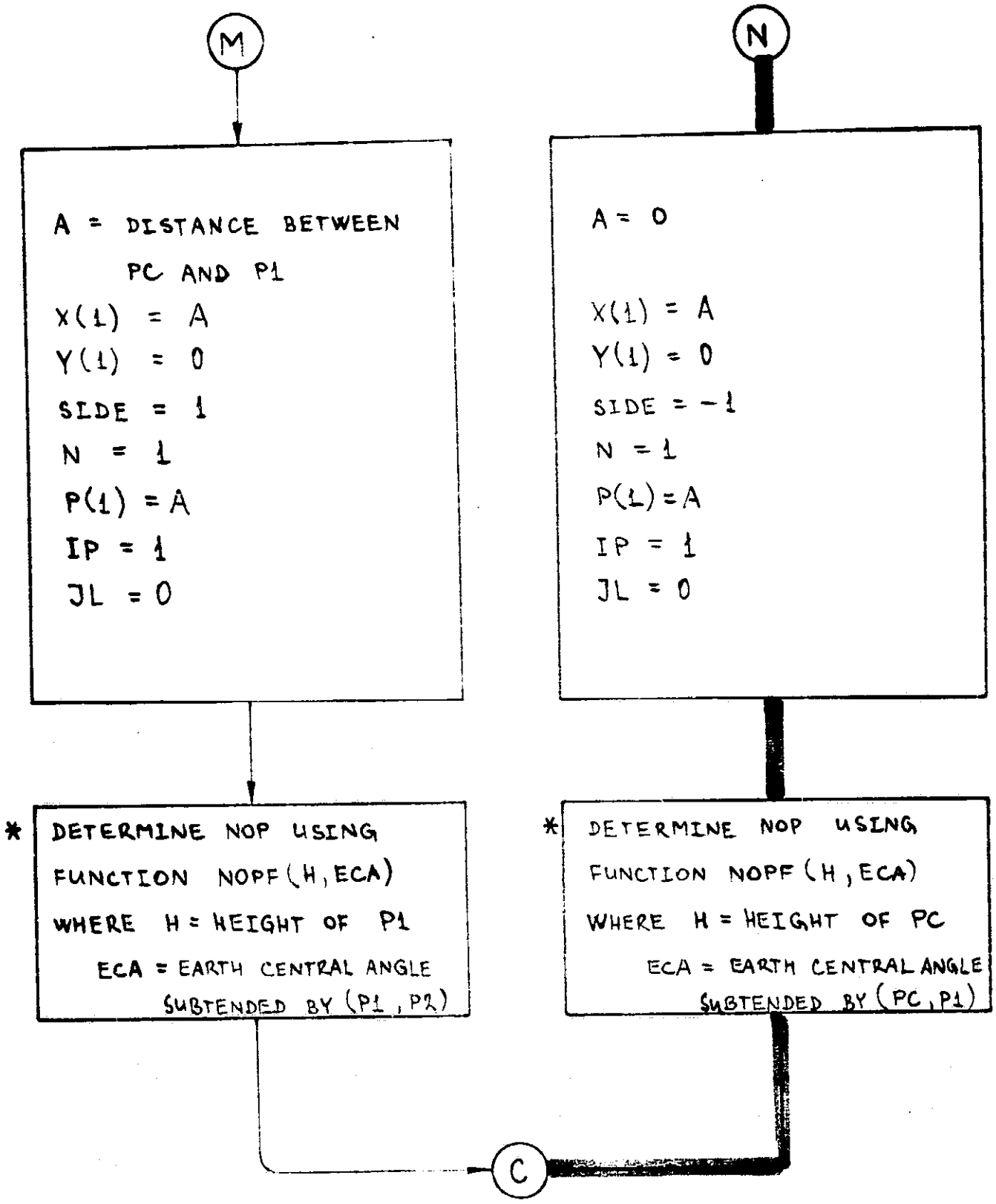

* NOP IS USUALLY ONE LESS THAN THE NUMBER OF POINTS NEEDED TO PROPERLY EVALUATE THE ELECTRON DENSITY DEVIATION FUNCTION BETWEEN TWO POINTS IN THE IONOSPHERE.

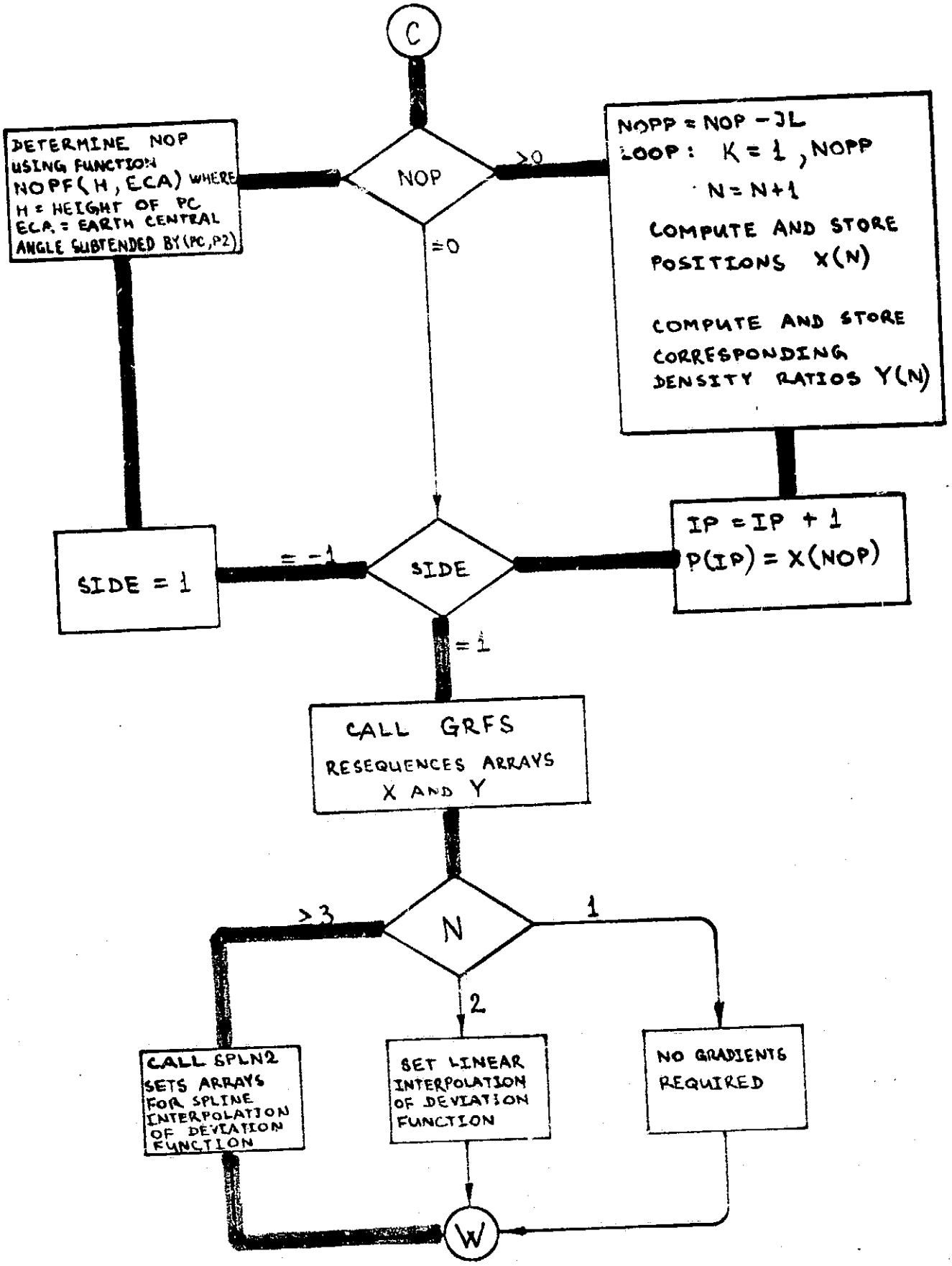
C
NOP
>0
=0
DETERMINE NOP USING FUNCTION NOPF(H, ECA) WHERE H = HEIGHT OF PC ECA = EARTH CENTRAL ANGLE SUBTENDED BY (PC, P2)
NOPP = NOP - JL
LOOP: K = 1, NOPP
N = N+1
COMPUTE AND STORE POSITIONS X(N)
COMPUTE AND STORE CORRESPONDING DENSITY RATIOS Y(N)
SIDE
= -1
SIDE = 1
IP = IP + 1
P(IP) = X(NOP)
= 1
CALL GRFS
RESEQUENCES ARRAYS X AND Y
N
>3
1
2
CALL SPLN2
SETS ARRAYS FOR SPLINE INTERPOLATION OF DEVIATION FUNCTION
SET LINEAR INTERPOLATION OF DEVIATION FUNCTION
NO GRADIENTS REQUIRED
W

ORIGINAL PAGE IS
OF POOR QUALITY

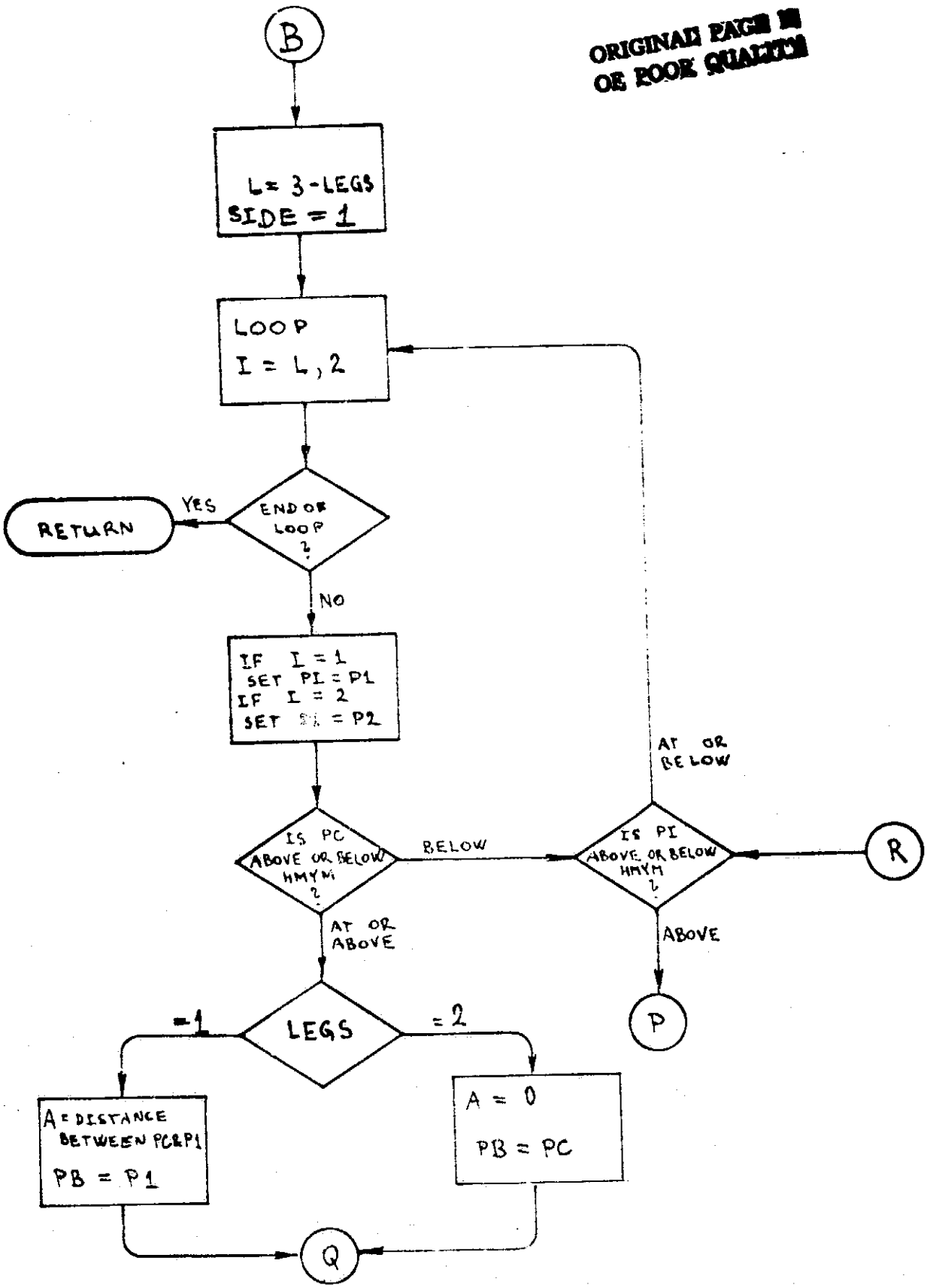

CONVERGE TO BOTTOM OF IONOSPHERE HMYM

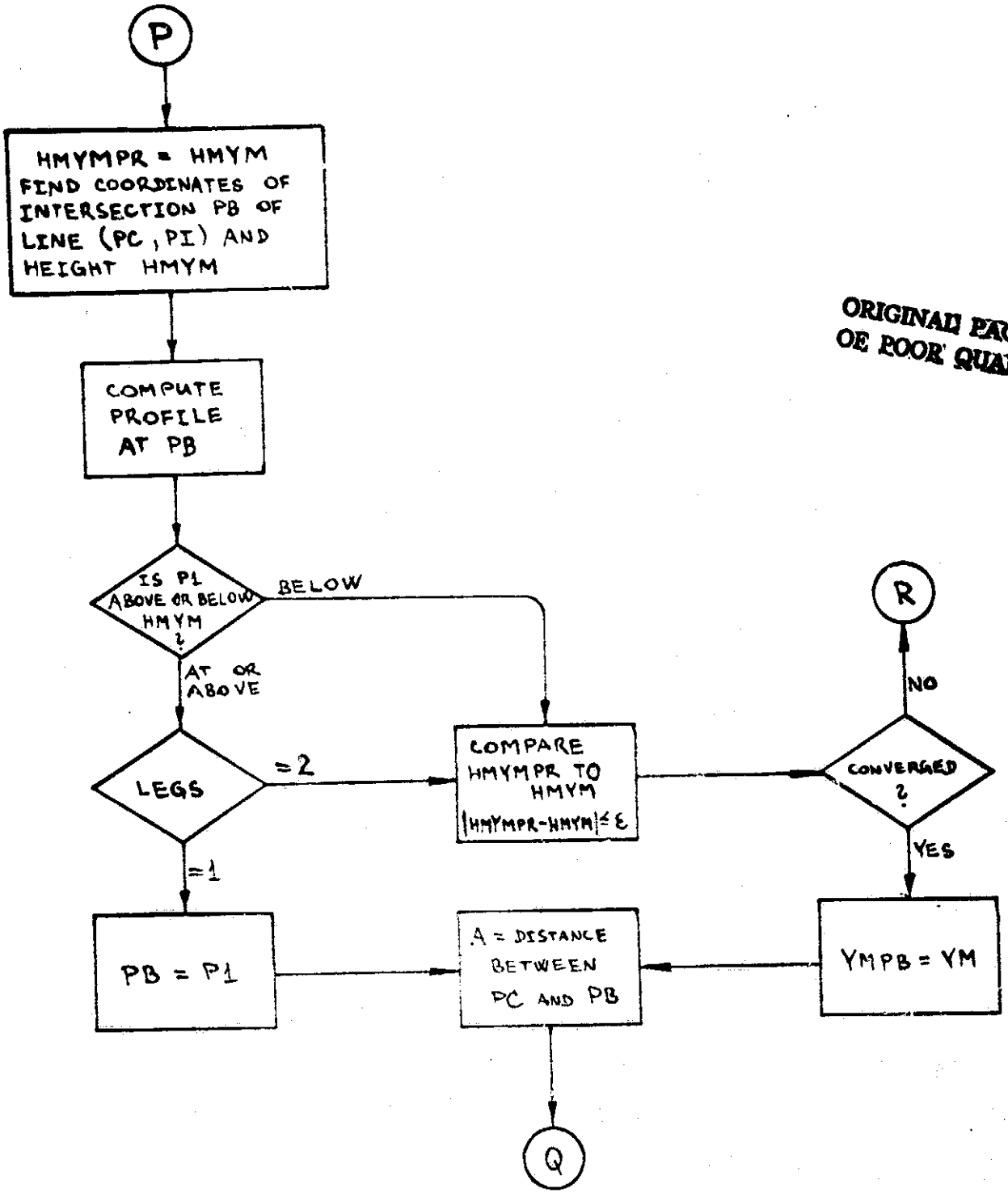

ORIGINAL PAGE IS OF POOR QUALITY

CONVERGE TO HEIGHT OF MAXIMUM ELECTRON DENSITY HM

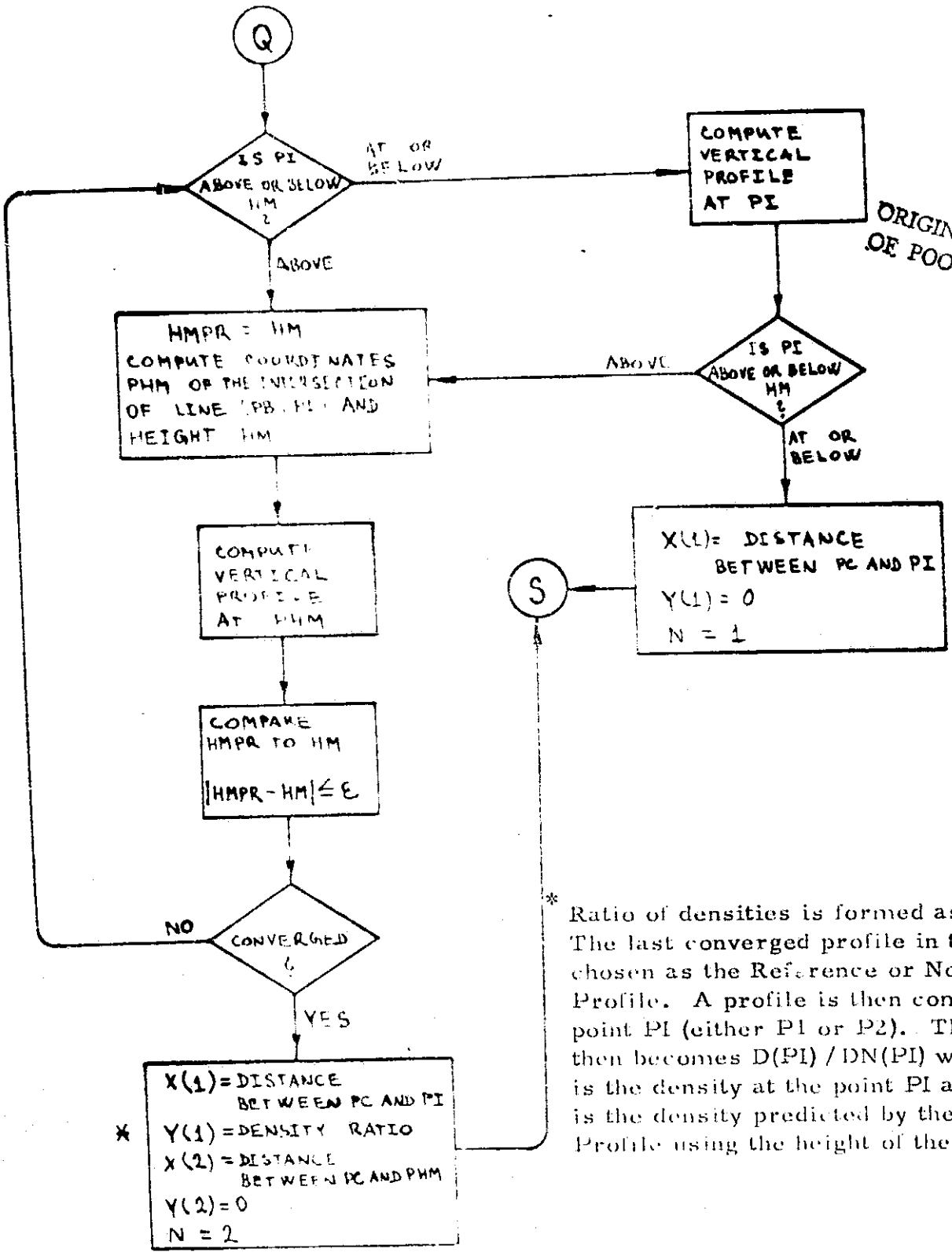

ORIGINAL PAGE IS OF POOR QUALITY

* Ratio of densities is formed as follows: The last converged profile in the loop is chosen as the Reference or Normalized Profile. A profile is then computed at the point PI (either P1 or P2). The ratio Y(1) then becomes D(PI) / DN(PI) where D(PI) is the density at the point PI and DN(PI) is the density predicted by the Reference Profile using the height of the point PI.

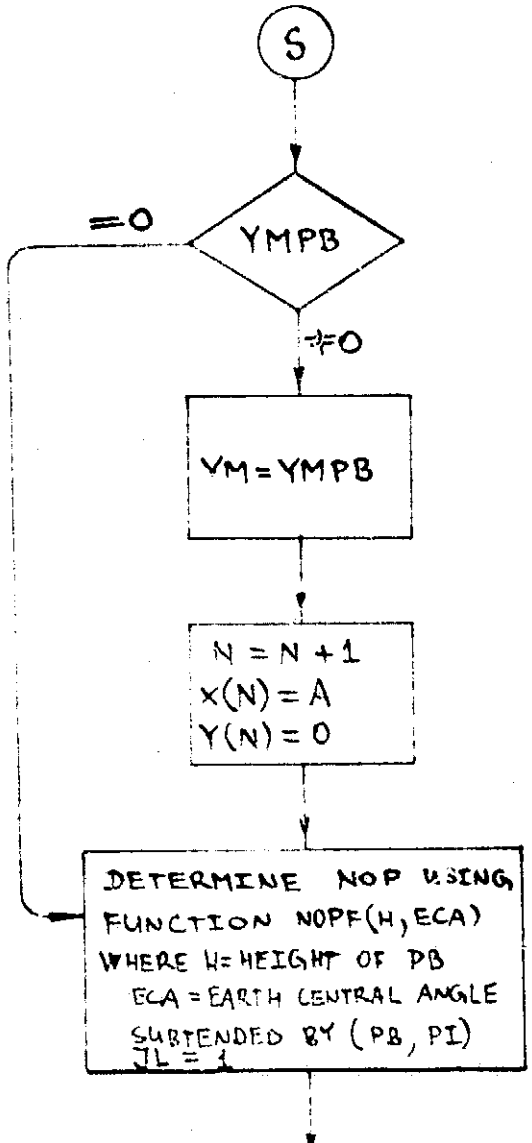

ORIGINAL PAGE IS
OF POOR QUALITY

INTEGRATOR 1

DETERMINE LIMITS OF INTEGRATION

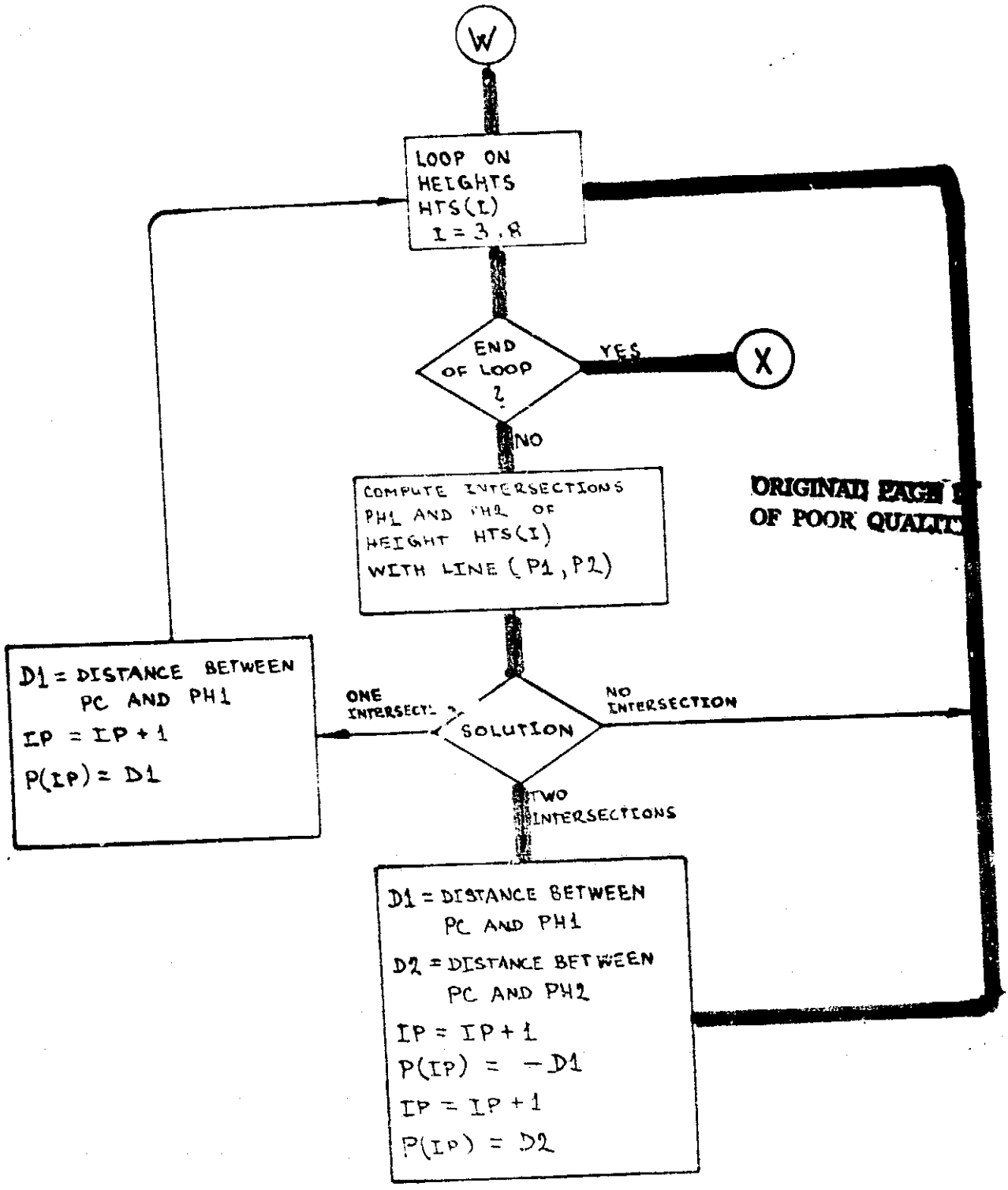

ORIGINAL PAGE IS
OF POOR QUALITY

INTEGRATOR 2

PERFORM NUMERICAL INTEGRATION OF TOTAL ELECTRON CONTENT

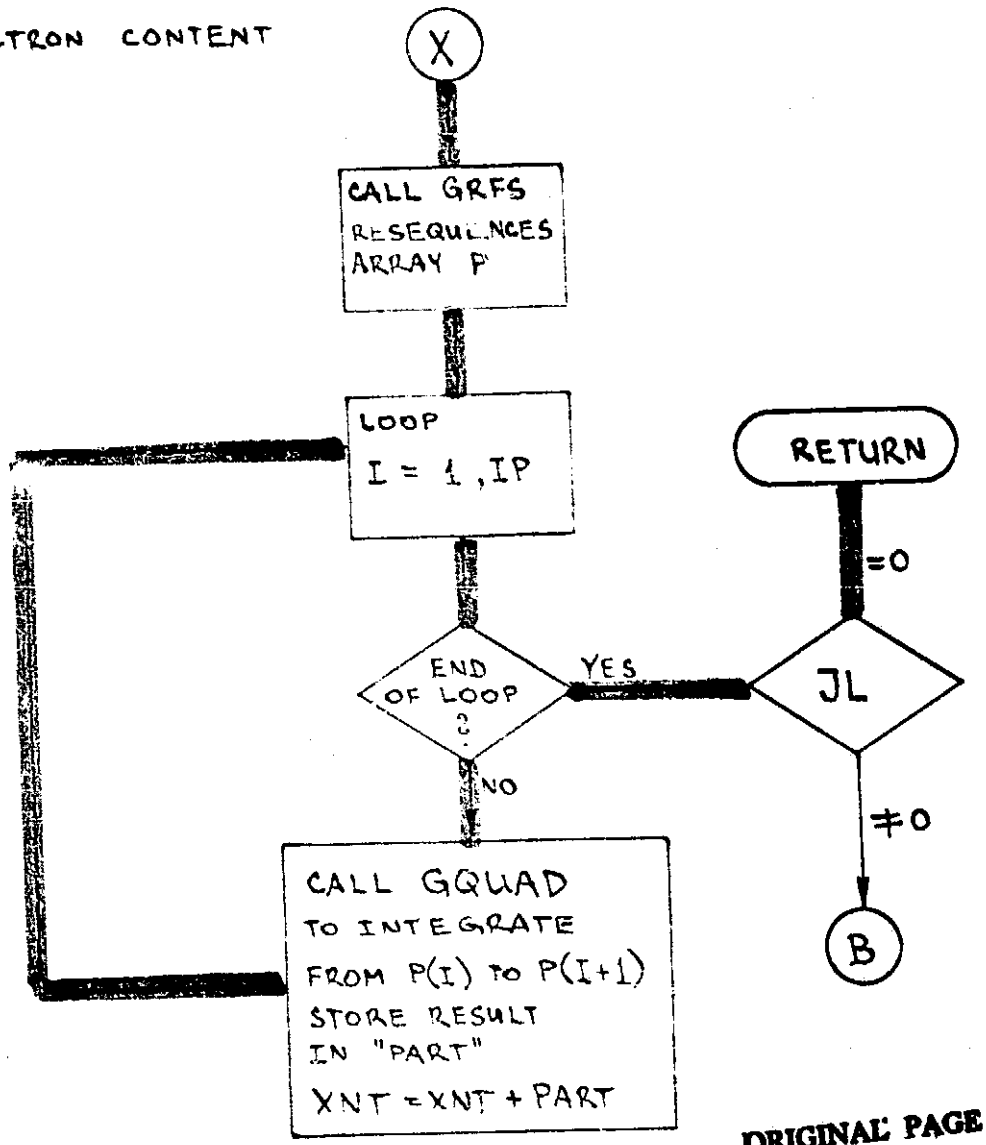

ORIGINAL PAGE IS
OF POOR QUALITY

APPENDIX D

SUBROUTINE IONSST

Flow diagram for Case 3 (Figure 8)

ORIGINAL PAGE IS
OF POOR QUALITY

PRECEDING PAGE BLANK NOT FILMED

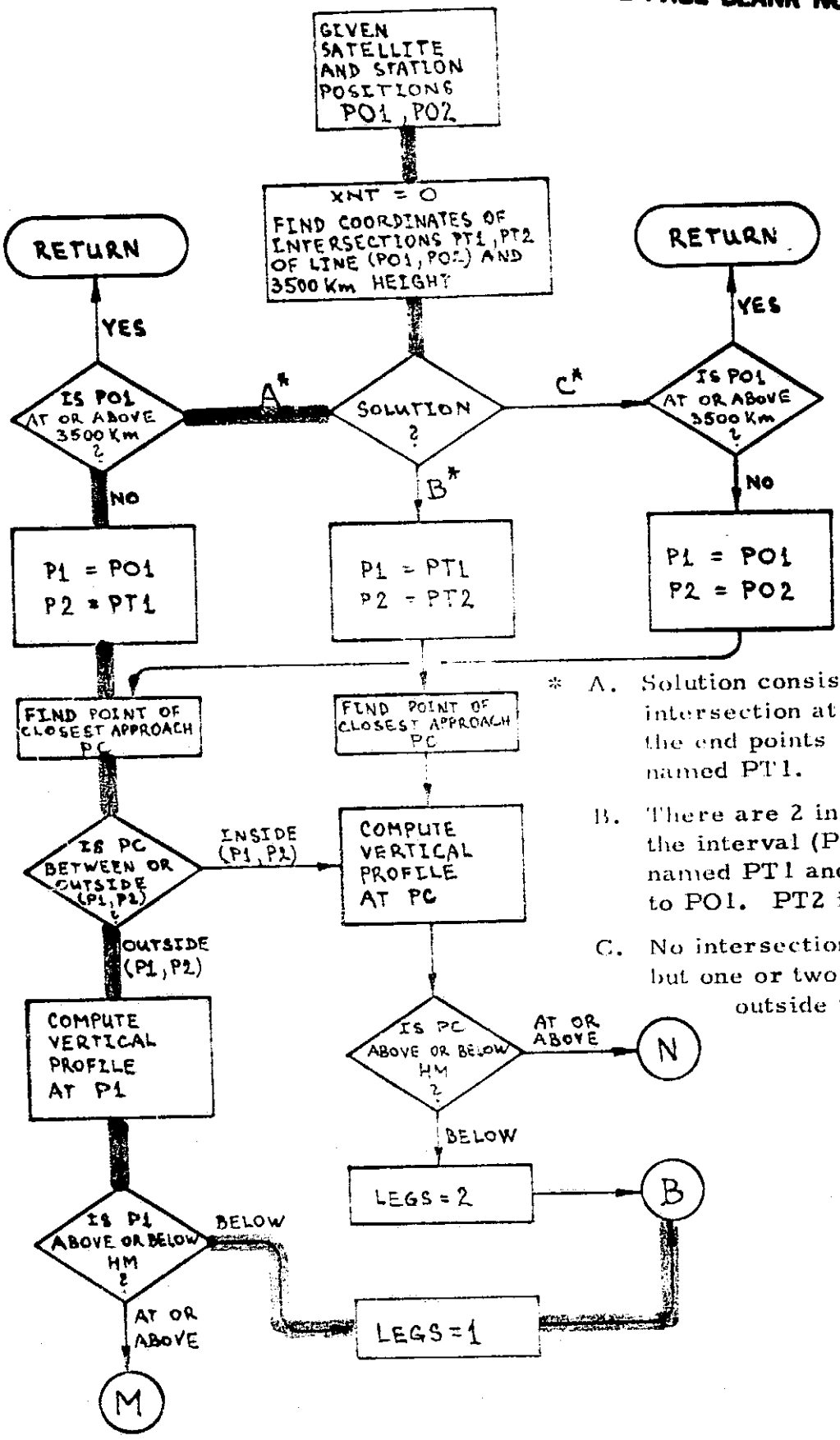

* A. Solution consists of one point of intersection at height 3500 km between the end points PO1 and PO2. It is named PT1.

B. There are 2 intersection points inside the interval (PO1, PO2). They are named PT1 and PT2. PT1 is closer to PO1. PT2 is closer to PO2.

C. No intersections between PO1 and PO2, but one or two intersections may exist outside the interval.

ORIGINAL PAGE IS OF POOR QUALITY

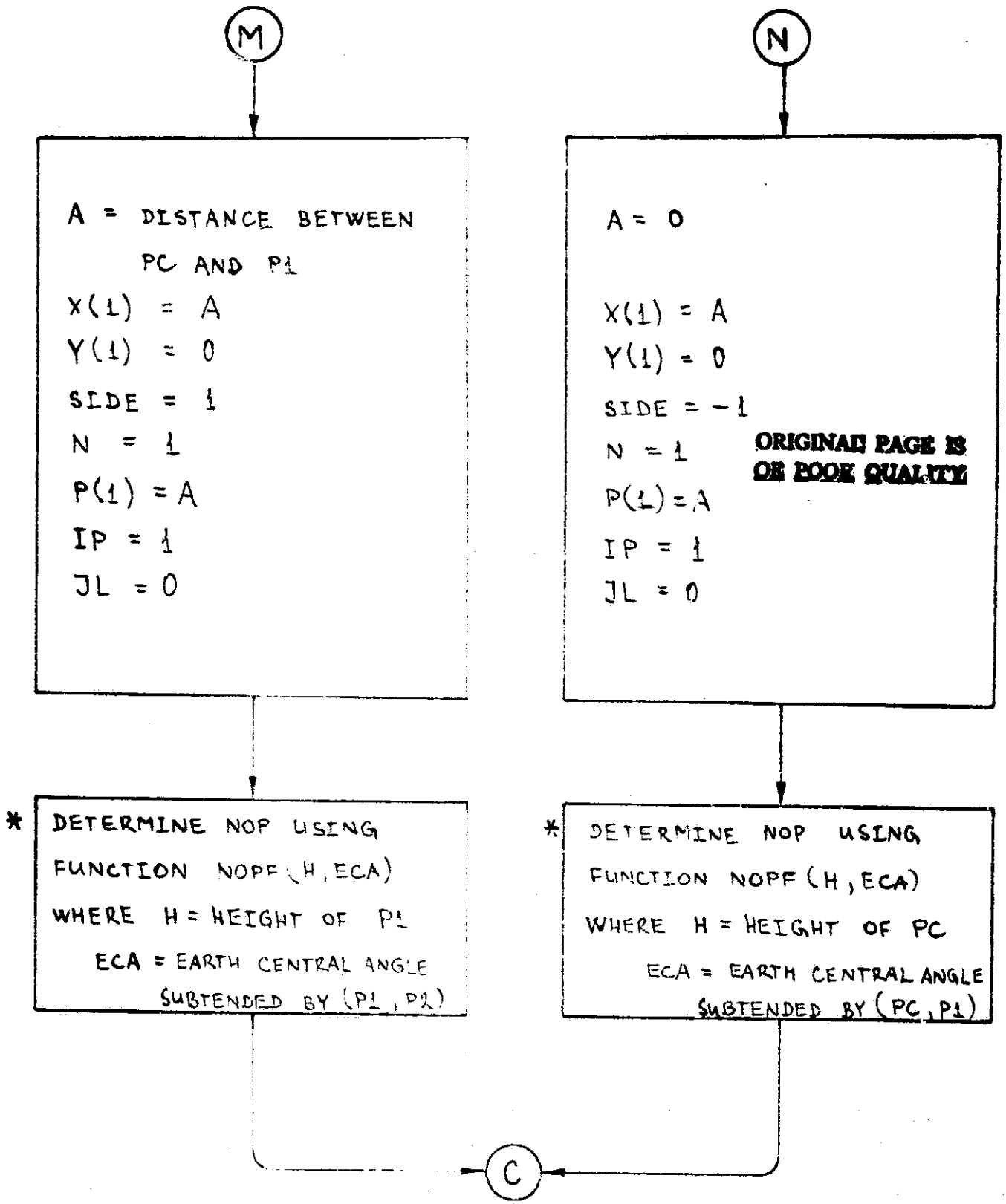

ORIGINAL PAGE IS OF POOR QUALITY

* NOP IS USUALLY ONE LESS THAN THE NUMBER OF POINTS NEEDED TO PROPERLY EVALUATE THE ELECTRON DENSITY DEVIATION FUNCTION BETWEEN TWO POINTS IN THE IONOSPHERE.

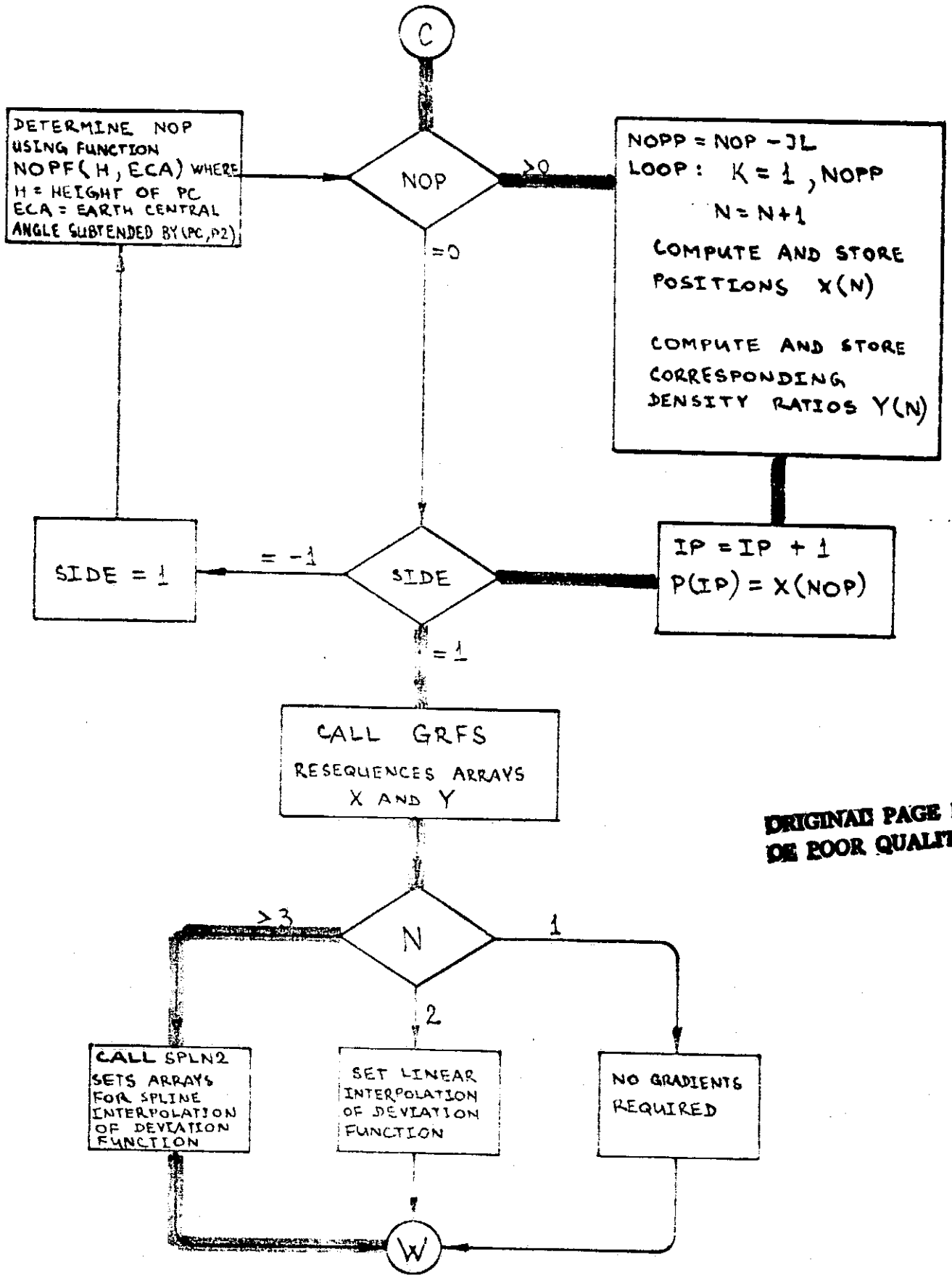

ORIGINAL PAGE IS OF POOR QUALITY

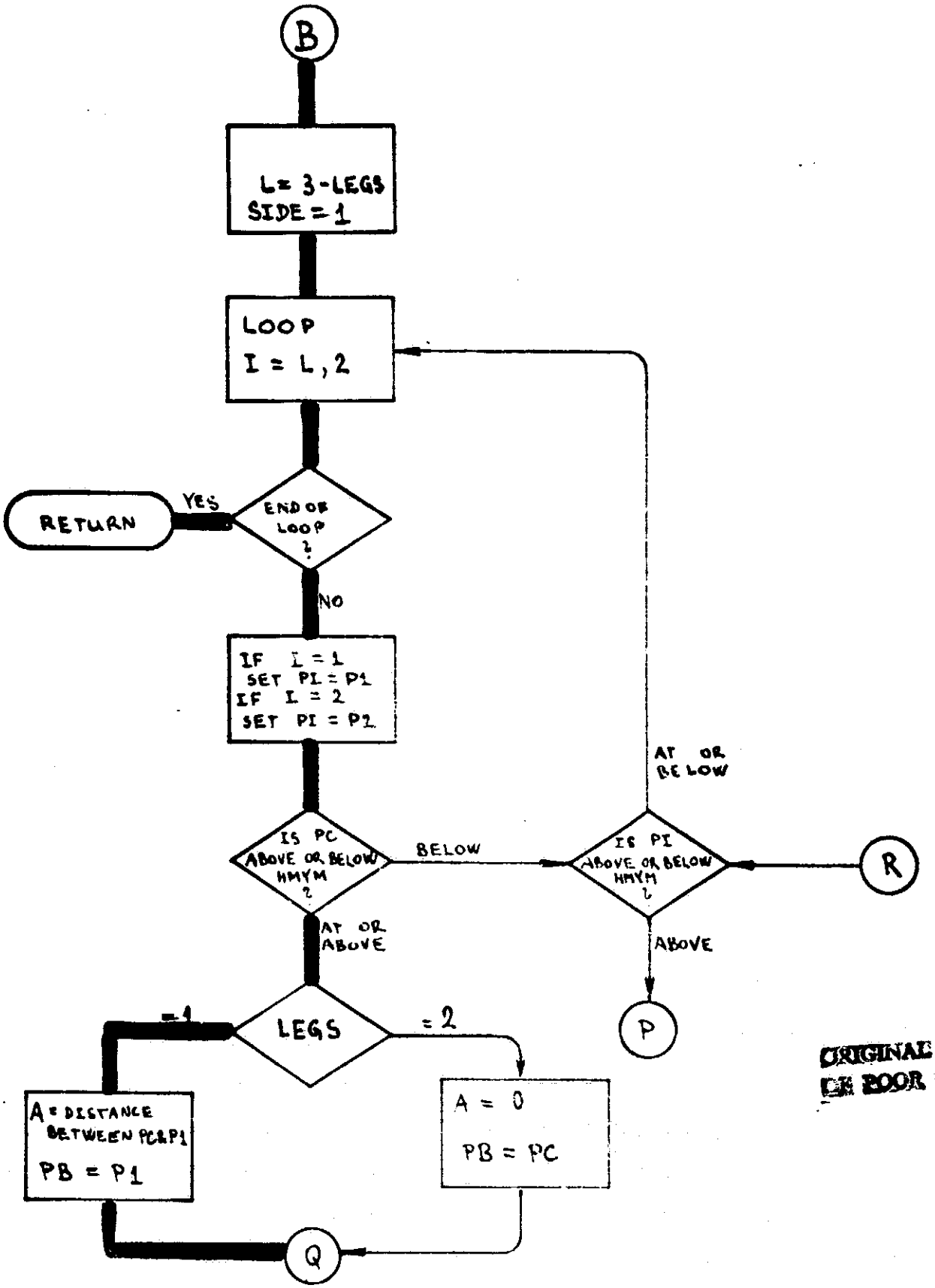

ORIGINAL PAGE IS
OF POOR QUALITY

CONVERGE TO BOTTOM OF IONOSPHERE HMYM

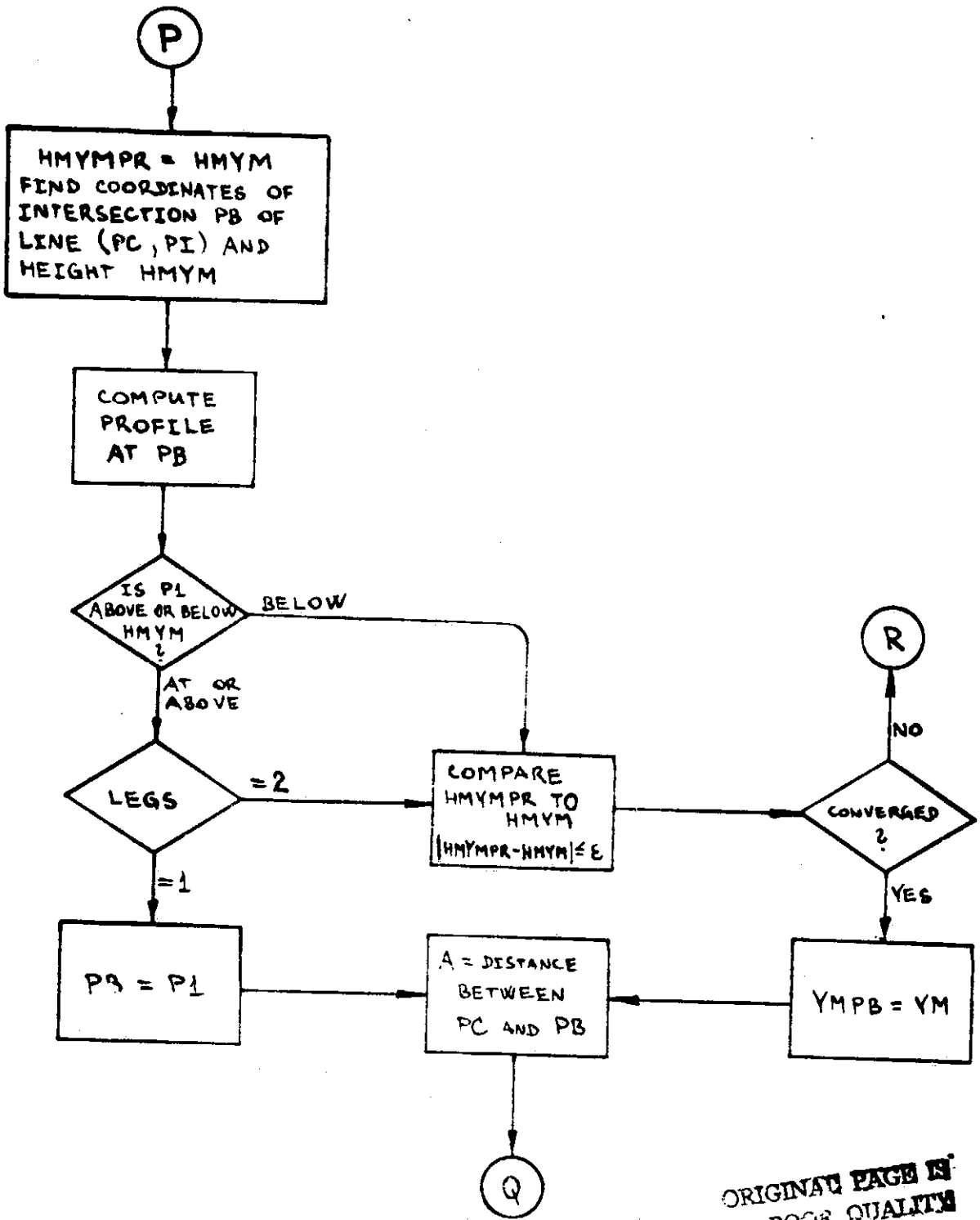

ORIGINAL PAGE IS
OF POOR QUALITY

CONVERGE TO HEIGHT OF MAXIMUM ELECTRON DENSITY HM

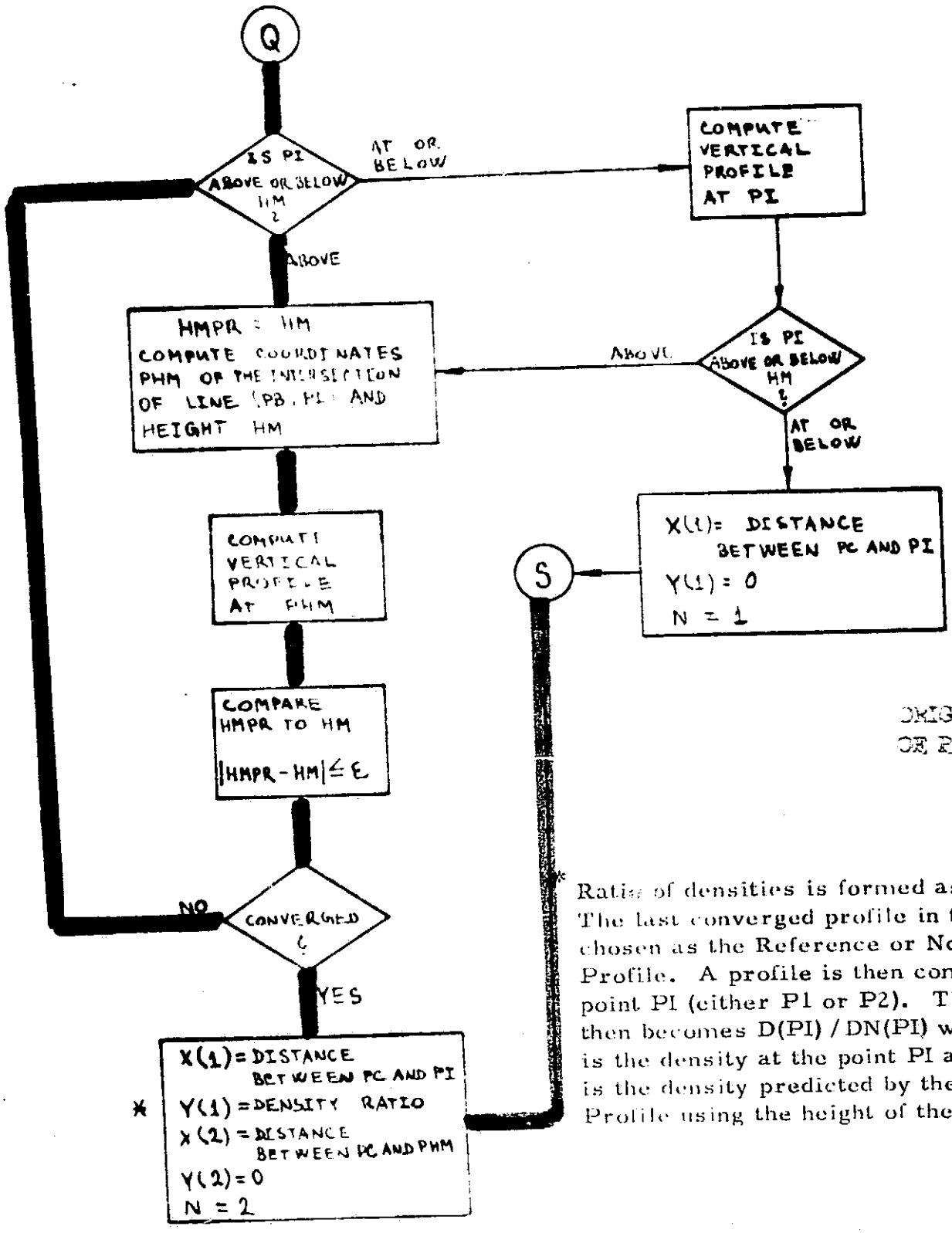

ORIGINAL PAGE IS
OF POOR QUALITY

* Ratios of densities is formed as follows: The last converged profile in the loop is chosen as the Reference or Normalized Profile. A profile is then computed at the point PI (either P1 or P2). The ratio Y(1) then becomes D(PI) / DN(PI) where D(PI) is the density at the point PI and DN(PI) is the density predicted by the Reference Profile using the height of the point PI.

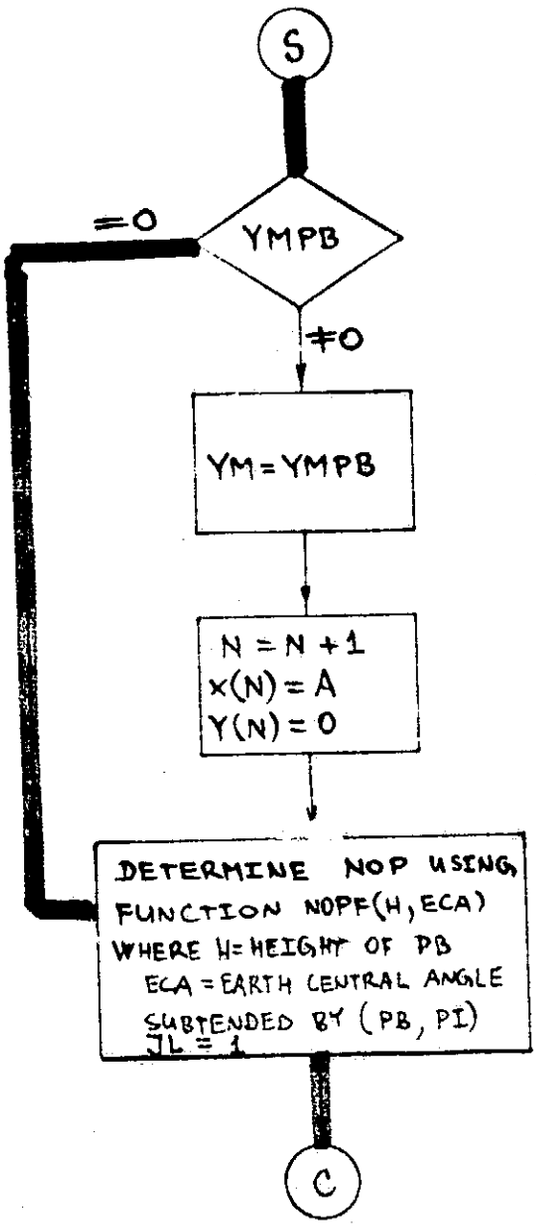

ORIGINAL PAGE IS
OF POOR QUALITY

C-2

INTEGRATOR 1

DETERMINE LIMITS OF INTEGRATION

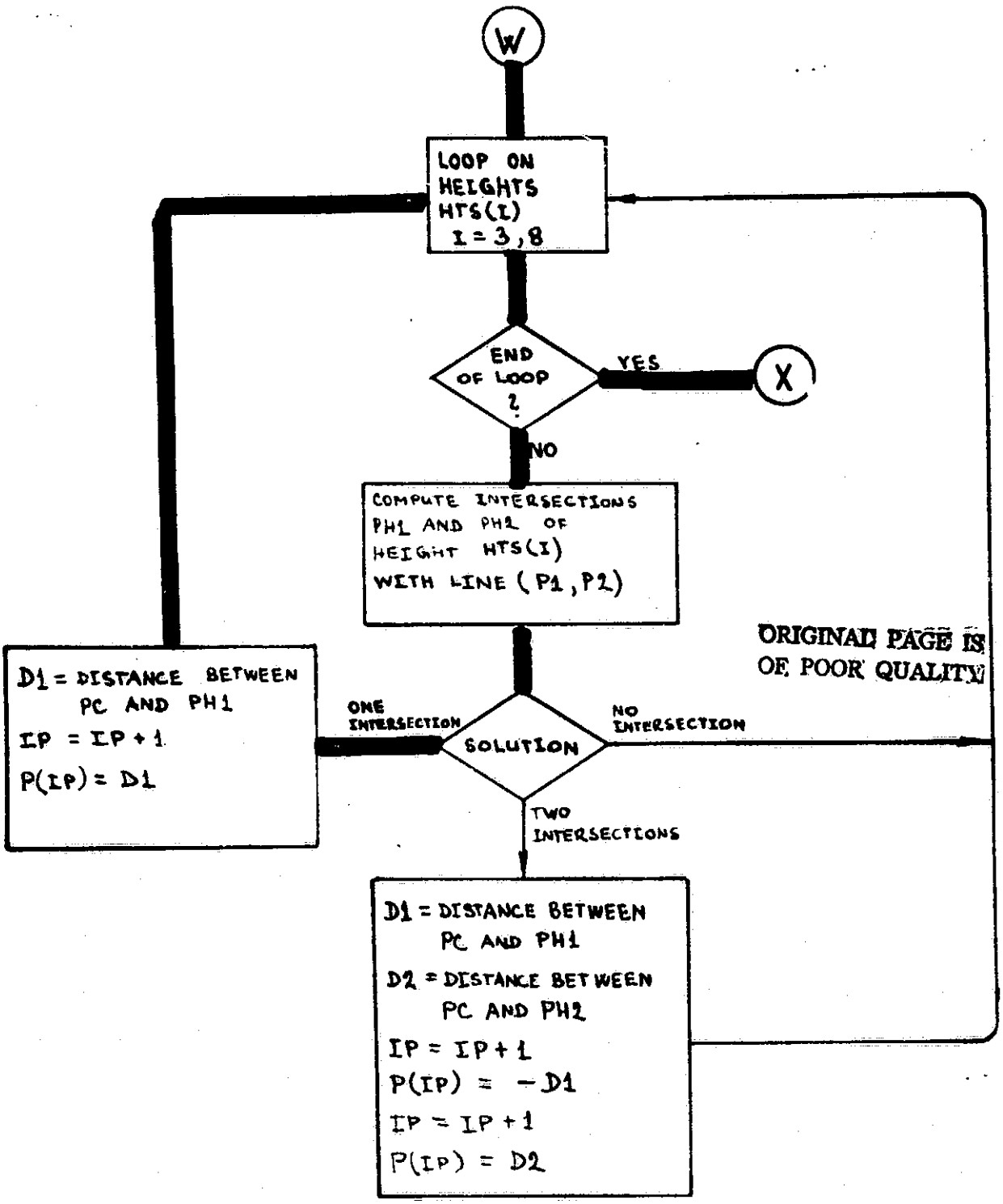

ORIGINAL PAGE IS OF POOR QUALITY

INTEGRATOR 2

PERFORM NUMERICAL INTEGRATION OF TOTAL ELECTRON CONTENT

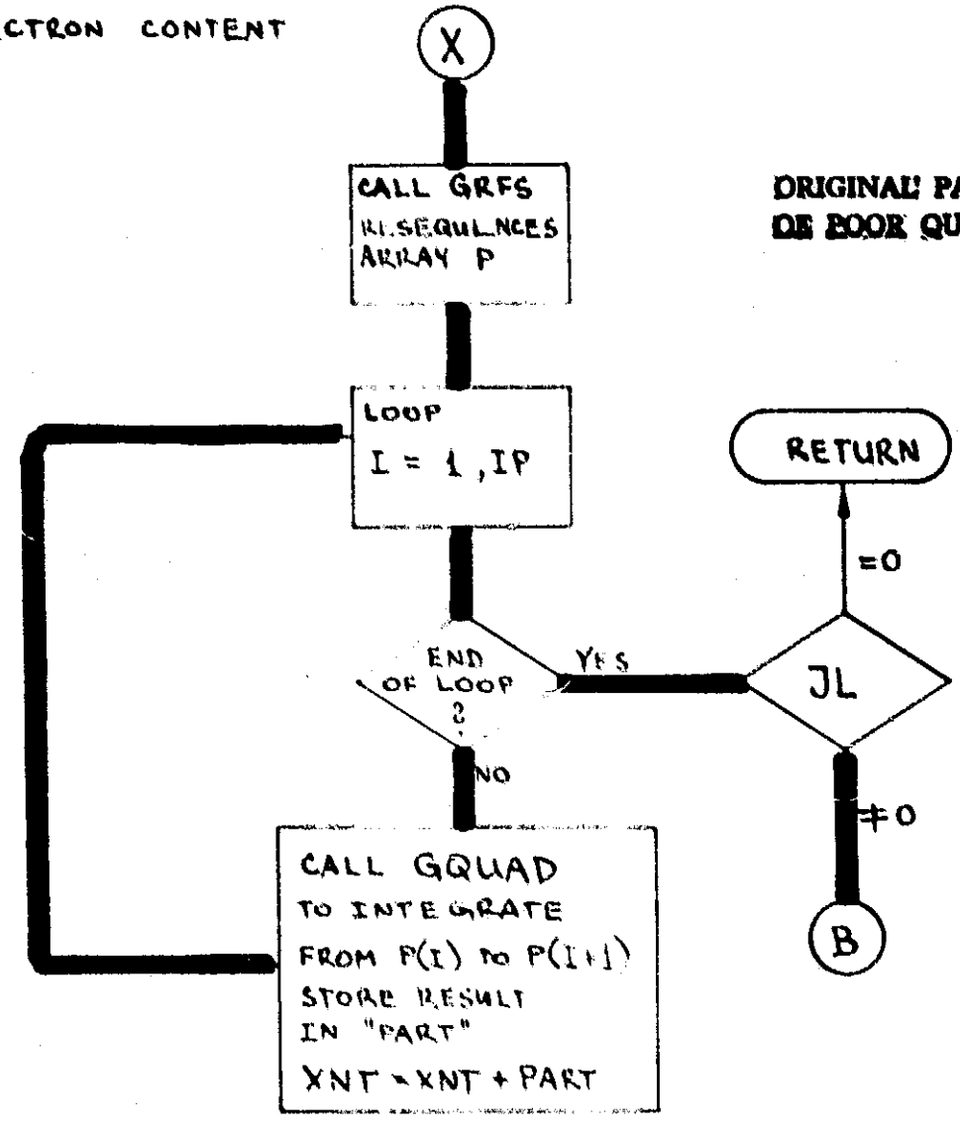

ORIGINAL PAGE IS
OF POOR QUALITY

APPENDIX E

SUBROUTINE IONSST

Flow diagram for Case 4 (Figure 9)

ORIGINAL PAGE IS
OF POOR QUALITY

PRECEDING PAGE BLANK NOT FILMED

ORIGINAL PAGE IS OF POOR QUALITY

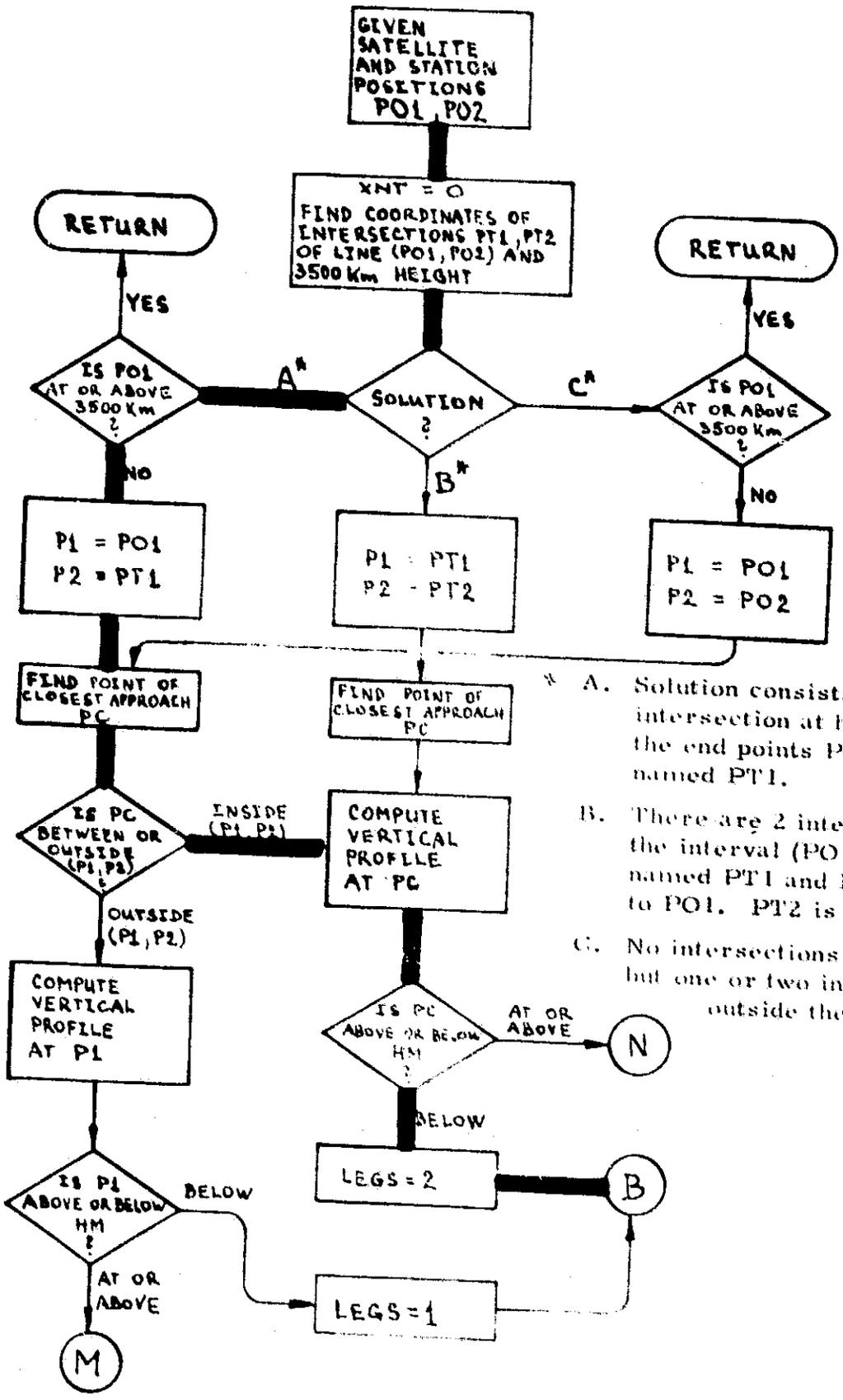

* A. Solution consists of one point of intersection at height 3500 km between the end points PO1 and PO2. It is named PT1.

B. There are 2 intersection points inside the interval (PO1, PO2). They are named PT1 and PT2. PT1 is closer to PO1. PT2 is closer to PO2.

C. No intersections between PO1 and PO2, but one or two intersections may exist outside the interval.

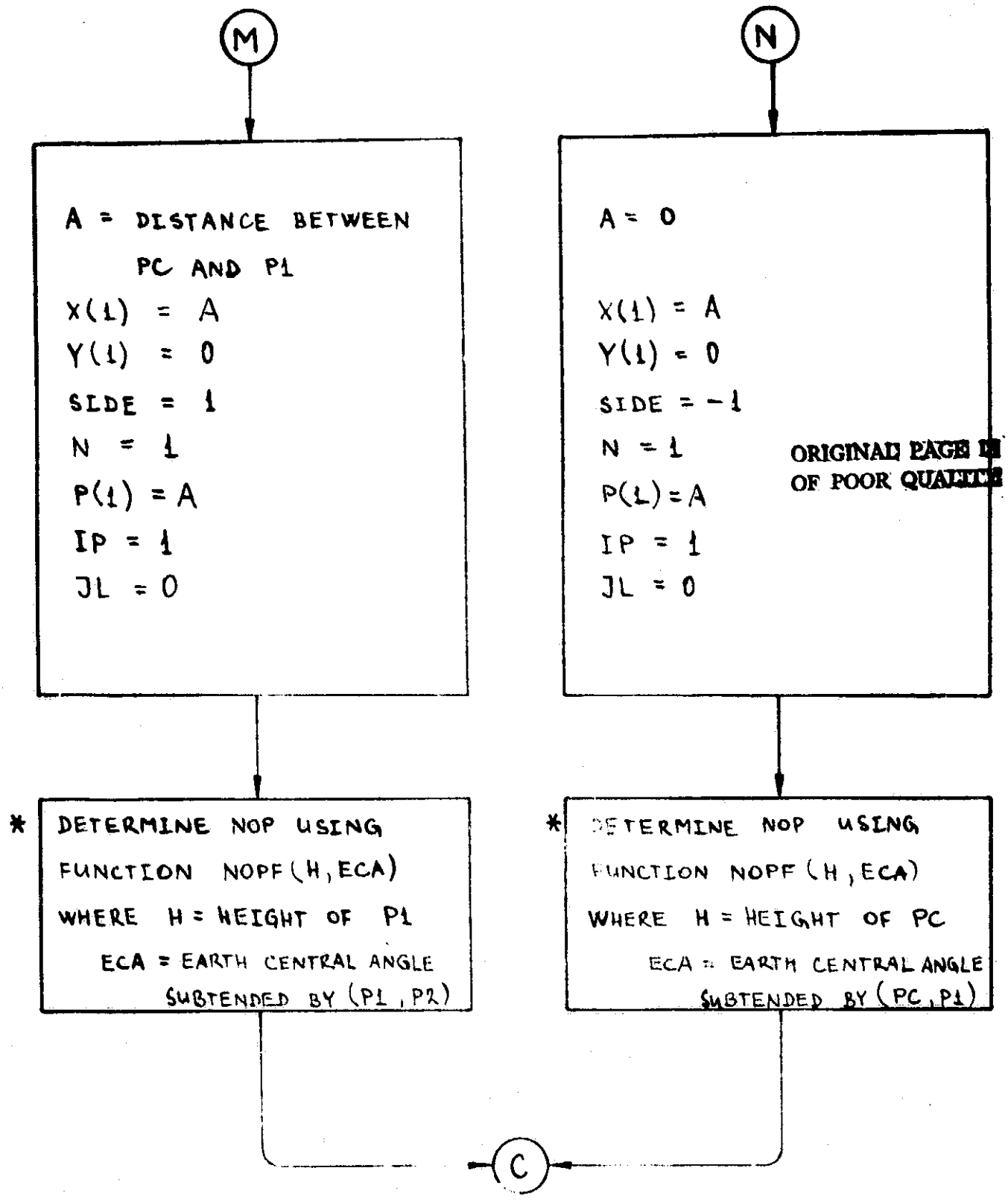

ORIGINAL PAGE IS OF POOR QUALITY

* NOP IS USUALLY ONE LESS THAN THE NUMBER OF POINTS NEEDED TO PROPERLY EVALUATE THE ELECTRON DENSITY DEVIATION FUNCTION BETWEEN TWO POINTS IN THE IONOSPHERE.

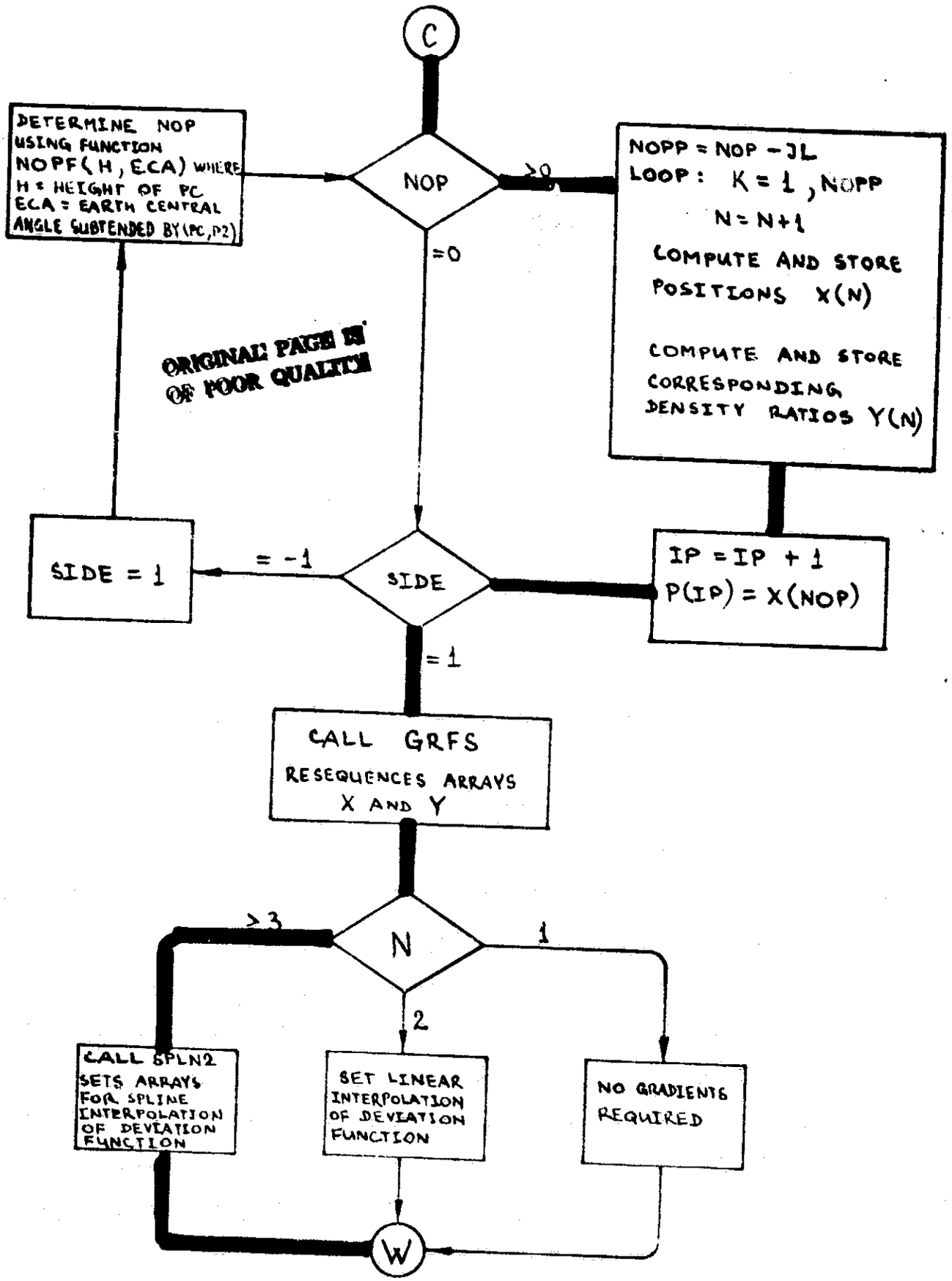

ORIGINAL PAGE IS OF POOR QUALITY

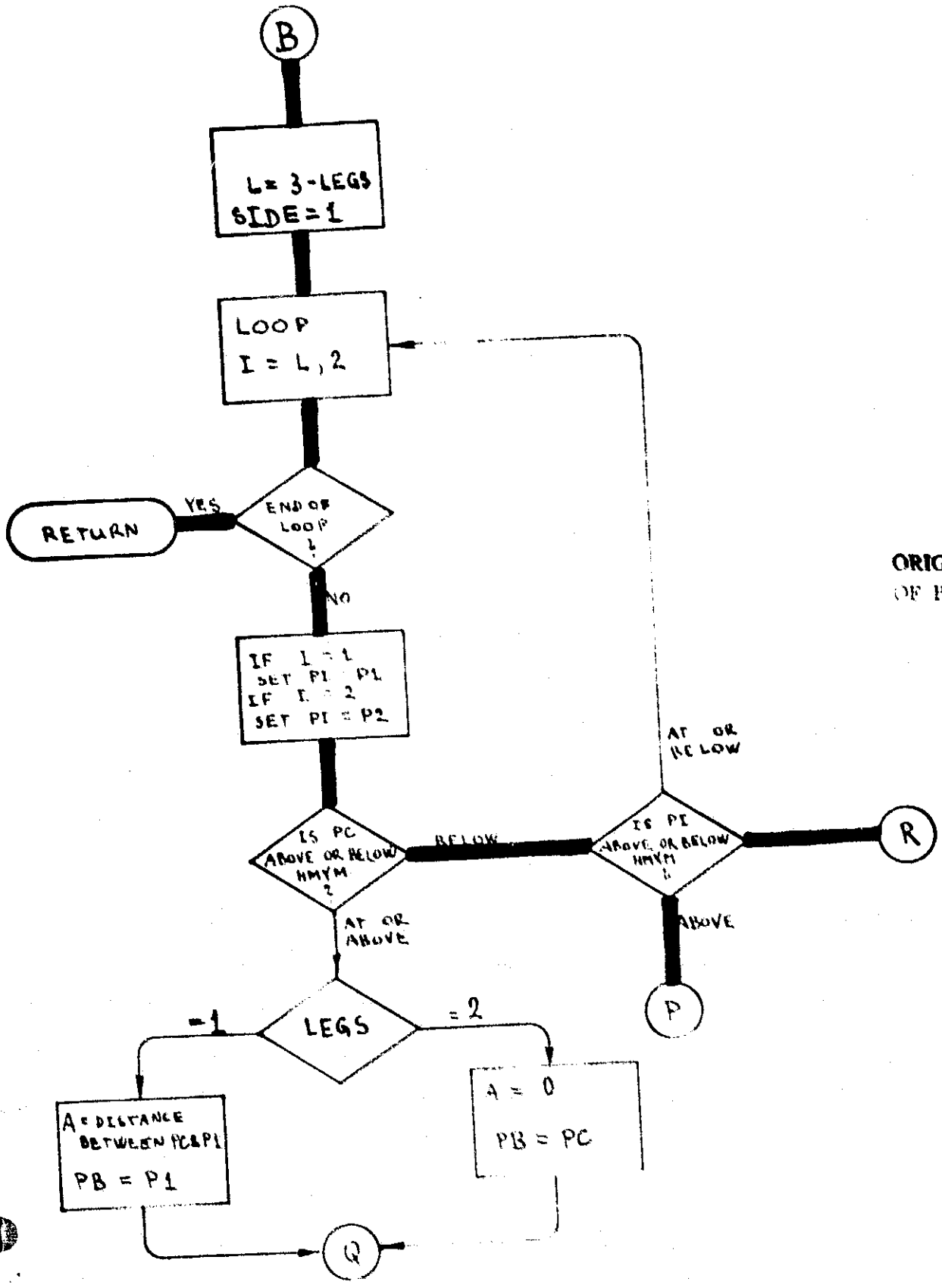

ORIGINAL PAGE IS
OF POOR QUALITY

CONVERGE TO BOTTOM OF IONOSPHERE HMYM

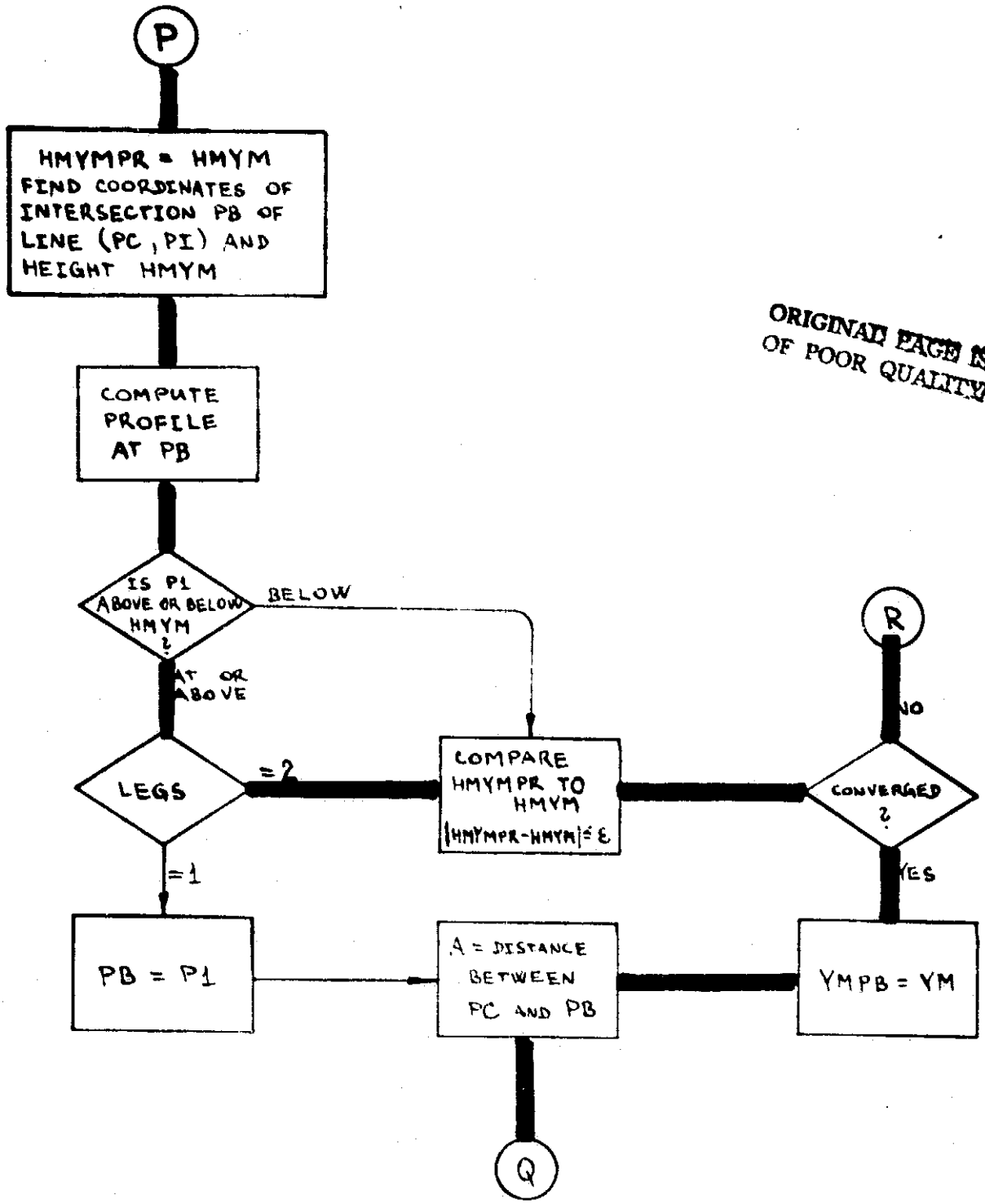

ORIGINAL PAGE IS OF POOR QUALITY

CONVERGE TO HEIGHT OF MAXIMUM ELECTRON DENSITY HM

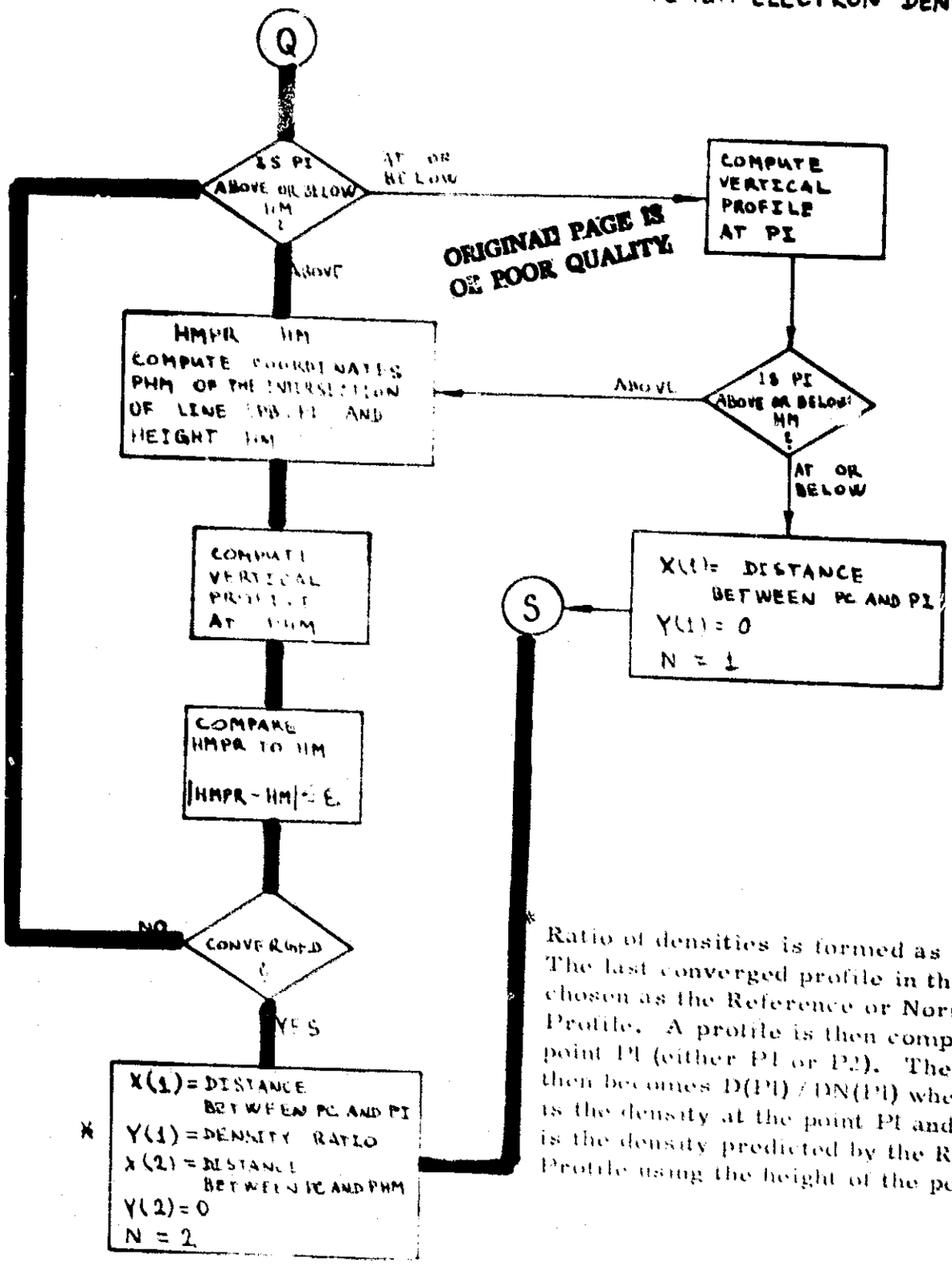

* Ratio of densities is formed as follows: The last converged profile in the loop is chosen as the Reference or Normalized Profile. A profile is then computed at the point PI (either PI or P2). The ratio Y(1) then becomes D(PI) / DN(PI) where D(PI) is the density at the point PI and DN(PI) is the density predicted by the Reference Profile using the height of the point PI.

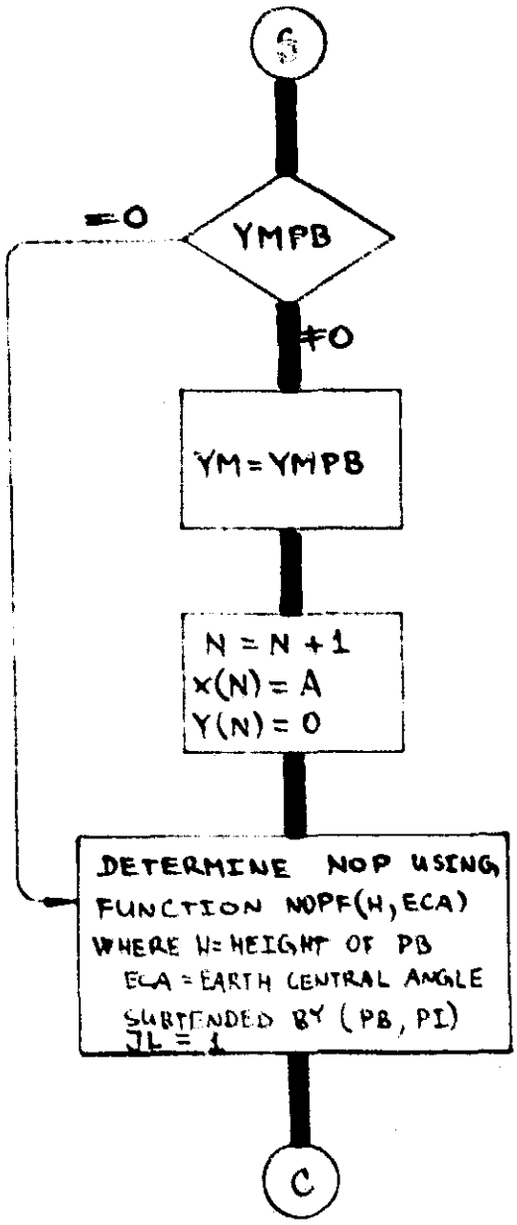

ORIGINAL PAGE IS
OF POOR QUALITY

INTEGRATOR 1

DETERMINE LIMITS OF INTEGRATION

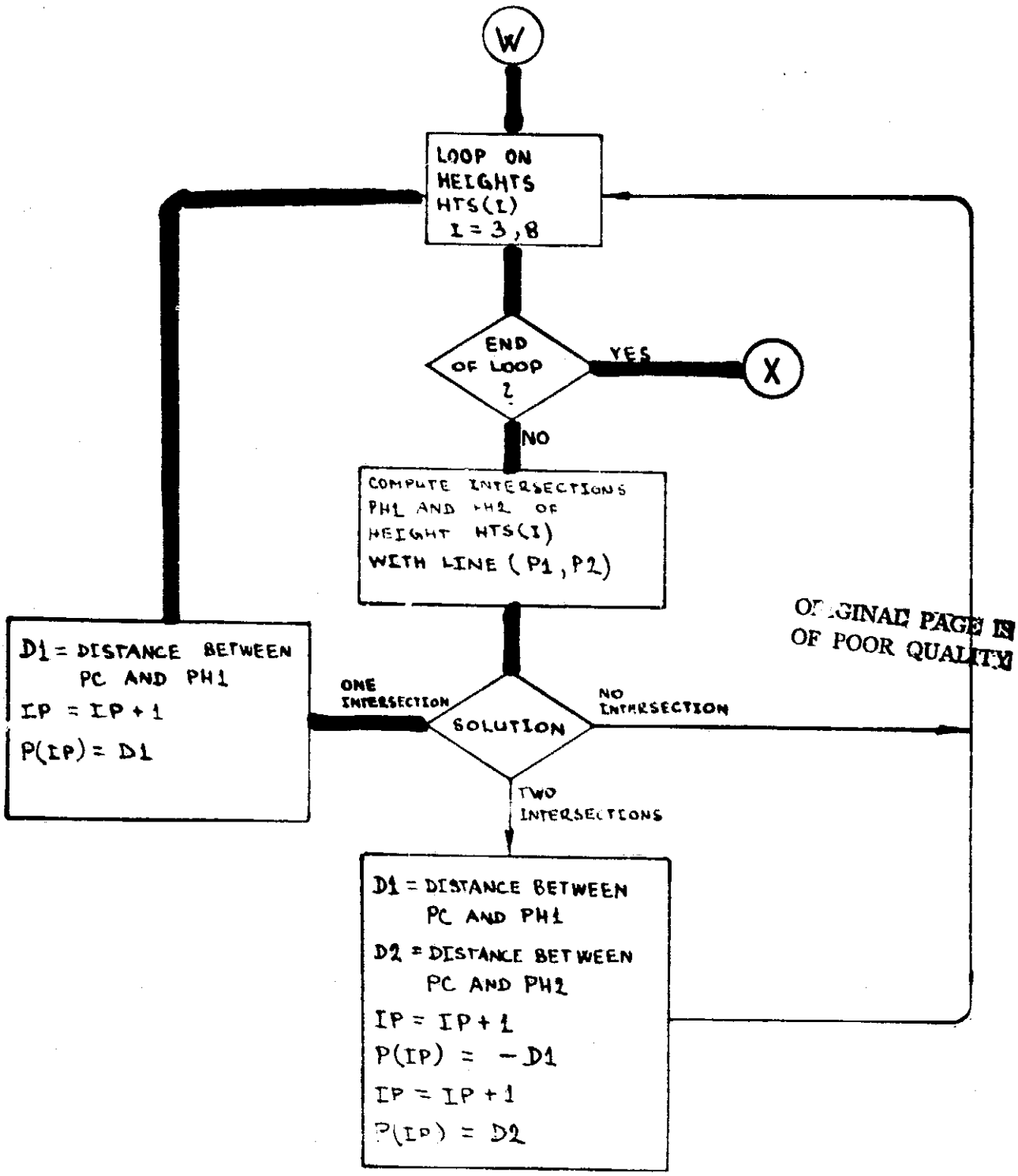

ORIGINAL PAGE IS OF POOR QUALITY

INTEGRATOR 2

PERFORM NUMERICAL INTEGRATION OF TOTAL ELECTRON CONTENT

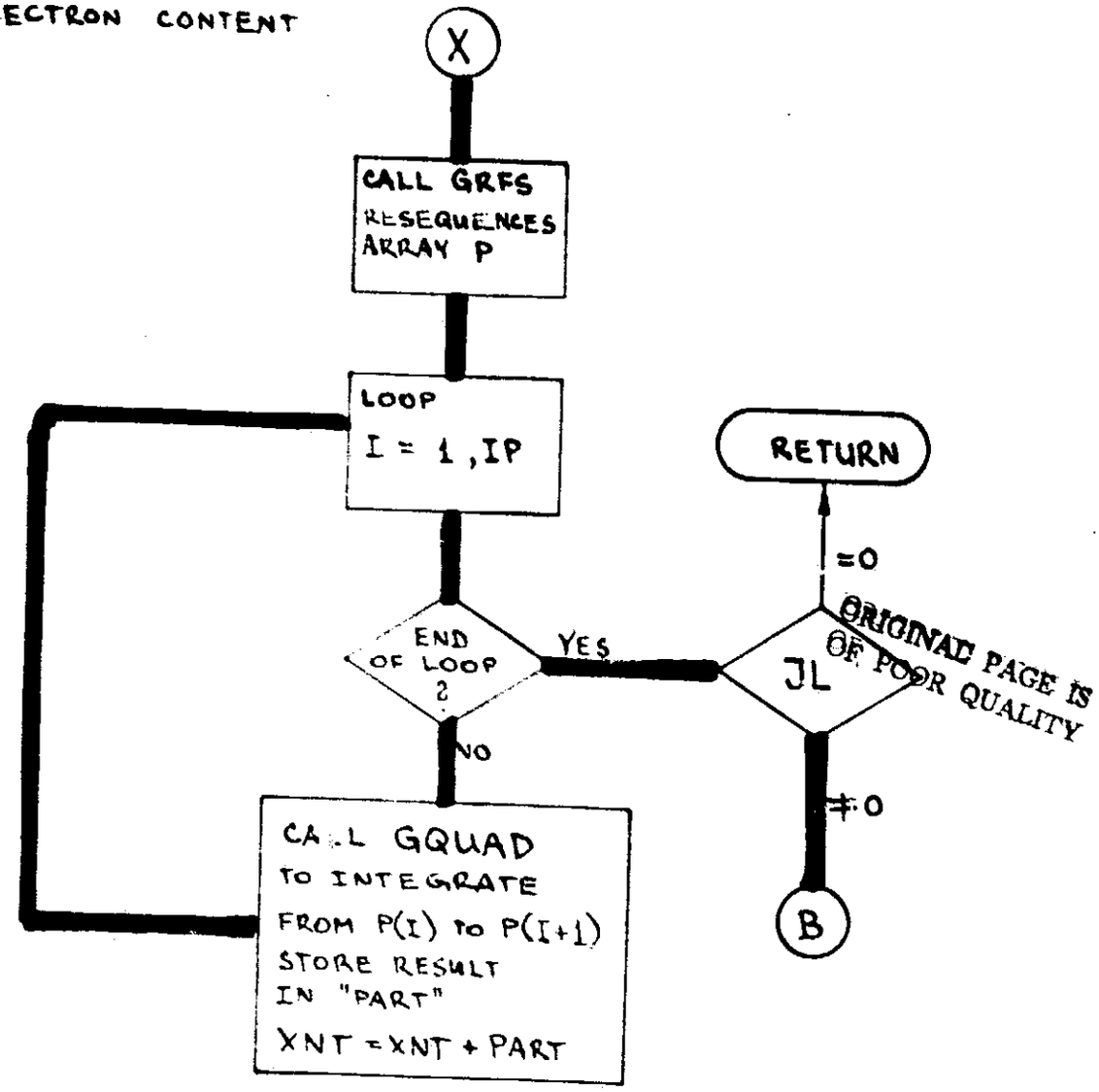

ORIGINAL PAGE IS
OF POOR QUALITY

APPENDIX F

SUBROUTINE IONSST

Flow diagram for Case 5 (Figure 10)

ORIGINAL PAGE IS
OF POOR QUALITY

PRECEDING PAGE BLANK NOT FILMED

ORIGINAL PAGE IS OF POOR QUALITY

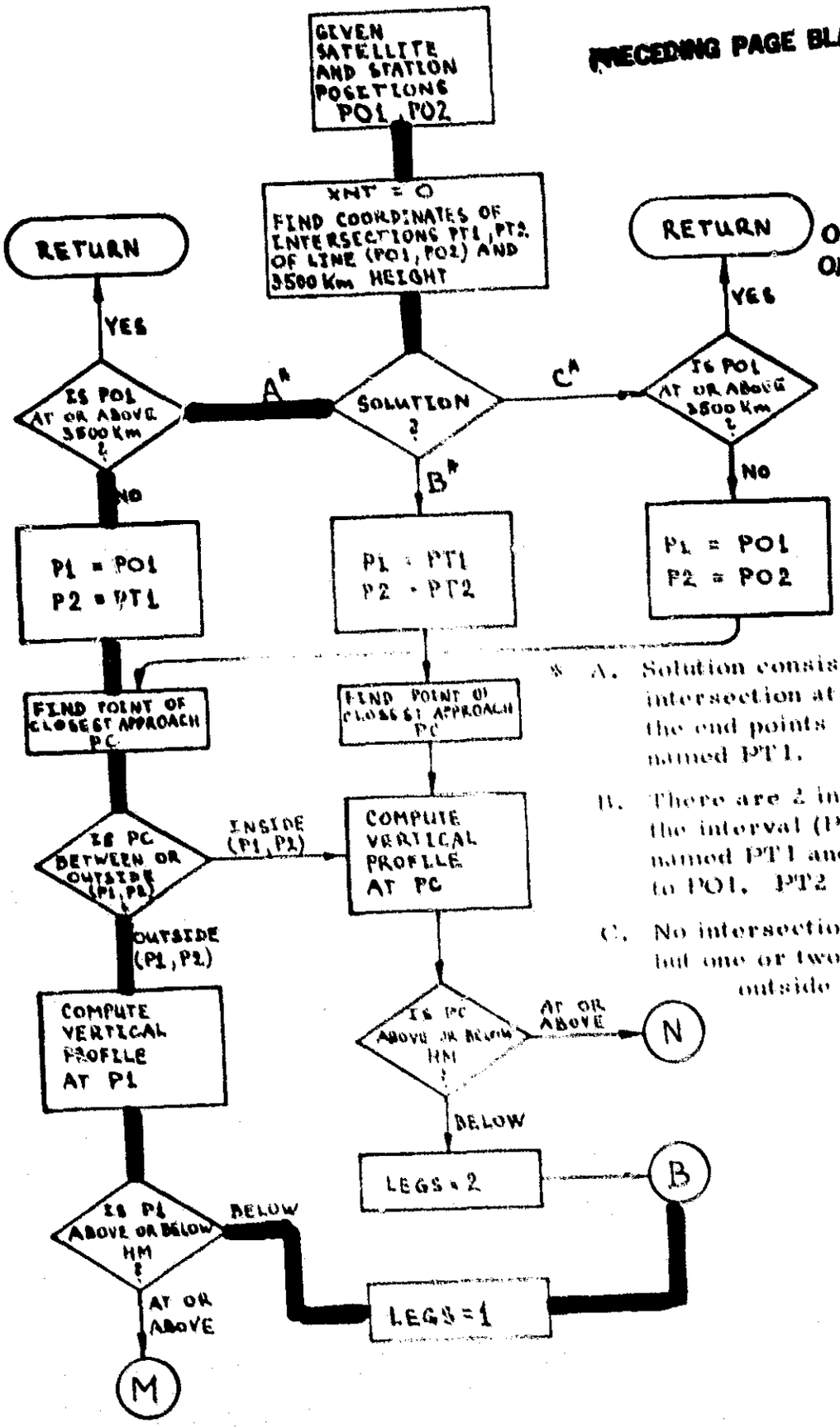

A. Solution consists of one point of intersection at height 3500 km between the end points PO1 and PO2. It is named PT1.

B. There are 2 intersection points inside the interval (PO1, PO2). They are named PT1 and PT2. PT1 is closer to PO1. PT2 is closer to PO2.

C. No intersections between PO1 and PO2, but one or two intersections may exist outside the interval.

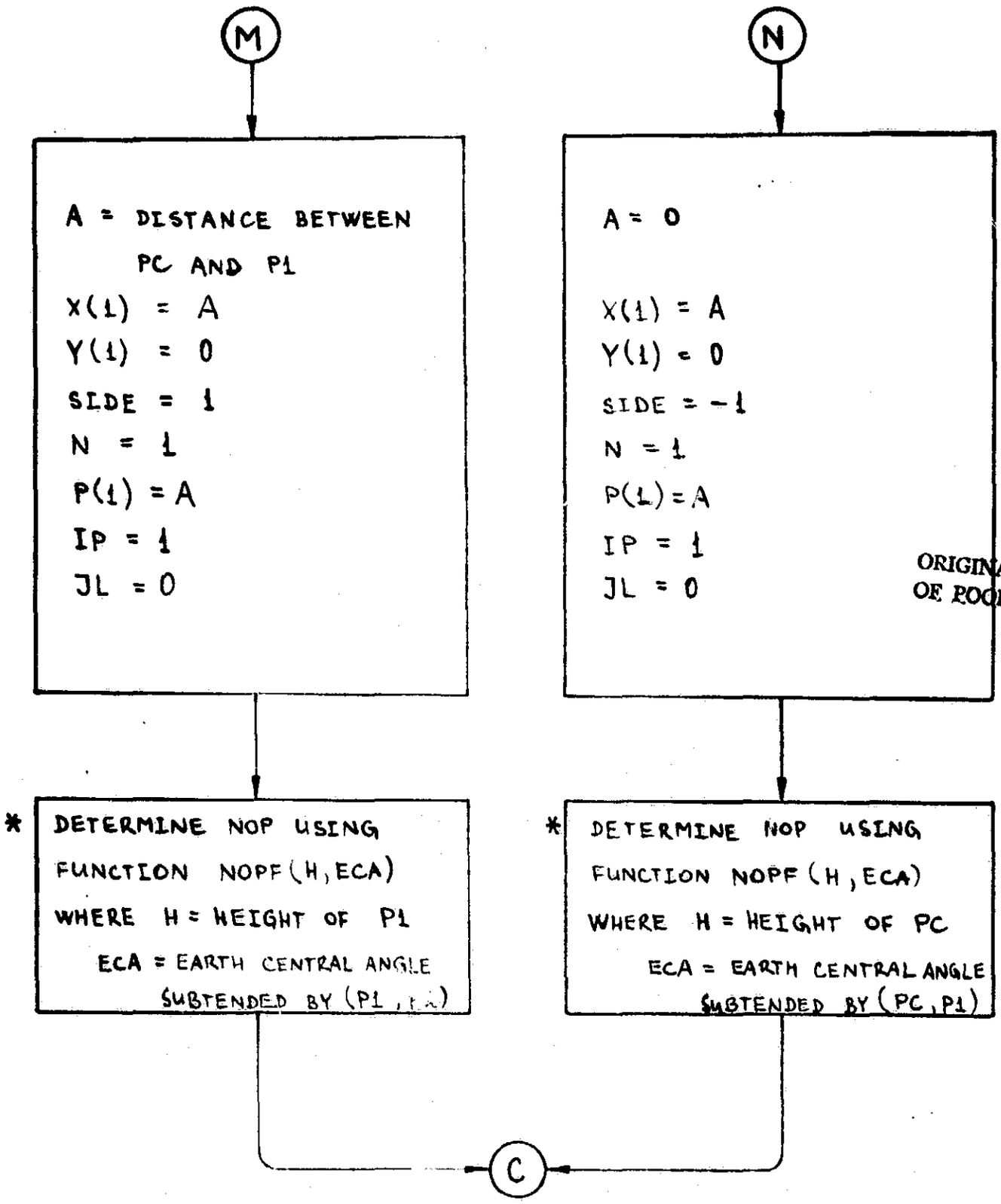

ORIGINAL PAGE
OF POOR QUALITY

* NOP IS USUALLY ONE LESS THAN THE NUMBER OF POINTS NEEDED TO PROPERLY EVALUATE THE ELECTRON DENSITY DEVIATION FUNCTION BETWEEN TWO POINTS IN THE IONOSPHERE.

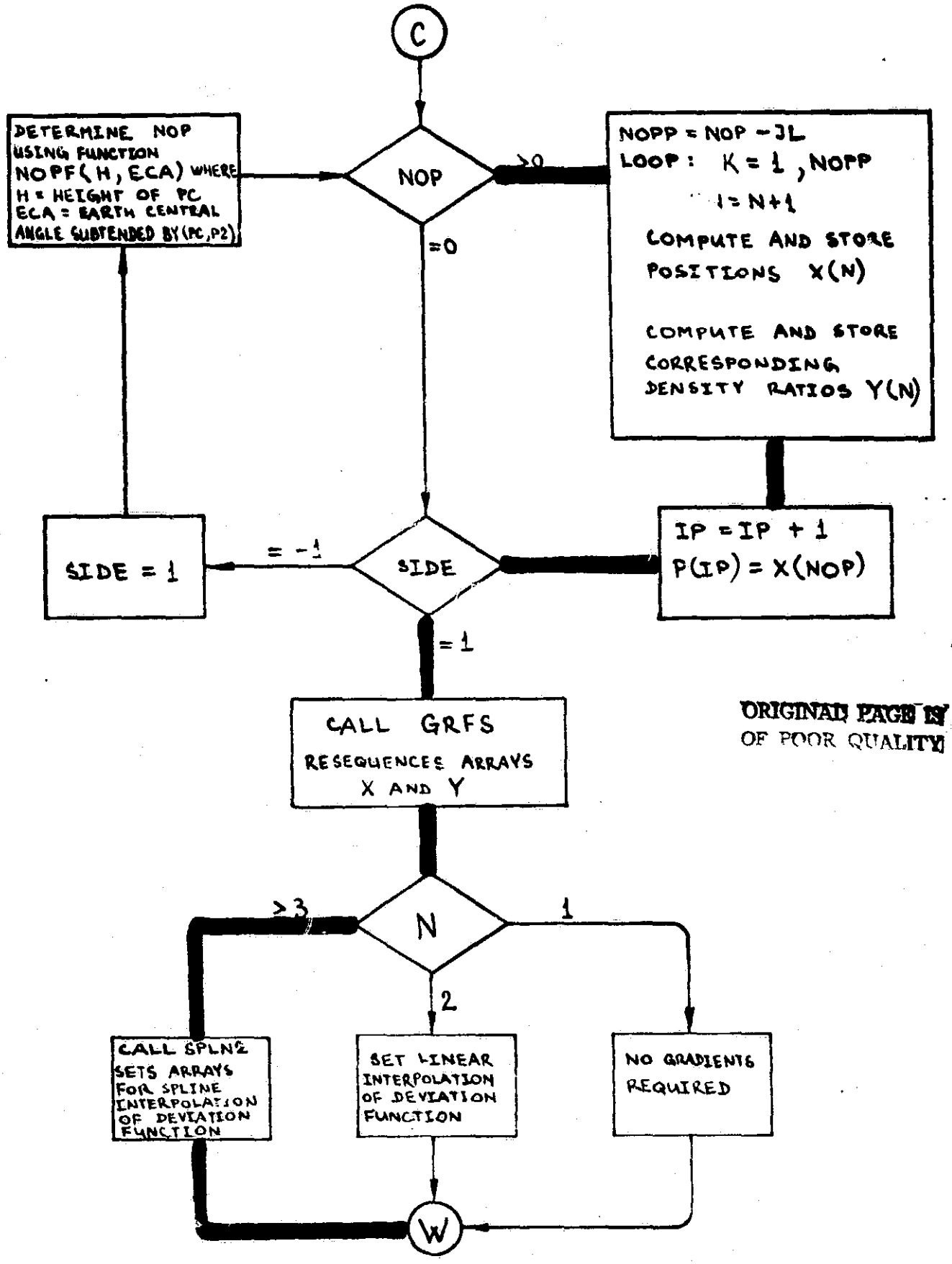

ORIGINAL PAGE IS
OF POOR QUALITY

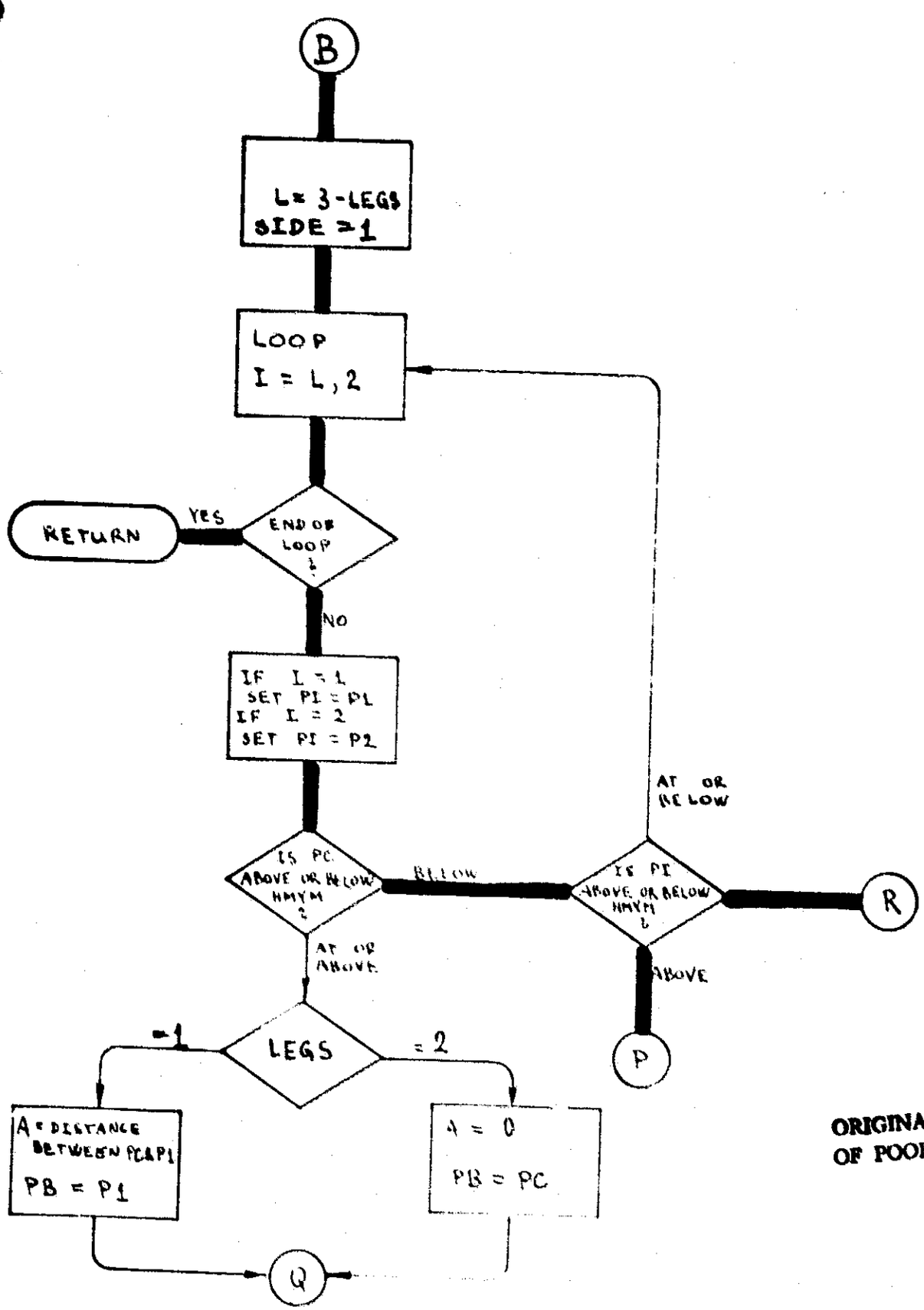

ORIGINAL PAGE IS
OF POOR QUALITY

CONVERGE TO BOTTOM OF IONOSPHERE HMYM

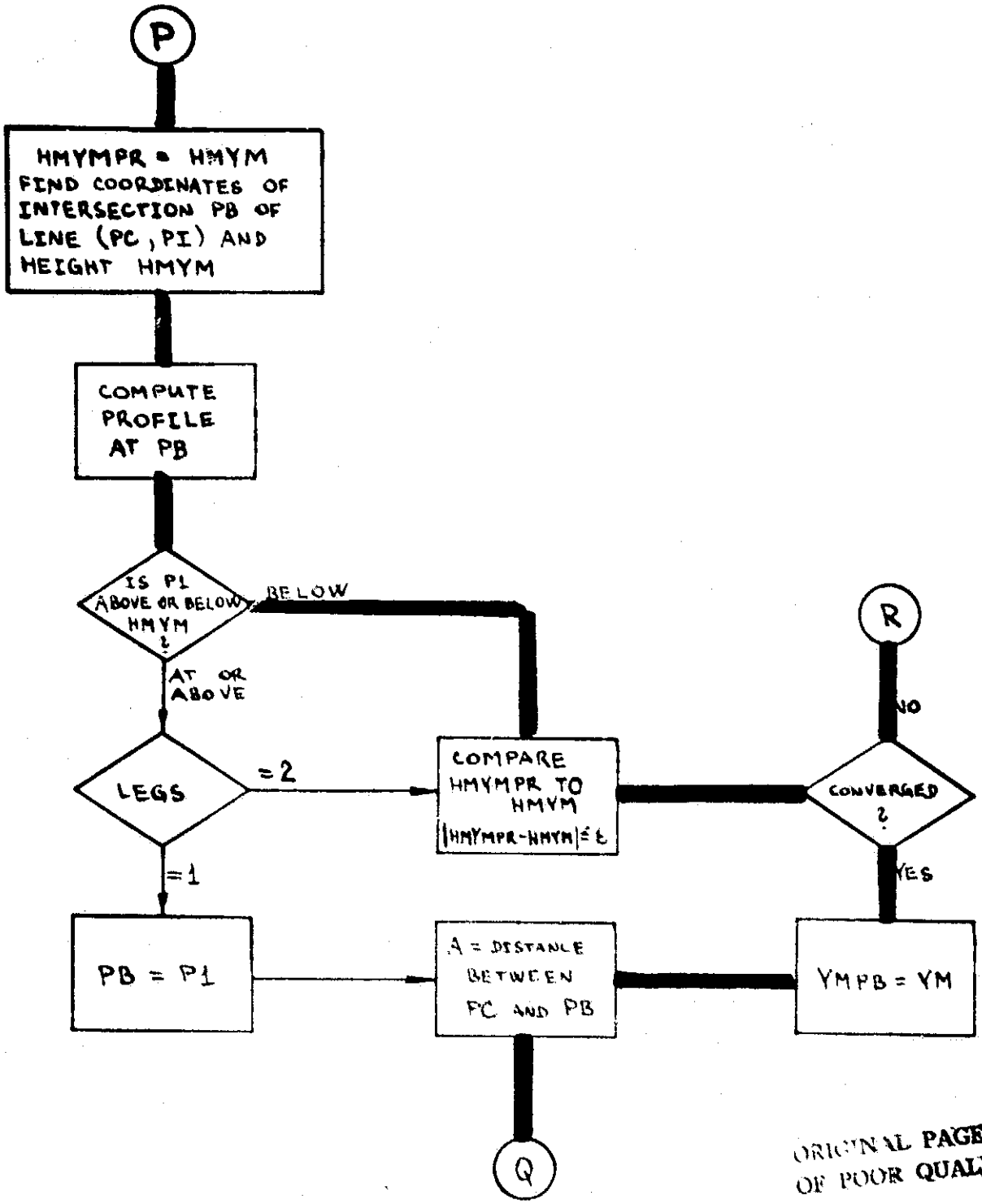

ORIGINAL PAGE IS
OF POOR QUALITY

CONVERGE TO HEIGHT OF MAXIMUM ELECTRON DENSITY HM

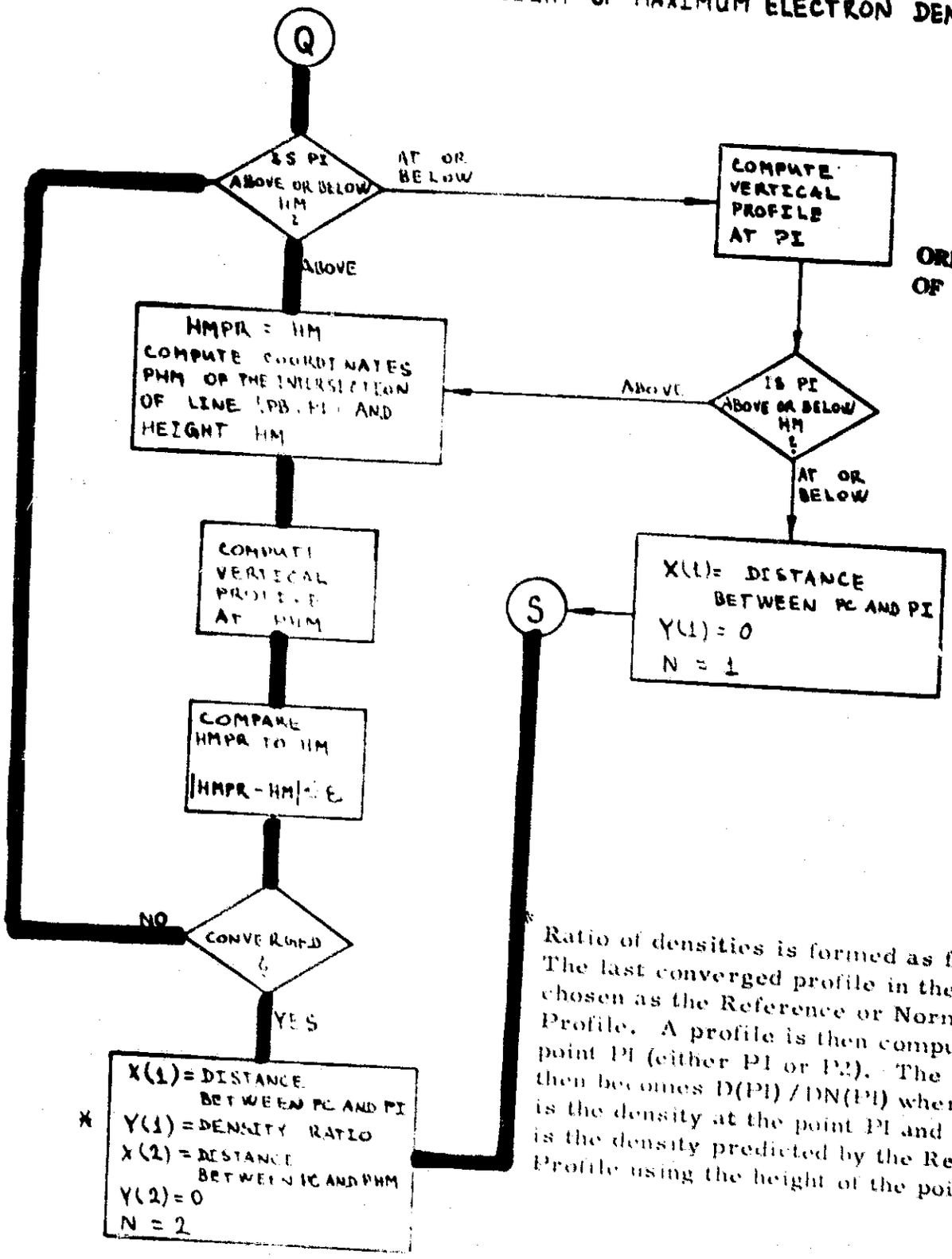

ORIGINAL PAGE IS OF POOR QUALITY

* Ratio of densities is formed as follows: The last converged profile in the loop is chosen as the Reference or Normalized Profile. A profile is then computed at the point PI (either PI or P2). The ratio Y(1) then becomes D(PI) / DN(PI) where D(PI) is the density at the point PI and DN(PI) is the density predicted by the Reference Profile using the height of the point PI.

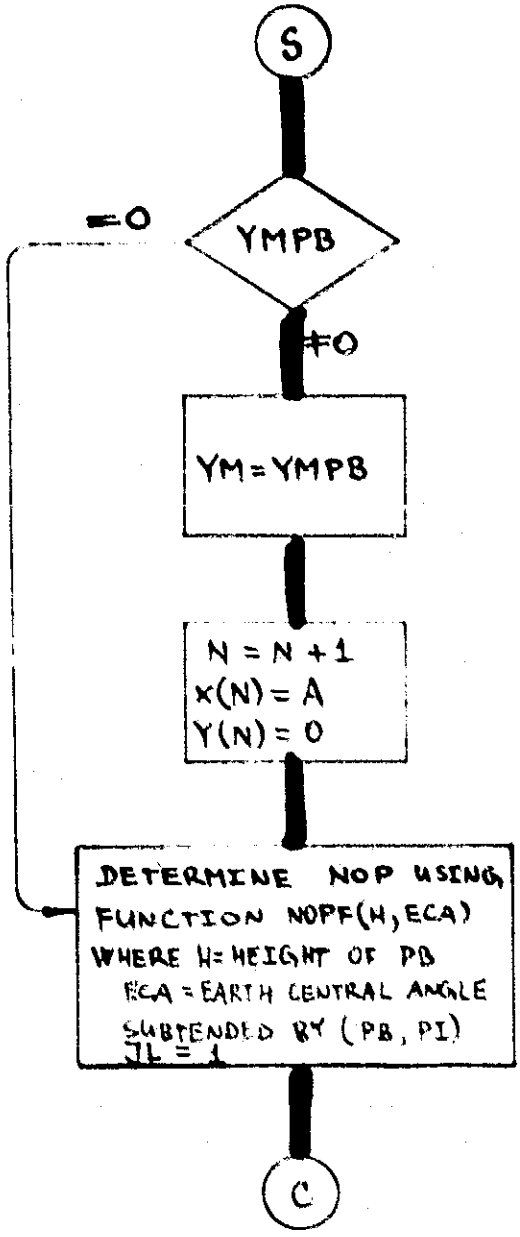

ORIGINAL PAGE IS
OF POOR QUALITY

INTEGRATOR 1

DETERMINE LIMITS OF INTEGRATION

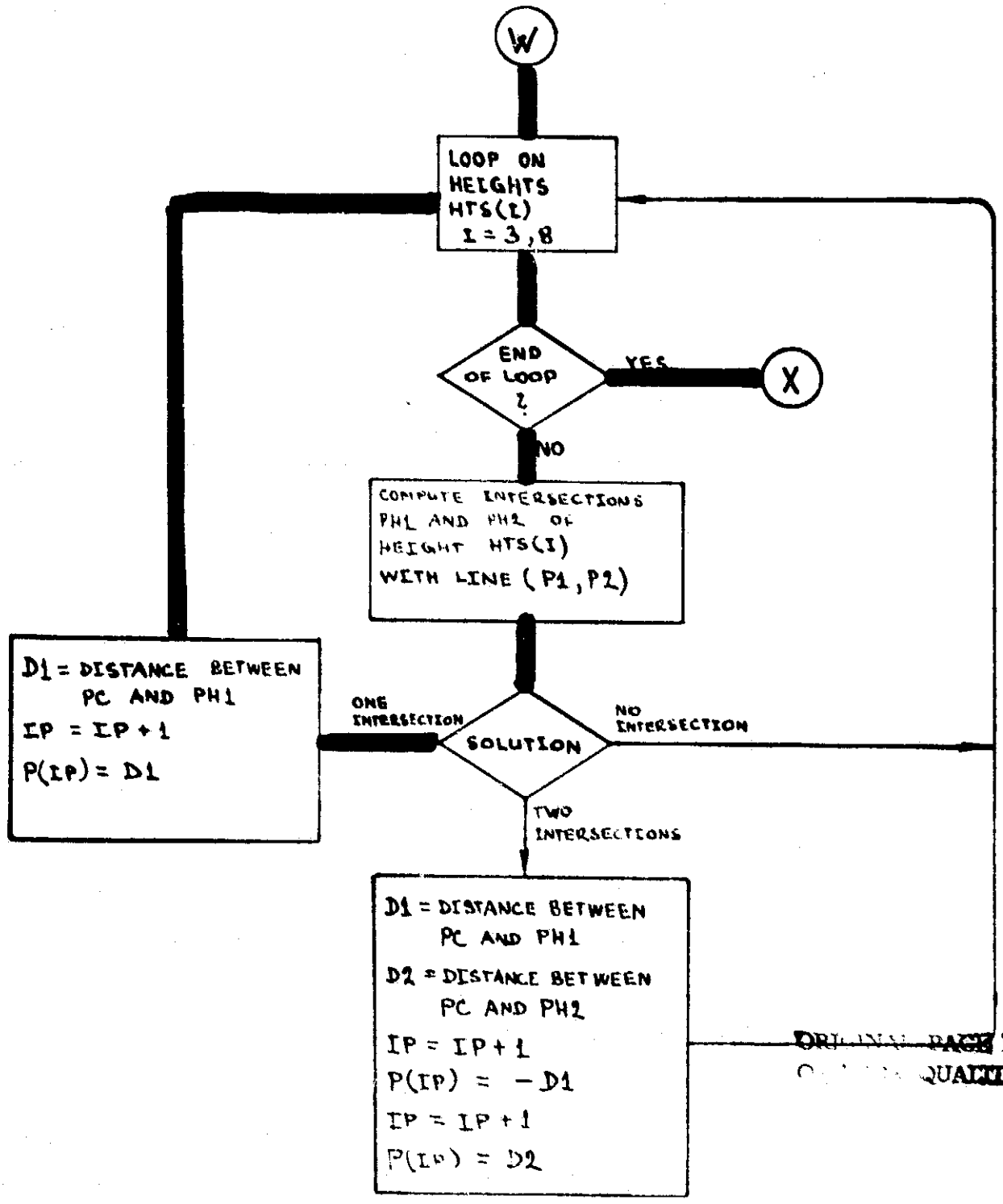

ORIGINAL PAGE IS OF POOR QUALITY

INTEGRATOR 2

PERFORM NUMERICAL INTEGRATION OF TOTAL ELECTRON CONTENT

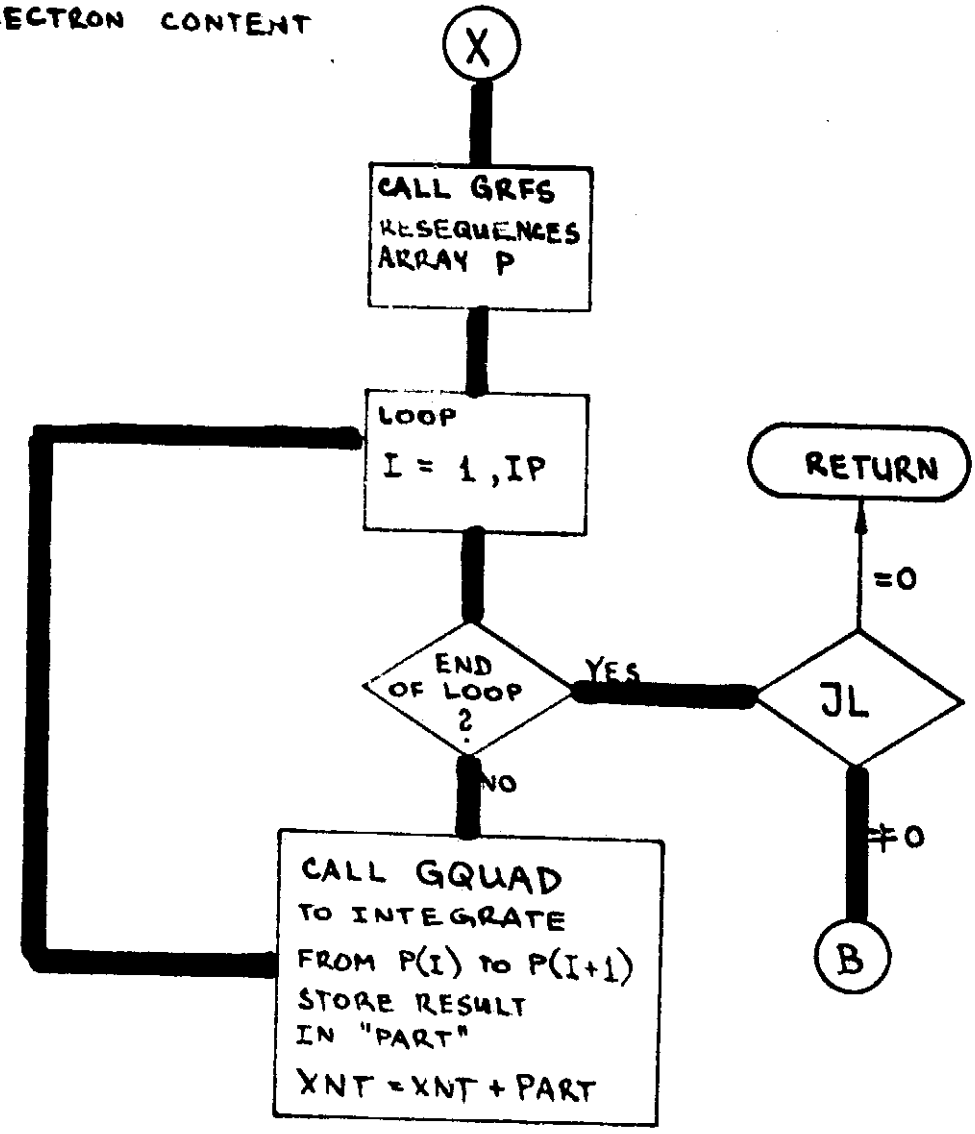

ORIGINAL PAGE IS
OF POOR QUALITY

APPENDIX G

JCL AND JOB SET-UP FOR SATELLITE TO SATELLITE IONOSPHERE RUNS

PRECEDING PAGE BLANK NOT FILMED

JCL SETUP TO RUN IONOSPHERIC CORRECTION IN SST MODE

```
//ZGJKKGD6 JOB (GS0031311G,T,G00001,008013),ZG,MSGLEVEL=(1,1)
//*MAIN CLASS=OVERNITE
//*MAIN LINES=25
// EXEC PGM=PACKUPD,REGION=180K
//STEPLIB DD DSN=GDJLM.UTIL.LCAD,DISP=SHR
//SYSPRINT DD SYSOUT=A
//SYSIN DD DDNAME=DATA5
//PACKIN DD DSN=ORBIT.GTDS.RD.FORT,DISP=SHR
//SEQOUT DD DSN=&SCR,DISP=(MOD,PASS),
//        SPACE=(CYL,(5,1),RLSE),UNIT=DISK
//SUBRLIST DD SYSOUT=A,SPACE=(CYL,(0,5),RLSE),UNIT=(DISK,3)
//PDSUP.DATA5 DD *
$SST
  (modifications)
$SSTCNS
  (modifications)
/*
```

ORIGINAL PAGE IS
OF POOR QUALITY

Satellite to satellite subroutines SST and SSTCNS are modified using the procedure PACKUPD. The subroutines are members of the data set ORBIT.GTDS.RD.FORT containing the source decks of the R&D version of GTDS. This data set is the procedure input data set as specified by the DD card PACKIN. The output data set specified by DD card SEQOUT carries the temporary name &SCR and contains the updated routines SST and SSTCNS. It is passed to the next job step where other subroutines are added.

```
// EXEC UCLEG,PARM.LINK='LET,LIST,MAP,OVLY,SIZE=(340K,56K)',
//        REGION.LINK=350K,REGION.GO=550K
//PDSUP.DATA5 DD *
```

Other subroutines to be modified are members of the data set ORBIT. GTDS.SORSLIB.FORT containing the source decks of the operational version of GTDS. In the first step of procedure UCLEG they are modified and added to the data set &SCR. In the second step of UCLEG the subroutines in &SCR are compiled and passed to the linkage editor.

$ASC
(modification - subprogram block data ASC is deleted)

$BETA
(modifications)

$CORDBA
(modifications)

$GQUAD
(modifications - needed only for inclusion of the subroutine in the data set &SCR) see note

$ALFA
(modifications) - see note

$ION
(modifications)

$PRFLPF
(modifications)

$SETDC
(modifications)

$SETDM
(modifications)

ORIGINAL PAGE IS
OF POOR QUALITY

$OUTCOR
(modifications)

$RH1
(modifications - new version is substituted)

$CORSST,ADD
(new subroutine)

$IONSST,ADD
(new subroutine)

$GRFS,ADD
(new subroutine)

$DLRSST,ADD
(new subroutine)

Note: Subroutines GQUAD and ALFA are members of the data set ORBIT.GTDS.SORSLIB.FORT but their compiled versions are not yet included in the data set ORBIT.GTDS.LOADMOD.LOAD.

$CONH,ADD
(new subroutine)

$CONX,ADD
(new subroutine)

$SPLN2,ADD
(new subroutine)

$SPLIN,ADD
(new subroutine)

ORIGINAL PAGE IS
OF POOR QUALITY

$TROPOA
(modifications)

$TROGET
(modifications - new version is substituted)

$DEVFCN,ADD
(new subroutine)

$TROWRK,ADD
(new subroutine)

```
/*
/*
//LINK.SYSLIB DD
//            DD
//            DD DSN=ORBIT.GTDS.RD.LOAD,DISP=SHR
//LINK.SYSLIN DD
//       DD *
```

(overlay control statement cards)

```
/*
/*
//GO.FT21F001 DD DSN=RVFXB,UNIT=2314,DISP=(NEW,DELETE),
//  SPACE=(CYL,(35,2))
//GO.FT45F001 DD SPACE=(CYL,(35,2))
//GO.FT91F001 DD DSN=GEOS.DAT,LABEL=(5,BLP),UNIT=2400-9,VOL=SER=35658
//GO.DATA5 DD *
```

(GTDS control deck)

```
/*
//
```

APPENDIX H

GLOSSARY

GLOSSARY

A	Distance between PC and P1. If PC lies between P1 and P2 then A=0.
GQUAD	Subroutine which performs the numerical integration of total electron content (XNT) between points P1 and P2 using Gaussian quadrature. GQUAD integrates by segments having end points defined by the array P.
GRFS	Subroutine used to resequence an array of up to 20 values in monotonically increasing order from largest negative value to largest positive value. GRFS can operate on a single array or on a pair of arrays. If one of the arrays contains positional values along (P1, P2), then GRFS will delete redundant points which are located too close (5km) to each other.
HM	Height of maximum electron density, meters above earth surface.
HMPR	Stores previous value of ionospheric profile parameter HM; used when converging on height HM.
HMYM	Height of bottom of ionosphere; meters above earth surface.
HMYMPR	Stores previous value of HMYM; used when converging on height HMYM.
IP	Number of elements in array P specifying the number of segments to be used to numerically integrate electron content between P1 and P2.
LEGS	Used in integrating electron content. If PC lies between P1 and P2 then LEGS 2 and the integration segments are (P1, PC) and (PC, P2). If PC lies outside (P1, P2) then LEGS 1 and integration segment is (P1, P2).
N	Number of elements in arrays X and Y used in calculating electron density deviation function.
NOP	Number of segments dividing the interval (P1, P2) into equal earth central angles. Used in determining the number of points N to be used in defining the deviation function which describes the variations in electron density between P1 and P2 or any other integration path.
N=NOP+1	+1 add a point where (P1, P2) crosses HM +0 no additional points

NOPF	Function which upon entry returns the number of points needed to properly define the electron density gradients between any two points in the ionosphere. The input parameters are a) the earth central angle subtended by the line segment joining the two points and b) the height above the surface of the earth of the point of closest approach of the line segment.
P	Array of positions along (P1, P2) marking the end points of the segments used to numerically integrate the total electron content between P1 and P2. The points chosen are the intersections of (P1, P2) with the heights HMYM, HM and the five heights delineating the topside exponential layers.
PB	Coordinates of intersection of the line of sight and the bottom of the ionosphere.
PC	Point of closest approach of the line (P01, P02) to earth center.
PI	Takes on value of coordinates of points P1 or P2, as appropriate. Used to define line segment end point for integration, either (PC, P1) or (PC, P2).
P01, P02	Body fixed XYZ coordinates of end points of line of sight. Ground to satellite mode: P01 is the position vector of ground station P02 is the position vector of satellite. Satellite to satellite mode: P01 is the position vector of target satellite P02 is the position vector of relay satellite
PT1, PT2	Body fixed XYZ coordinates of intersections of line of sight and 3500 km sphere.
P1, P2	Body fixed XYZ coordinates of end points of that segement of the line of sight (P01, P02) which lies entirely within the ionosphere.
SIDE	Parameter used to distinguish between path segments on opposite sides of PC. If PC lies between P1 and P2 then for segment (P1, PC) SIDE= -1 and for (PC, P2) SIDE= +1. If PC lies outside (P1, P2) then SIDE = +1.
SPLN2	Subroutine which computes and sets up arrays necessary to perform a spline interpolation within an array of vlues. Interpolation is performed by subroutine SPLIN.
X	Array of positions along (P1, P2) at which the density ratios Y are computed. The positions are in meters of distance from PC along (P1, P2).

XNT Total electron content integrated along the line of sight from P01 to P02.

Y Array of electron density ratios used in computing the deviation function which defines the electron density gradients along (P1, P2), (P1, PC) or (PC, P2) depending on the geometry.

$$Y = \frac{DEN(\lambda, \theta, h)}{DENREF(h)} - 1$$

Where DEN indicates electron density at position λ, θ, h and DENREF is density of reference profile at height h.

YMPB Ionospheric profile thickness parameter YM of lower ionosphere at the point PB.

REFERENCES

1. a) Bent, R.B.,Llewellyn, S.K., Nesterczuk, G., Schmid, P.E., "The Development of a Highly Successful Worldwide Empirical Ionospheric Model and its Use in Certain Aspects of Space Communication and Worldwide Total Electron Content Investigations". Proceeding 1975 Symposium on the Effect of the Ionosphere on Space Systems and Communications, Naval Research Laboratory, (January 20-22, 1975).

   b) S.K. Llewellyn, R.B. Bent "Documentation and Description of the Bent Ionospheric Model", AFCRL TR-73-0657, SAMSO TR-73-253 (July 1973).

   c) P.E. Schmid, R.B. Bent, S.K. Llewellyn, G. Nesterczuk, S. Rangaswamy "NASA-GSFC Ionospheric Corrections to Satellite Tracking Data", NASA-GSFC x-591-73-281 (December 1973).

2. Davis, K. "Ionospheric Radio Propagation", NBS Monograph 80, Government Printing Office (1965).

3. Thompson, R.F., "Spline Interpolation on a Digital Computer", NASA-GSFC x-692-70-261 (July 1970).

4. "Handbook of Mathematical Functions", ed. M. Abramowitz and I.A. Stegun, Dover Publications, New York (1965).

5. Behuncik, J.A. "Refraction Corrections as Applied to MSFN Measurements", NASA-GSFC x-832-70-10) (April 1970).

6. Nesterczuk, G., Kozelsky, J.K., Behuncik, J.A., "Line of Sight Electron Density Gradients as Deduced From an Empirical Ionospheric Model", COSPAR Symposium on the Geophysical uses of Satellite Beacon Observations, Boston University, June 1976 (Proceedings to be published).

7. Nesterczuk,G., Kozelsky, J.K., "Effect of Line of Sight Electron Density Gradients on Satellite Tracking Data", NASA-GSFC Contractor Final Report, Contract # NAS 5-22302, Atlantic Science Corporation, Final Report Number 76 W 110F5 (Sept. 1976)

REFERENCES

8. Nesterczuk, G., Kozelsky, J.K., Bent, R.B., Llewellyn, S.K., "Evaluation of the Ionospheric Refraction Correction Algorithm in the GTDS", NASA-GSFC Contractor Final Report, Contract # NAS 5-22302, Atlantic Science Corporation Final Report # 76 W 110F4 (August 1976)